PHOSPHATE OVERLOAD INHIBITS FEMALE FERTILITY IN MICE

APPROVED BY SUPERVISORY COMMITTEE

Makoto Kuro-o, M.D., Ph.D.

Steven Kliewer, Ph.D.

Carol Elias, Ph.D.

Joel Elmquist, D.V.M., Ph.D.

DEDICATION

I would like to thank my mentor Makoto Kuro-o for his endless support in my academic endeavors. Thank you, Makoto, for allowing me full freedom to pursue any and every experiment I have come up with along the way. Thank you for your guidance and mentorship throughout this amazing journey.

Next, I would like to thank the members of the Kuro-o lab, both past and present. Thank you Hiroshi Kurosu, Lei Wang, Olga Sineshchekova, Yuji Nakada, George John, Shigehiro Doi, Chung-Yi Cheng, Hidekazu Sugiura, Johanne Pastor, Kazuhiro Shiizaki, and Joel Schwartz-Moretti. Hiroshi, thank you for teaching me how to be a scientist. Thank you for challenging me to always ask why and for helping me to formulate the original hypotheses of my thesis project. Lei, thanks for all the mice and help with cloning! Dearest Olga, thank you for being such a great friend, ear, and advisor. Yuji, thank you for all your discussions of Lost. George, thank you for your friendliness and expertise. Shige, thank you for teaching the lab about nephrology. Chung-Yi, thank you for your never-ending drive and devotion to your experiments– your zeal served as a true inspiration to me. Hide, thank you for your kindness. Johanne, thank you for taking care of all of us and for your help with immunohistochemistry. Kazu, thank you for your smile– your happiness is truly contagious. Joel, I cannot thank you enough for your discussions (academic and otherwise), support, and wry

sense of humor– it has been my pleasure to be your fellow graduate student in the lab.

My thesis committee members have been a tremendous resource to me throughout the pursuit of my Ph.D. Thank you all for your critical comments and suggestions during our meetings. Steven Kliewer, thank you for your insight and endless use of your qPCR machine. Joel Elmquist, thank you for your advice on all things hypothalamic and for technical support and use of equipment in your lab. Carol Elias, a special thanks to you for your amazing guidance and mentorship to me throughout this process. I appreciate all your help with *in situ* hybridization and your superior knowledge of your field.

Thanks to all members of the Department of Molecular Pathology for your administrative support, for kindly lending supplies when I ran out, and for always being great neighbors. Special thanks to James Richardson and John Shelton, and all members of the Molecular Pathology Core for their exquisite histological preparations.

I would also like to thank the Integrative Biology Graduate Program for providing a challenging and encouraging research environment. Special thanks to Priyarama Sen for her administrative support and to Yi Liu, Ilya Bezprozvanny, and Alec Zhang for their helpful comments and criticism during our Works in Progress Seminars.

My deepest gratitude goes out to my fellow classmates, colleagues, and dear friends at UT Southwestern. Specifically, I would like to thank those who have been with me in this adventure since the beginning– Meredith Akins, Angie Bookout, Meredith Goertz, Bethany Gray, Sharon Kuss, Kathleen Lee, and Laura Sullivan. Team Girl– how could I have ever survived core course without you? Angie and Meredith Akins, our girls' nights truly sustain me. Angie, thank you to the end of the earth and back for your help with experiments and your emotional support along the way. Meredith Goertz, my Princess, thank you and Oliver for being my partners in crime.

Special thanks to the wonderful cougars of Life Group Central. Kay DeBlance, Lisa Embrey, Megan Otto, Kristen Hart, Cara Keuck, Melissa Ashworth, Amanda Ham, and Amy Spaur, thank you for your constant prayers and endless emotional support. Where would I be without each of you, my beautiful sisters in Christ? An enormous thank you goes out to Megan Otto (and the Focus Fairy) for being my constant motivator throughout my dissertation writing!

Abby Cannon, I owe my sanity and mental well-being to you. My love, my other half, my psychic connection, thank you from the bottom of my heart for listening all those long nights on the phone. Thanks for being there for me through all the tears and all the happy times as well. Thanks also for understanding me and my crazy laundry room dancing ways no matter what.

I want to thank my two dearest friends from Shreveport, Emily Pellegrin and Robbie Dayton. Emily, you've been there with me since the very beginning. I value our friendship more than you could ever imagine. I love you, my friend. Robbie, you and Penny brighten my life in so many ways. Thanks for always always caring for me and looking out for me. Thanks for teaching me about the universe too!

Dave, my love, I can't even find the words to express my gratitude to you for your support in my life. Throughout writing this dissertation and otherwise, you have pushed me and challenged me to be better and do more. You're always thinking of others and trying to save the world, and I truly admire you for that.

Finally, I want to dedicate this dissertation to my family. Mom, without you I would be utterly lost in life. Seriously. I am so lucky to have you not only as a mother, but as a great friend. I deeply cherish our relationship, and I wuv you too much! Michael and Denise, thank you for being amazing big siblings and for always looking out for me (when you're not teasing me of course!). Michael, I'm so happy for you and Anna, and I can't wait to welcome my new niece or nephew to the family! New additions to the crew, Bill, Cameron, and Taylor, I am so happy that we are a family– thank you for your laughter and life and your never-ending flinkiness! The newest furry little addition to my family, Riley, I love you no matter what.

A huge and heartfelt thank you to those who have gone on before me in this journey- Peepaw, Meemaw, Grandmommy, and Dad. Peepaw, I am going to be a doctor now, but I know there is certainly much more to life than being smart– thank you for teaching me that. Meemaw, thank you for your contagious happiness and joy for life, and thank you for teaching me that of all the things I've lost, I miss my mind the most! Grandmommy, thank you for teaching me to be the young lady that I am today– I love you Boolie! Also, a special thanks to my sweet dog Lucy, who passed away last Christmas. Lulu, thank you for greeting me with a smile every day– you brought immeasurable joy to my life!

Dad, oh Dad, I cannot begin to express how much you mean to me. You inspired me to become a scientist, Dad. Thank you for teaching me about nature, and sunsets, and dogs, and horses, and howling at the moon. I love you dearly, and I miss you, and I dedicate this dissertation to you.

PHOSPHATE OVERLOAD INHIBITS FEMALE FERTILITY IN MICE

by

ADDIE SMITH DICKSON

DISSERTATION

Presented to the Faculty of the Graduate School of Biomedical Sciences at

The University of Texas Southwestern Medical Center

In Partial Fulfillment of the Requirements

For the Degree of

DOCTOR OF PHILOSOPHY

The University of Texas Southwestern Medical Center

Dallas, Texas

May, 2012

PHOSPHATE OVERLOAD INHIBITS FEMALE FERTILITY IN MICE

ADDIE SMITH DICKSON, Ph.D.

The University of Texas Southwestern Medical Center, 2012

MAKOTO KURO-O, M.D., Ph.D.

Phosphate (P_i) is a mineral that is essential for life and is found in many important biological molecules as well as comprising the structural material of bone and teeth. However, when animals fail to excrete ingested P_i, P_i overload occurs. P_i overload causes hyperphosphatemia associated with multiple aging-like phenotypes, including infertility. We have employed two mouse models to study the effects of P_i overload on female fertility. The first model is Klotho mutant mice, which suffer P_i overload due to decreased renal P_i excretion. The second

model is wild-type mice fed a high P_i diet, which develop P_i overload due to increased intestinal P_i absorption. Both mouse models of P_i overload are infertile, do not undergo proper puberty, do not ovulate, and have hypotrophic uteri. These animals have aberrant hypothalamic-pituitary-gonadal (HPG) axis function typified by low expression of Kiss1 mRNA in the hypothalamus, altered serum luteinizing hormone (LH) levels, and low mRNA expression of steroidogenic enzymes in the ovary. However, the HPG axis in these animals appears to be functional if stimulated with the proper hormonal cues. Estradiol administration stimulates Kiss1 expression in the anteroventral periventricular nucleus while inhibiting Kiss1 expression in the arcuate nucleus of the hypothalamus. Acute administration of Kisspeptin-10 elicits an LH surge. Additionally, gonadotropin administration induces ovulation. These results suggest that the HPG axis in female mouse models of P_i overload is capable of proper function but that upstream hormonal cues may be absent in these mice. We propose that low Kiss1 expression is the primary cause of HPG axis dysfunction in these mice since it is a master regulator of puberty onset in females. Our models of P_i overload-induced female infertility may serve as a novel rodent model system in which to study sexual dysfunction and hormonal aberrations in women and children with chronic kidney disease who suffer from P_i overload due to decreased renal P_i excretion.

TABLE OF CONTENTS

PRIOR PUBLICATIONS

Dwyer, D. S. and **A. Dickson** (2007). "Neuroprotection and enhancement of neurite outgrowth with small molecular weight compounds from screens of chemical libraries." Int Rev Neurobiol **77**: 247-289.

Kurosu H, Choi M, Ogawa Y, **Dickson AS**, Goetz R, Eliseenkova AV, Mohammadi M, Rosenblatt KP, Kliewer SA, Kuro-o M. (2007). "Tissue-specific expression of betaKlotho and fibroblast growth factor (FGF) receptor isoforms determines metabolic activity of FGF19 and FGF21." J Biol Chem 282(37): 26687-26695.

LIST OF FIGURES

LIST OF TABLES

LIST OF DEFINITIONS

129 – 129S1/SvImJ Mouse Strain

3β-HSD-II – 3β-Hydroxysteroid Dehydrogenase Type II

17β-HSD-1– 17β-Hydroxysteroid Dehydrogenase Type 1

ACSF – Artificial Cerebrospinal Fluid

ACTH – Adrenocorticotropic Hormone

ADHR – Autosomal Dominant Hypophosphatemic Rickets/Osteomalacia

Arc – Arcuate nucleus

ARHR – Autosomal Recessive Hypophosphatemic Rickets/Osteomalacia

ATP – Adenosine Triphosphate

AVPV – Anteroventral Periventricular Nucleus

B6 – C57BL/6 Mouse Strain

BBB – Blood Brain Barrier

cAMP – Cyclic Adenosine Monophosphate

cDNA – Complementary Deoxyribonucleic Acid

Cga – Common Glycoprotein Alpha-subunit

CKD – Chronic Kidney Disease

cpm – Counts Per Minute

CRH – Corticotropin-releasing Hormone

CRHR1 – Corticotropin-releasing Hormone Receptor 1

CSF – Cerebrospinal Fluid

DAB – 3,3-Diaminobenzidine

DEPC – Diethylpyrocarbonate

DEPC-PBS – Diethylpyrocarbonate-treated Phosphate Buffered Saline

DMP1 – Dentin Matrix Protein 1

DNA – Deoxyribonucleic Acid

E2 – 17β-Estradiol

EAR – Estimated Average Requirement

ECL – Enhanced Chemiluminescence

eGFP – Enhanced Green Fluorescent Protein

ELISA – Enzyme-linked Immunosorbent Assay

ERK1/2 – Extracellular Signal-related Kinase 1/2

ESRD – End Stage Renal Disease

FGF – Fibroblast Growth Factor

FGF7 – Fibroblast Growth Factor 7

FGF21 – Fibroblast Growth Factor 21

FGF23 – Fibroblast Growth Factor 23

$FGF23^{-/-}$ – Fibroblast Growth Factor 23-null genotype

FGFR1 – Fibroblast Growth Factor Receptor 1

FGFR3 – Fibroblast Growth Factor Receptor 3

FGFR4 – Fibroblast Growth Factor Receptor 4

FACS – Fluorescence Activated Cell Sorting

FRS2α – Fibroblast Growth Factor Receptor Substrate 2α

FSH – Follicle Stimulating Hormone

FSHR – Follicle Stimulating Hormone Receptor

FTC – Familial Tumoral Calcinosis

GFP – Green Fluorescent Protein

GFP+ – Green Fluorescent Protein -positive

GH – Growth Hormone

GnRH – Gonadotropin Releasing Hormone

GnRHR – Gonadotropin Releasing Hormone Receptor

GPR54 – G Protein-coupled Receptor 54, Kiss1 Receptor

H&E – Hematoxylin and Eosin

H_2O_2 – Hydrogen Peroxide

HPA – Hypothalamic-pituitary-adrenal

$H_2PO_4^-$ – Dihydrogen Phosphate Ion

H_3PO_4 – Phosphoric Acid

hCG – Human Chorionic Gonadotropin

HPG – Hypothalamic-pituitary-gonadal

HPO_4^{2-} – Hydrogen Phosphate Ion

HRP – Horseradish Peroxidase

IGF-1 – Insulin-like Growth Factor 1

IRMA – Immunoradiometric Assay

KISS1 – KiSS-1 Metastasis-suppressor

KL – Klotho Gene

$KL^{-/-}$ – Klotho-deficient Genotype

LH – Luteinizing Hormone

LHCGR – Luteinizing Hormone/Choriogonadotropin Receptor

LRH-1 – Liver Receptor Homolog-1

MAPK – Mitogen-activated Protein Kinase

MAS/FD – McCune-Albright Syndrome/Fibrous Dysplasia

MEPE – Matrix Extracellular Phosphoglycoprotein

mRNA – Messenger Ribonucleic Acid

NaPi – Sodium-phosphate Cotransporter

NBF – Neutral Buffered Formalin

P450arom – Cytochrome P450 Aromatase

P450c17 – 17 Hydroxylase

P450scc – Side-chain Cleavage P450

PBS – Phosphate Buffered Saline

PBT – Phosphate Buffered Saline + 0.25% Triton X-100

PeN – Periventricular Nucleus

PHEX – Phosphate-regulating Gene with Homologies to Endopeptidases on the X Chromosome

P_i – Inorganic Phosphate, Phosphate Ion

PMSG – Pregnant Mare's Serum Gonadotropin

PO_4^{3-} – Phosphate Ion

PRL – Prolactin

PTH – Parathyroid Hormone

RDA – Recommended Dietary Allowance

RIA – Radioimmunoassay

RNA – Ribonucleic Acid

ROMK1 – Potassium Inwardly-rectifying Channel Subfamily J Member 1

RPM – Revolutions Per Minute

RT – Room Temperature

SDS – Sodium Dodecyl Sulfate

SDS-PAGE – Sodium Dodecyl Sulfate Polyacrylamide Gel Electrophoresis

SF-1 – Steroidogenic Factor 1

sFRP-4 – Secreted Frizzled-related Protein 4

StAR – Steroidogenic Acute Regulatory Protein

TCA – Trichloroacetic Acid

TIO – Tumor-induced Rickets/Osteomalacia

TRHR – Thyrotropin-releasing Hormone Receptor

TRPV5 – Transient Receptor Potential Cation Channel Subfamily V Member 5

TSH – Thyroid-stimulating Hormone

UL – Tolerable Upper Intake Level

WT – Wild-type

XLH – X-linked Hypophosphatemic Rickets/Osteomalacia

CHAPTER ONE
Introduction and Literature Review

PHOSPHATE HOMEOSTASIS

Introduction to Phosphate

Nomenclature

Phosphate is a general term used to describe inorganic and organic compounds (inorganic phosphates and organophosphates, respectively) derived from elemental phosphorus. Inorganic phosphate (P_i) exists in biological systems in a state of equilibrium between four forms, including the phosphate ion (PO_4^{3-}), the hydrogen phosphate ion (HPO_4^{2-}), the dihydrogen phosphate ion ($H_2PO_4^-$), and phosphoric acid (H_3PO_4), in the following equation:

$$PO_4^{3-} \leftrightarrow HPO_4^{2-} \leftrightarrow H_2PO_4^- \leftrightarrow H_3PO_4$$

The predominant biological form of phosphate is inorganic phosphate in its ionized form as $H_2PO_4^-$ or HPO_4^{2-} (Taal, Chertow et al. 2011). For the rest of this dissertation, the notations "phosphate" and "P_i" will be synonymous and will refer to these ions.

Biological Functions

Phosphate is a nutrient that is necessary for the survival of all living organisms. In human tissue, phosphate is a highly profuse mineral, only second to calcium in abundance (Gerrior, Bente et al. 2004; Hiza and Bente 2011). P_i is essential for many biological phenomena, including but not limited to the following examples. In the form of calcium phosphate, P_i comprises the major structural components of bone and teeth. Cellularly, the plasma membrane is made of phosphate in the form of phospholipids. The nucleotides that make up deoxyribonucleic acids (DNA) and ribonucleic acids (RNA) are all nucleoside-monophosphate molecules. Phosphate is an important high energy molecule in the form of the cell's main energy transport molecule, adenosine triphosphate (ATP). Phosphorylation, or the addition of a phosphate ion to a protein, is an indispensible cell signaling mechanism. Furthermore, phosphate salts are important intracellular and extracellular buffers for maintaining physiological pH (Taal, Chertow et al. 2011).

Dietary Sources

Since phosphate is essential for life, it is present in all plant and animal food sources. Particularly, meats, fish, and dairy are rich sources of dietary P_i, containing approximately 100-300 mg per serving (United States Nutrient Data Laboratory 2005). Large non-natural sources of dietary phosphate include carbonated soda beverages (approximately 40 mg per serving) and polyphosphate

food additives and preservatives (Calvo and Park 1996; United States Nutrient Data Laboratory 2005). These phosphate-based preservatives are estimated to account for approximately 20-30% of adult phosphate consumption (Calvo and Park 1996).

The United States Food and Nutrition Board has determined that the Estimated Average Requirement (EAR), or the "average daily nutrient intake level estimated to meet the requirements of half the individuals in a group" for phosphate is 580 mg/day for adult men and women (United States Institute of Medicine Standing Committee on the Scientific Evaluation of Dietary Reference Intakes 1997). Based on these nutritional requirements, the Food and Nutrition Board suggests a Recommended Dietary Allowance (RDA) of 700 mg P_i/day for adult men and women, with an estimated Tolerable Upper Intake Level (UL) of 4000 mg P_i/day (United States Institute of Medicine Standing Committee on the Scientific Evaluation of Dietary Reference Intakes 1997).

Over the past century, phosphate consumption in America has risen considerably due to increased consumption of dairy and grain-based foods (Gerrior, Bente et al. 2004). Currently adult P_i intake is more than double EAR and RDA values at a level of 1700 mg/day (Hiza and Bente 2011). While the United States Department of Agriculture (USDA), does include food enrichments and fortifications in their calculations of nutrient consumption, their current methodology does not include nutrient contents contained in food preservatives

(Hiza and Bente 2011). Therefore, the current USDA estimates of phosphate consumption per capita may grossly underestimate actual amounts of phosphate consumed, especially for individuals who eat highly processed foods.

Physiology of Phosphate Handling

Phosphate Balance

In a healthy individual with a normal rate of phosphate consumption (800-1500 mg/day), phosphate is maintained in a net zero balance, meaning that the amount of P_i consumed through the diet is equal to that excreted in the feces and urine on a daily basis (Taal, Chertow et al. 2011). In humans, blood phosphate concentration is maintained within a narrow range (3-4.5 mg/dL), and this homeostasis achieved through coordinated actions of the several organ systems including the intestine, kidney, bone, and parathyroid glands (Taal, Chertow et al. 2011). Upon food consumption, phosphate is absorbed from the lumen of the small intestine by sodium/phosphate (NaPi) cotransporters (type IIb) expressed on the apical membrane of the intestinal epithelia (Hilfiker, Hattenhauer et al. 1998; Feild, Zhang et al. 1999). Once phosphate enters the bloodstream, the vast majority of it (85-90%) is filtered by the glomeruli in the kidney (Taal, Chertow et al. 2011). Only a small portion of the filtered phosphate is excreted in the urine (3-20%) because most filtered phosphate (80-97%) is reabsorbed by NaPi

cotransporters (predominantly type IIa but also type IIc) expressed by proximal tubular cells (~80% of filtered P_i) and distal convoluted tubular cells (~10% of filtered P_i) in the kidney (Beck, Karaplis et al. 1998; Segawa, Kaneko et al. 2002; Razzaque 2009; Taal, Chertow et al. 2011). The P_i that has been reabsorbed is then stored throughout the body mainly in the bone (80-85%) but also in cells and soft tissues (14%) and in the blood and other extracellular fluids (1%). Although intestinal absorption, renal reabsorption, and modeling and remodeling of bone all contribute to serum phosphate levels, the kidney is thought to be the major regulator of serum P_i levels in the body (Taal, Chertow et al. 2011).

Phosphate Homeostatic Hormones

One way that expression of NaPi cotransporters is controlled is directly through dietary phosphate content. A diet low in P_i upregulates messenger RNA (mRNA) levels of NaPi cotransporter in order to maintain appropriate phosphate reabsorption (Kido, Miyamoto et al. 1999), while a diet high in P_i downregulates expression of NaPi transporters (Ritthaler, Traebert et al. 1999). In addition to this dietary regulation, several hormone systems have evolved to further control expression of NaPi transporters and thus ensure proper phosphate balance in the body. These hormones include vitamin D, parathyroid hormone (PTH), and Fibroblast Growth Factor 23 (FGF23), and signaling through these hormonal

systems is inextricably linked and has evolved to contain multiple levels of feed-forward and feedback control (Taal, Chertow et al. 2011).

Vitamin D is a hormone that is produced in an inactive, prehormone form in the skin as vitamin D3. In order for it to become active, vitamin D3 is sequentially hydroxylated in the liver and then the kidney to produce its active form 1,25-dihydroxyvitamin D3 (simply referred to as "vitamin D" in this dissertation) (Kronenberg, Melmed et al. 2008). Vitamin D is normally converted to its active form under conditions of low serum calcium and/or low serum phosphate, and it subsequently acts to increase intestinal absorption of calcium and P_i (Kronenberg, Melmed et al. 2008). It also acts to increase bone resorption by increasing osteoclast differentiation and activation (McSheehy and Chambers 1986). Increasing bone resorption releases calcium and phosphate, thus increasing their serum concentrations. Vitamin D also acts to feedback onto other phosphate-regulating hormones by inhibiting PTH transcription (Silver, Russell et al. 1985) and stimulating FGF23 transcription (Kolek, Hines et al. 2005).

PTH is normally secreted from the parathyroid gland in response to hypocalcemia (sensed by calcium-sensing receptor) and acts to increase serum calcium levels (Brown and MacLeod 2001), but it also serves to regulate phosphate homeostasis. In the kidney, PTH modifies the activity of NaPi-IIa and NaPi-IIc by increasing their endocytic retrieval from the apical membrane of proximal tubular cells, thereby decreasing renal P_i reabsorption (Lotscher,

Scarpetta et al. 1999; Segawa, Yamanaka et al. 2007). Also in the kidney, PTH acts to increase vitamin D synthesis by increasing 1α-hydroxylase (the final and critical enzyme in vitamin D synthesis), which in turn increases intestinal absorption of calcium and phosphate (Bergwitz and Juppner 2010). PTH also acts on bone to increase osteoclast number and activity (Bergwitz and Juppner 2010), which increases bone resorption, thereby increasing serum calcium and phosphate levels. Since PTH targets have opposing effects on regulating serum P_i (i.e. decreasing renal P_i reabsorption versus increasing intestinal absorption and increasing P_i release from the skeleton), it is important to note that the net effect of PTH is to slightly lower serum phosphate (Bergwitz and Juppner 2010). Although PTH secretion is mainly regulated by serum calcium levels, high phosphate levels can directly stimulate PTH secretion to complete a feedback loop in this hormonal circuit (Moallem, Kilav et al. 1998).

FGF23 is a phosphaturic hormone that is secreted from the bone (osteoblasts and osteocytes) in response to high serum phosphate and/or vitamin D concentrations (Liu, Guo et al. 2003; Riminucci, Collins et al. 2003; Weber, Liu et al. 2003; Mirams, Robinson et al. 2004; Sitara, Razzaque et al. 2004; Collins, Lindsay et al. 2005; Kolek, Hines et al. 2005; Yoshiko, Wang et al. 2007). Unlike vitamin D and PTH, the main function of FGF23 is to regulate serum phosphate concentrations but not serum calcium. FGF23 acts on the kidneys to downregulate proximal tubular expression of NaPi type IIa and IIc,

thus increasing P_i excretion in urine (Shimada, Hasegawa et al. 2004). Additionally, FGF23 acts on the kidneys to reduce expression of 1α-hydroxylase and to stimulate expression of 1,25-dihydroxyvitamin D3 24-hydroxylase (a vitamin D-degrading enzyme), thereby effectively reducing active vitamin D levels (Shimada, Hasegawa et al. 2004). This action of FGF23 ensures that excess phosphate will not be absorbed from the diet under conditions in which serum phosphate concentrations are already high. Finally, FGF23 exerts another level of feedback control by decreasing synthesis and secretion of PTH (Ben-Dov, Galitzer et al. 2007).

Klotho is a transmembrane receptor that is crucial for maintaining proper phosphate homeostasis (Razzaque 2009). Klotho is upregulated by a low phosphate diet (Morishita, Shirai et al. 2001; Segawa, Yamanaka et al. 2007), and vitamin D also stimulates transcription of Klotho mRNA (Forster, Jurutka et al. 2011). Klotho is a single-pass transmembrane protein that forms a complex with Fibroblast Growth Factor Receptor 1 (FGFR1), and together these two proteins act as a cell-surface co-receptor for FGF23 (Kurosu, Ogawa et al. 2006; Urakawa, Yamazaki et al. 2006). Because of Klotho's critical function in the FGF23 co-receptor complex, mice lacking Klotho cannot support FGF23 signaling and therefore have serum phosphate and high levels of vitamin D (Kuro-o, Matsumura et al. 1997; Yoshida, Fujimori et al. 2002). These mice will be described in great

detail in this dissertation as we have chosen them as a model system in which to study the physiological effects of phosphate overload.

Importantly, aside from its function in the FGF23 co-receptor complex, the extracellular domain of Klotho can be cleaved from the membrane by ADAM-10 and ADAM-17 metalloproteinases and is thought to enter the circulation and act at distant sites (Chen, Podvin et al. 2007). This shed form of Klotho can directly inhibit NaPi-IIa activity by removing glucosyl residues from the cotransporter, thereby increasing its retrieval from the plasma membrane (Hu, Shi et al. 2010). Thus, Klotho that has been shed from the cell membrane can increase phosphate excretion into urine independently from its activity as an FGF23 co-receptor.

DISEASES OF PHOSPHATE IMBALANCE

Because of the critical and diverse roles that phosphate plays in cell signaling, metabolism, and physiology, disorders of phosphate imbalance affect multiple tissues and organ systems and have profound health effects. These disorders fall into two categories: hypophosphatemic diseases, in which patients have low serum phosphate levels, or hyperphosphatemic diseases, in which patients have high serum phosphate levels.

Hypophosphatemic Diseases

Aside from patients with genetic disorders, idiopathic hypophosphatemia is rare (less than 1% of hospitalized patients) and appears mostly in acutely or critically ill patients (Kronenberg, Melmed et al. 2008). In these patients, hypophosphatemia is often caused by chronic alcoholism and/or malnutrition.

Non-idiopathic hypophosphatemic diseases share many clinical features including osteomalacia and rickets (Kronenberg, Melmed et al. 2008). Osteomalacia is a condition in which the bones are softened and weak, leading to bone pain and fractures; when this condition occurs during childhood, it is referred to as rickets. Hypophosphatemic diseases are characterized by low serum phosphate associated with impaired renal phosphate reabsorption and low levels of vitamin D (Fukumoto 2009). Rickets can be caused by dietary deficiency in vitamin D, but genetic causes of the disease are more prevalent in the areas of the world where vitamin D deficient diet is uncommon (Winters, Graham et al. 1958; Mankin 1974). These diseases have been attributed to excess FGF23 expression/function (Fukumoto 2009), and in fact FGF23 was originally cloned as the causative factor in two of these diseases (ADHR Consortium 2000; Shimada, Mizutani et al. 2001).

X-linked Hypophosphatemic Rickets/Osteomalacia (XLH)

XLH is the most common genetic hypophosphatemic disease and is characterized as vitamin D-resistant rickets/osteomalacia (Fukumoto 2009). XLH is caused by over 100 different inactivating mutations in the phosphate-regulating gene with homologies to endopeptidases on the X chromosome (PHEX) gene (The HYP Consortium 1995; Bianchetti, Oudet et al. 2002; Jonsson, Zahradnik et al. 2003). The function of the PHEX gene is still unknown, and it is not known if it is indeed an endopeptidase, and if so, what its substrate is. Elevated FGF23 in patients with XLH is thought to be causative in this disease; however, it is not known how mutations in the PHEX gene result in the accumulation of FGF23 (Fukumoto 2009).

Autosomal Recessive Hypophosphatemic Rickets/Osteomalacia (ARHR)

ARHR is caused by mutations in the dentin matrix protein 1 (DMP1) gene, which is expressed in bone and teeth (Feng, Ward et al. 2006; Lorenz-Depiereux, Bastepe et al. 2006). High levels of FGF23 in patients with ARHR are again thought to be causative in this disease (Lorenz-Depiereux, Bastepe et al. 2006), but it is not clear how mutations in DMP1 directly contribute to increased levels of FGF23 seen in these patients (Razzaque 2009).

Autosomal Dominant Hypophosphatemic Rickets/Osteomalacia (ADHR)

FGF23 has been cloned as the gene responsible for ADHR (ADHR Consortium 2000). Mutations reported in this disease occur in codons for two arginines in the protein– ^{176}Arg and ^{179}Arg (Fukumoto 2009). These arginines are critical for FGF23 processing and reside in a ^{176}Arg-X-X-^{179}Arg motif that is a target for proteolytic cleavage (Shimada, Mizutani et al. 2001). When these arginines become mutated, FGF23 becomes "non-degradable" and is thought to accumulate and/or exert excess function, resulting in hypophosphatemia and low vitamin D levels in these patients (White, Carn et al. 2001; Shimada, Muto et al. 2002).

Tumor-induced Rickets/Osteomalacia (TIO)

TIO is caused by hyper-FGF23-secreting tumors (Shimada, Mizutani et al. 2001; White, Jonsson et al. 2001). In addition to FGF23-overexpressing tumors, TIO can be caused by tumors overexpressing other genes such as secreted frizzled-related protein 4 (sFRP-4), matrix extracellular phosphoglycoprotein (MEPE), and Fibroblast Growth Factor 7 (FGF7). Serum levels of FGF23 are also high in these patients, but it remains unknown how sFRP-4, MEPE, and FGF7 contribute directly to phosphaturia and elevated FGF23.

Hypophosphatemic Rickets/Osteomalacia Associated with McCune-Albright Syndrome/Fibrous Dysplasia (MAS/FD)

Patients suffering from fibrous dysplasia with or without McCune-Albright Syndrome can experience hypophosphatemia, which may be associated with FGF23 overproduction in bone regions affected by the fibrous dysplasia (Riminucci, Collins et al. 2003).

Hyperphosphatemic Diseases

Hyperphosphatemic diseases show opposite characteristics to hypophosphatemic diseases including high serum phosphate, increased renal phosphate reabsorption, high serum vitamin D, low FGF23, and/or FGF23 resistance (Kronenberg, Melmed et al. 2008; Fukumoto 2009). Hyperphosphatemia occurs in the genetic disease Familial Hyperphosphatemic Tumoral Calcinosis (FTC) and also as a consequence of renal dysfunction in Chronic Kidney Disease (CKD).

Familial Hyperphosphatemic Tumoral Calcinosis (FTC)

FTC is caused by mutations in three genes– GALNT3, FGF23, and Klotho (Benet-Pages, Orlik et al. 2005; Frishberg, Topaz et al. 2005; Ichikawa, Imel et al. 2007). Patients with mutations in GALNT3 have low circulating levels of full-length (fully functional) FGF23 but high levels of C-terminal (inactive) fragments of FGF23, suggesting a lack of proper FGF23 function is responsible for

phosphate retention in this disease (Fukumoto 2009). The GALNT3 gene encodes an enzyme called ppGaNTase-T3 that is responsible for attaching an O-linked glycan to ^{178}Thr in FGF23 (in the ^{176}-Arg-X-X-^{179}Arg proteolytic processing site) (Ten Hagen, Fritz et al. 2003; Kato, Jeanneau et al. 2006; Frishberg, Ito et al. 2007). The addition of this glycan moiety to FGF23 prevents it proteolytic cleavage (Frishberg, Ito et al. 2007). Therefore, inactivating mutations in GALNT3 lead to loss of O-linked glycosylation of FGF23, thus increasing proteolytic processing and accumulation of the inactive C-terminal fragment of the protein. This leads to decreased phosphate excretion into urine and increased levels of circulating vitamin D seen in the disease.

In addition to mutations in GALNT3, missense mutations in FGF23 itself have been reported in FTC (Fukumoto 2009). These mutations appear to affect FGF23 processing in a similar manner to loss of GALNT3 function because low levels of full-length FGF23 but high levels of the C-terminal peptide are observed in these patients as well (Fukumoto 2009).

Additionally, one case of FTC is reportedly caused by a homozygous mutation in the Klotho gene (Ichikawa, Imel et al. 2007). Since Klotho is part of the co-receptor complex required for FGF23 signaling, loss of Klotho function renders FGF23 non-functional as well. In fact there is a compensatory upregulation of FGF23 levels seen in this patient, which is similar to the

extremely high levels of FGF23 seen in Klotho-deficient ($KL^{-/-}$) mice (Urakawa, Yamazaki et al. 2006; Ichikawa, Imel et al. 2007).

Chronic Kidney Disease (CKD)

The most significant type of hyperphosphatemic disease in terms of public health is CKD, which, according to the National Kidney Foundation, affects 26 million Americans. CKD is characterized by a slow decline in kidney function, usually over several years. Most commonly, CKD results as a consequence of diabetes and/or high blood pressure. CKD is divided into 5 stages based on glomerular filtration rate (GFR). Unfortunately, symptoms often do not occur until later stages of the disease once significant kidney function has been lost. Advanced stage kidney disease, often called end-stage renal disease (ESRD), requires treatment with dialysis or kidney transplantation (Taal, Chertow et al. 2011).

CKD is a major health concern in the United States, and is associated with significant risk, including increased risk for cardiovascular and all-cause mortality (Foley, Parfrey et al. 1998; Sarnak, Levey et al. 2003; Go, Chertow et al. 2004). Strikingly, risk of cardiovascular mortality increases by 10% per 1-mg/dL increase in serum phosphate in these patients, and risk of all-cause mortality increases by 18-35% per 1-mg/dL increase in serum P_i (Palmer, Hayen et al.

2011). These figures suggest that serum phosphate is an extremely important and contributing factor to the prognosis of CKD.

As CKD progresses, patients develop deranged phosphate homeostasis and a positive phosphate balance as a result of decreased kidney function (Hruska, Mathew et al. 2008). This positive phosphate balance eventually results in hyperphosphatemia (Craver, Marco et al. 2007). Additionally, patients with CKD have high serum levels of FGF23 (which rise progressively as renal function worsens), low vitamin D, and secondary hyperparathyroidism (Taal, Chertow et al. 2011). Although elevated serum FGF23 levels precede hyperphosphatemia in CKD (Gutierrez, Isakova et al. 2005), the role of elevated FGF23 in contributing to disease progression remains controversial (Quarles 2012; Wahl and Wolf 2012).

Apropos to this dissertation, adult patients (both male and female) with CKD and ESRD experience sexual dysfunction and juvenile patients often experience delayed or deranged puberty (Taal, Chertow et al. 2011). These topics will be further discussed in Section 1.4.2, but first we will provide an introduction to normal reproductive health women and adolescents.

FEMALE REPRODUCTIVE BIOLOGY

The following is a general overview of the hormonal axes involved in female reproductive biology as they pertain to this dissertation research. This introduction does not comprise a comprehensive description of all hormones involved in female reproductive physiology but rather descriptions of key regulators for the sake of clarity and relevance to this dissertation research.

The Hypothalamic-pituitary-gonadal Axis

The hypothalamus, pituitary gland, and ovaries work together in a tight circuit to regulate and promote female fertility. Coordinated actions of each of these organs are necessary for the cyclic ovulation patterns that both humans and mice undergo. Simply viewed, hormones secreted from the hypothalamus act on the pituitary, those secreted from the pituitary act on the ovaries, and those secreted from the ovaries provide feedback to the hypothalamus, completing a hormonal loop. For this reason, the hypothalamus, pituitary, and ovaries function rather as a unit than as separate entities. Together this unit is referred to as the hypothalamic-pituitary-gonadal (HPG) axis (Kronenberg, Melmed et al. 2008).

The Hypothalamus

The main function of the hypothalamus in terms of female reproductive biology is the maintenance of gonadotropin releasing hormone (GnRH) pulsatility

(Kronenberg, Melmed et al. 2008). The frequency and amplitude of the GnRH pulse are critical regulators of the entire HPG axis, since low frequency or tonic release of GnRH both result in anovulation. GnRH is a 10-amino-acid peptide hormone that is produced in the preoptic area of the hypothalamus and is secreted into the hypophyseal portal, which allows it to access the anterior pituitary gland (Seeburg and Adelman 1984). GnRH neurons originate from the olfactory bulb in the rostral portion of the brain and migrate caudally during development to their final location in the hypothalamus (Kronenberg, Melmed et al. 2008). The proper migration of GnRH neurons is essential for normal reproductive physiology as inadequate GnRH neuronal migration leads to hypogonadotropic hypogonadism (lack of sex steroid production due to defects in the pituitary gland or hypothalamus), as seen in Kallmann's syndrome (Cariboni and Maggi 2006).

The Pituitary Gland

GnRH signals through the GnRH receptor (GnRHR) in gonadotroph cells in the anterior pituitary to stimulate the production of luteinizing hormone (LH) and follicle stimulating hormone (FSH) (Kronenberg, Melmed et al. 2008). GnRH pulse frequency is a critical transcriptional regulator of LH and FSH common α subunit (Cga) and their unique β subunits, as well as dimerization and post-translational modification of α and β subunits, and is responsible for cyclic patterns of LH and FSH expression across the menstrual cycle (in humans) and

the estrus cycle (in mice) (Knobil 1980; Haisenleder, Dalkin et al. 1991; Kronenberg, Melmed et al. 2008).

Once secreted from the pituitary gland, LH and FSH enter the circulation and act on the ovary to stimulate hormone production, egg development, and ovulation (Kronenberg, Melmed et al. 2008). LH specifically acts through its receptor LHCGR in theca cells in the ovary to stimulate the production of androstenedione (a steroid estrogen precursor). FSH acts through the FSH receptor (FSHR) in a different cell type in the ovary, the granulosa cells, to further regulate estradiol production and to stimulate follicle growth (as the name of the hormone suggests). In both humans and mice, the mid-cycle rise in serum LH levels triggers the release of an egg from a mature ovarian follicle (ovulation). After ovulation, the ruptured follicle is transformed into a different structure, the corpus luteum (plural corpora lutea), which secretes high levels progesterone under the control of LH. However, if pregnancy does not occur, the corpus luteum involutes and regresses into a structure called the corpus albicans (Kronenberg, Melmed et al. 2008).

The ovaries

The main function of the ovaries is the production of female reproductive hormones, estradiol and progesterone, and the ovulation of mature eggs. Under control of the GnRH pulse, the ovaries remain quiescent during childhood but

become active upon puberty initiation. They remain active through adulthood until after menopause, at which time no oocytes remain and many steroidogenic cells in the ovary have died. Estradiol stimulates uterine growth and prepares the endometrial layer of the uterus for implantation of the fertilized egg. Additionally, estradiol provides positive and negative feedback regulation on hypothalamic hormone secretion and thereby highly impacts the HPG axis as a whole (Kronenberg, Melmed et al. 2008).

In terms of egg development and hormone secretion, the ovarian follicle is the most important functional unit in this organ. There are progressive stages of follicular development which are defined as primary, secondary, tertiary, and Graafian. The first three stages are not dependent on pituitary hormones and appear to be mediated by ovarian factors (Kronenberg, Melmed et al. 2008). In each ovary, many follicles at different stages of development exist, and much of this development is FSH independent. However, the rise in FSH at the end of the luteal phase is required to stimulate certain follicles to continue development toward the Graafian stage, and if FSH and other intraovarian signals are not present these follicles will become atretic (Schipper, Hop et al. 1998). Following this stage of follicular development, there is a midcycle rise in estradiol and a strong LH surge that induces ovulation of the dominant mature follicle (in humans) or several follicles (in mice) (Richards, Jonassen et al. 1980; Richards and Bogovich 1982; Kronenberg, Melmed et al. 2008).

Estradiol Production

Estradiol is produced by preovulatory follicles in a series of six enzymatic steps. All steroid hormones produced by the ovary are derived from cholesterol, and the first and rate-limiting step in estradiol production is the transport of cholesterol into the mitochondria by the enzyme steroidogenic acute regulatory protein (StAR) (Miller and Strauss 1999). Within the mitochondria, cholesterol is converted to pregnenolone by the enzyme side-chain cleavage P450 (P450scc). In the cytoplasm, pregnenolone is converted by two enzymes, 17 hydroxylase (P450c17) and 3β-hydroxysteroid dehydrogenase type II (3β-HSD-II), into androstenedione. Androstenedione is aromatized by aromatase P450 (P450arom) to estrone. The final step in estradiol production is the conversion of estrone to estradiol (the biologically active form of estrogen) by the enzyme 17β-hydroxysteroid dehydrogenase type 1 (17β-HSD-1) (Kronenberg, Melmed et al. 2008).

In the preovulatory follicle the first four steps in this conversion occur in the theca cells under the control of LH (Bogovich and Richards 1982). LH signals through the LHCGR to induce the production of cyclic adenosine monophosphate (cAMP), which acts as a second messenger to increase flux through the steroidogenesis pathway (Kronenberg, Melmed et al. 2008).

Activation of LHCGR also induces the master regulator transcription factor steroidogenic factor 1 (SF-1), which upregulates transcription of StAR, P450scc, P450c17, and 3β-HSD-II (Hanley, Ikeda et al. 2000).

The final two steps in the production of estradiol occur in the neighboring granulosa cells of the preovulatory follicle (Dorrington, Moon et al. 1975). These steps are under the control of FSH signaling through FSHR (Dorrington, Moon et al. 1975). Again, activation of FSHR upregulates intracellular cAMP levels, and activates SF-1 and another transcription factor liver homologue receptor-1 (LRH-1) (Peng, Kim et al. 2003). In rodents, LRH-1 is the major mediator signaling downstream of FSHR and upregulates transcription of P450arom (Falender, Lanz et al. 2003; Hinshelwood, Repa et al. 2003).

Puberty

Puberty is a continuation of gonadal maturation and developmental that is initially begun during fetal development (Kronenberg, Melmed et al. 2008). During puberty, the central nervous system awakens the HPG axis (Boyar, Rosenfeld et al. 1974; Plant 2001), and this results in a full maturation of the ovaries. Subsequent ovarian sex steroid production and secretion stimulates the development of secondary sex characteristics and the achievement of fertility. In addition to the Tanner stages of sexual maturation, the ovaries also increase in

size and the uterus increases in size and diameter (Kronenberg, Melmed et al. 2008). Also during puberty, there is an adolescent growth spurt that is dependent upon both estradiol and growth hormone (GH) (Kronenberg, Melmed et al. 2008).

GnRH Pulsatility

GnRH is secreted in a pulsatile fashion during early embryonic development, but then becomes quiescent during a period called the juvenile pause (Plant 2001). During this time, the GnRH pulse generator is silenced by inhibitory factors. It is not until puberty that GnRH pulsatility is resumed, and this pulsatility remains constant throughout adulthood.

One hormone that may be a critical regulator of puberty initiation and disinhibition of the GnRH pulse generator is Kisspeptin. Kisspeptins are peptide products of various lengths of the Kiss1 gene that are expressed in the anteroventral periventricular nucleus (AVPV), the periventricular nucleus (PeN), and the arcuate nucleus (Arc) of the hypothalamus (Gottsch, Cunningham et al. 2004; Clarkson and Herbison 2006; Clarkson, d'Anglemont de Tassigny et al. 2009; Oakley, Clifton et al. 2009). Kisspeptins signal through their receptor GPR54 (Oakley, Clifton et al. 2009), which is expressed in GnRH neurons (Han, Gottsch et al. 2005). Kisspeptin signaling through GPR54 was discovered to be a key regulator of sexual development and reproductive function because mutations in GPR54 in humans and mice were shown to be associated with

hypogonadotropic hypogonadism (de Roux, Genin et al. 2003; Funes, Hedrick et al. 2003; Seminara, Messager et al. 2003). Since then, it has been appreciated that Kisspeptins potently stimulate GnRH secretion and downstream luteinizing hormone (LH) release, and it has been noted that the Kisspeptin/GPR54 system is indeed a "gatekeeper" of puberty (Oakley, Clifton et al. 2009). Importantly, expression of KISS1 is regulated by positive and negative feedback from ovarian hormones. Specifically, estradiol is thought to stimulate Kiss1 expression in the AVPV but repress its expression in the Arc (Oakley, Clifton et al. 2009). This differential expression of Kiss1 may be important for puberty initiation and maintenance of fertility throughout adulthood.

Similarly to the GnRH pulse, pituitary gonadotropins LH and FSH are high during early development and infancy, but then they become inhibited and their pulse amplitude remains low until puberty (Kronenberg, Melmed et al. 2008). About a year before puberty, LH pulse amplitude rises (Wu, Butler et al. 1996; Mitamura, Yano et al. 1999; Mitamura, Yano et al. 2000). In addition to LH and FSH, the pituitary also begins to produce more prolactin during puberty (Kronenberg, Melmed et al. 2008).

Puberty in Mice

The same hormones and regulatory mechanisms that mediate puberty in humans are also required for puberty initiation and progression in mice

(Kronenberg, Melmed et al. 2008; Oakley, Clifton et al. 2009). The time of puberty onset in mice can differ from strain to strain, but it follows a general scheme described as follows. Around day 26 post-birth, mice undergo vaginal canalization marking the beginning of puberty. Around day 40, female mice will experience their first estrus and initiate estrus cycling thereafter. Approximately day 60 marks the completion of puberty and the achievement of sexual maturity.

REPRODUCTIVE DYSFUNCTION IN WOMEN

Infertility due to anovulation is one of the most common gynecologic problems in reproductive-age women. This is commonly associated with menstrual symptoms including lack of menses (amenorrhea), infrequent menses (oligomenorrhea), irregular menses, or excessive menstrual bleeding. Anovulatory patients can be divided into two main groups: women who are estrogen-deficient or those with excess androgen production. There are five major etiological factors that contribute to anovulation in reproductive-age women including hypothalamic anovulation, hyperprolactinemia, androgen excess, premature ovarian failure, or chronic illness (including liver and kidney failure and acquired immunodeficiency syndrome) (Kronenberg, Melmed et al. 2008).

Functional Hypothalamic Anovulation

A disruption of pulsatile GnRH release from the hypothalamus leads to dysregulation of downstream signaling through the HPG axis, and can cause anovulation, termed "hypothalamic anovulation". Rarely, genetic disorders, anatomical abnormalities, infection, tumors, or head trauma can cause hypothalamic anovulation; however, most often, this form of anovulation is not associated with any known neurologic causes (Kronenberg, Melmed et al. 2008). More commonly, unknown factors lead to misregulation/downregulation of HPG axis hormones and signaling, and this situation is termed "functional hypothalamic anovulation" (Knobil 1980). Importantly, functional hypothalamic anovulation is completely reversible if the proper health and lifestyle changes are implemented (Kronenberg, Melmed et al. 2008).

A diagnosis of functional hypothalamic anovulation is reached by ruling out other organic causes of anovulation such as hyperprolactinemia, hypothyroidism, or androgen excess (as seen in polycystic ovary syndrome). The following clinical observations are also important for diagnosing hypothalamic anovulation. Women usually present with secondary (or rarely primary) amenorrhea. They have normal secondary sexual characteristics but evidence of poorly-estrogenized sex organs (thin vaginal mucosa, little to no cervical mucus, and normal to small-sized uterus). Additionally low gonadotropin levels are

usually measured. LH secretion patterns vary from individual to individual with hypothalamic anovulation, and prepubertal patterns can be seen (Kronenberg, Melmed et al. 2008).

Reproductive Health in CKD

Adult CKD Patients

Men and women with CKD nearly universally suffer from reproductive dysfunction (Kronenberg, Melmed et al. 2008; Taal, Chertow et al. 2011). In women, symptoms such as infertility, anovulation, dysmenorrhea, amenorrhea, oligomenorrhea, premature menopause, decreased libido, and anorgasmia are common (Handelsman 1985). These symptoms are caused by alterations in reproductive hormone levels that occur in early disease stages and progressively worsen with CKD progression (Anantharaman and Schmidt 2007). Hormonal disruption appears to occur at all levels of the HPG axis in these patients (Holley 2004). Although hormonal aberrations vary among different patients, commonalities observed in premenopausal women include lack of preovulatory surges in estradiol and LH, high/normal but acyclic LH and FSH, low/normal estradiol levels during the follicular phase, very low progesterone, and elevated prolactin (Holley 2004; Anantharaman and Schmidt 2007).

It has been suggested that a defect in the hypothalamus is responsible for reproductive dysfunction in women with CKD (Holley 2004; Anantharaman and Schmidt 2007). Indeed, administration of estrogens in women with chronic renal failure could not induce a midcycle LH surge, suggesting that the hypothalamus is unresponsive to this normal positive feedback control (Lim, Henriquez et al. 1980). There are many other organic causes that potentially contribute to reproductive dysfunction in women with renal failure including hyperprolactinemia, anemia, hyperparathyroidism, hypothyroidism, elevated stress hormone levels, elevated growth hormone levels, malnutrition/uremic anorexia, zinc and other vitamin deficiencies, and/or uremic toxins (Handelsman 1985; Holley 2004; Anantharaman and Schmidt 2007).

Renal transplantation can restore normal menstrual function and fertility in women, and is the best treatment for reproductive dysfunction in women with CKD (Handelsman 1985). Successful pregnancy in uremic women is rare, but rates are improved after kidney transplant (Anantharaman and Schmidt 2007). However, irregular menses may still be common after renal transplantation (Ghazizadeh and Lessan-Pezeshki 2007). Hormone replacement therapy can be effective for uremic women with low estradiol and progesterone levels, but is not effective in all patients and may not improve all sexual symptoms (Anantharaman and Schmidt 2007). It is clear that a better understanding of the underlying causes

of reproductive dysfunction in women with CKD is needed to improve treatment strategies and patient outcomes.

Juvenile CKD Patients

CKD is vastly an adult disease; however, children and adolescents can develop CKD usually as a consequence of developmental disorders resulting in kidney malformation (Taal, Chertow et al. 2011). Juvenile patients with CKD, both male and female, often suffer from delayed or blunted puberty (Lane 2005). On average, children with CKD have a 2 year delay in puberty onset and progression compared to healthy individuals (Hokken-Koelega, Saenger et al. 2001). Because of its effects on puberty, CKD in children and adolescents also potently inhibits linear growth (Hokken-Koelega, Saenger et al. 2001). Hormonal aberrations are observed in juvenile CKD patients at all levels of the HPG axis (Hokken-Koelega, Saenger et al. 2001; Holley 2004). Specifically, these patients lose pulsatile secretion patterns of LH, but LH pulsatility can be restored by successful kidney transplantation (Schaefer, Seidel et al. 1991; Schaefer, Veldhuis et al. 1994).

It has long been established that CKD affects puberty in adolescents, but it should also be noted that a reciprocal relationship exists as well. Unfortunately, kidney function in children with CKD dramatically deteriorates during puberty (Ardissino, Dacco et al. 2003; Lane 2005). It is unknown what factors in puberty

contribute to kidney decline during puberty in these patients, but elevation of systemic blood pressure, production of sex steroids (both androgens and estrogens), and elevated growth hormone signaling may be involved (Lane 2005). There is an extreme paucity of literature available on the relationship between CKD and puberty and vice versa, and it is clear that enhanced understanding of this interplay will be necessary for improved patient outcomes and kidney survival.

MOUSE MODELS OF PHOSPHATE OVERLOAD

For this dissertation research, we have employed two mouse models of phosphate overload: Klotho-deficient mice ($KL^{-/-}$) and wild-type (WT) mice fed a high phosphate diet. We have defined "phosphate overload" to mean conditions (genetic, dietary, or otherwise) resulting in a state of positive phosphate balance. As described in Section 1.1.2, positive phosphate balance is a state resulting in phosphate retention when phosphate input exceeds phosphate output. This can occur due to excess phosphate uptake (through the diet) or decreased renal excretion of phosphate into urine.

Klotho-deficient Mice

We have chosen to use Klotho-deficient mice (Kuro-o, Matsumura et al. 1997) as a model of phosphate overload. For the rest of this dissertation, these mice will be denoted as $KL^{-/-}$.

Due to Klotho's role as a co-receptor for the phosphaturic hormone FGF23 (see Section 1.2.2), mice lacking Klotho cannot support FGF23 signaling and therefore experience severe phosphate retention due to decreased renal excretion of phosphate (Kuro-o, Matsumura et al. 1997; Kurosu, Ogawa et al. 2006; Urakawa, Yamazaki et al. 2006). Phosphate retention is manifest in these mice as hyperphosphatemia. In addition to hyperphosphatemia, these mice exhibit multiple premature aging-like phenotypes including shortened lifespan, growth retardation, skin and muscle atrophy, and soft-tissue calcification (Kuro-o, Matsumura et al. 1997). Importantly for this dissertation research, $KL^{-/-}$ mice (both males and females) are also infertile. However, for the rest of this dissertation, we will only describe infertility phenotypes of $KL^{-/-}$ females.

Wild-type Mice Fed High Phosphate Diet

We have employed wild-type (WT) mice fed a high phosphate diet as a second model of phosphate overload. These mice experience a positive phosphate balance due to increased dietary intake and intestinal absorption of phosphate that exceeds renal excretion capacity (unpublished findings from our laboratory).

Differing from $KL^{-/-}$ mice, high phosphate-fed mice excrete high levels of phosphate into urine in response to their positive phosphate balance. We will investigate fertility phenotypes in these mice and again only describe experiments using female mice.

RESEARCH GOALS

The goal of this dissertation research is to investigate the effects of phosphate overload on female fertility in mice. Previous reports have described female infertility in $KL^{-/-}$ mice but have failed to provide a comprehensive mechanism underlying this phenotype (Kuro-o, Matsumura et al. 1997; Toyama, Fujimori et al. 2006). To our knowledge, no previous reports have been made detailing the effects of dietary phosphate overload on fertility (male or female). Therefore, we will present our novel findings herein.

In humans, phosphate overload becomes relevant in the case of CKD. Since adult and juvenile forms of CKD are associated with reproductive dysfunction, we hope that our studies of the effects of phosphate overload on female fertility in mice will provide novel mechanistic insight for this disease. Additionally, phosphate consumption in the United States has risen over the past century due to increased food availability and increased consumption of processed foods containing phosphate-based preservatives. Perhaps our studies might

suggest that increased phosphate consumption may lead to decreased fertility in otherwise healthy individuals.

CHAPTER TWO
Female mice experiencing phosphate overload display aberrant HPG axis function.

INTRODUCTION AND RATIONALE

In this chapter, we will examine female infertility in two models of phosphate overload: $KL^{-/-}$ female mice and WT female mice fed a high phosphate diet. Infertility phenotypes of $KL^{-/-}$ mice have been somewhat understudied and have only been previously investigated in two reports (Kuro-o, Matsumura et al. 1997; Toyama, Fujimori et al. 2006). Kuro-o et al. noted that $KL^{-/-}$ females have atrophied external and internal genital organs, including both the uterus and ovaries (Kuro-o, Matsumura et al. 1997). Additionally, these mice were incapable of mating (Kuro-o, Matsumura et al. 1997). Upon histological examination of the ovary, Kuro-o et al. concluded that $KL^{-/-}$ females suffer from impaired gonadal cell maturation because they could only observe immature follicles but not mature secondary follicles, Graafian follicles, or corpora lutea in ovaries of 6-9 week old mice (Kuro-o, Matsumura et al. 1997).

Toyama et al. later conducted a more thorough investigation of the infertility phenotype of $KL^{-/-}$ females and suggested that decreased production of pituitary hormones LH and FSH may be primarily responsible for reproductive deficits in $KL^{-/-}$ females (Toyama, Fujimori et al. 2006). They found that $KL^{-/-}$

females had significantly less variation in LH and FSH hormone levels than their WT littermates across the estrus cycle (Toyama, Fujimori et al. 2006). Upon immunohistochemical examination of the pituitary gland, Toyama et al. found that $KL^{-/-}$ mice had almost no LH-positive cells; however, this was not the case for FSH-positive cells (Toyama, Fujimori et al. 2006). Downstream of LH and FSH, Toyama et al. again described a lack of follicular maturation in $KL^{-/-}$ ovaries and found that follicles did not progress beyond the preantral stage (Toyama, Fujimori et al. 2006). They noted a lack of LHCGR mRNA expression as well as a lack of P450arom expression in $KL^{-/-}$ ovaries (Toyama, Fujimori et al. 2006).

Toyama et al. have suggested that a lack of GnRH stimulation of pituitary gonadotrophs may be responsible for low circulating LH and FSH in $KL^{-/-}$ females. In this chapter, we have investigated this possibility by measuring GnRH mRNA levels and immunoreactivity $KL^{-/-}$ females and their WT littermates. Additionally, we have measured upstream regulators of GnRH pulsatility, including Kiss1 and its receptor GPR54. Furthermore, we have confirmed previous reports of disturbed pituitary function in $KL^{-/-}$ females and conducted a thorough ovarian gene expression analysis in these animals and their WT littermates. These data will be presented herein.

It has been demonstrated that many premature aging-like phenotypes of $KL^{-/-}$ mice are due to improper phosphate balance in these mice and can therefore be corrected by dietary restriction of phosphate or genetic manipulation of

phosphate handling (Morishita, Shirai et al. 2001; Segawa, Yamanaka et al. 2007; Ohnishi, Nakatani et al. 2009). Feeding $FGF23^{-/-}$ mice, which have an identical phenotype to $KL^{-/-}$ mice, a phosphate-deficient diet corrected their hyperphosphatemia and rescued their early lethality (Shimada, Kakitani et al. 2004; Sitara, Razzaque et al. 2004; Stubbs, Liu et al. 2007). Because of these findings, we will investigate the effects of phosphate-restricted diet on fertility phenotypes of $KL^{-/-}$ females in this chapter.

Since we believe that infertility in $KL^{-/-}$ mice may be secondary to hyperphosphatemia, we also decided to investigate the effects of positive phosphate balance on female fertility in WT mice. In this chapter, we will present data from two WT strains of mice, 129S1/SvImJ and C57BL/6, that underwent dietary phosphate overload. Several groups have investigated the effects of high phosphate diet on various aspects of rodent physiology, including effects on renal function and phosphate handling, phosphate homeostatic hormones, soft tissue and vascular calcifications, tumorigenicity, protein phosphorylation, and intracellular signaling (van den Broek and Beynen 1998; Saito, Maeda et al. 2005; Jin, Hwang et al. 2006; Tani, Sato et al. 2007; El-Abbadi, Pai et al. 2009; Camalier, Young et al. 2010; Weinman, Biswas et al. 2011). These studies indicate that dietary phosphate content is an important mediator of rodent health and that excess phosphate consumption can have adverse physiological effects. However, to our knowledge, no group has yet investigated the effects of elevated

dietary phosphate content on reproductive health (in rodents or otherwise). Our novel results will be presented herein.

RESULTS

$KL^{-/-}$ females display aberrant HPG axis function.

To begin our investigation of reproductive phenotypes in the $KL^{-/-}$ model of phosphate overload, we performed a gross characterization of 8 week old $KL^{-/-}$ females and their WT littermates. As previously reported, $KL^{-/-}$ females are hyperphosphatemic (Figure 2-1A), they exhibit growth retardation as evidenced by their low body weight (Figure 2-1B), and they display several reproductive abnormalities (Figure 2-1, C-E) (Kuro-o, Matsumura et al. 1997). Outwardly, $KL^{-/-}$ females do not undergo vaginal canalization (data not shown), which is one of the first indicators of pubertal initiation in mice (Caligioni 2009). $KL^{-/-}$ females have extremely hypotrophic uteri, weighing 6.6 mg on average (average uterus weight for WT littermates is 40.4 mg) (Figure 2-1C), and when corrected for their low body weight, they still display a significantly reduced uterus to body weight ratio compared to their WT littermates (Figure 2-1D). Histological examination of ovaries taken from 8 week old WT mice revealed the presence of corpora lutea (white arrowheads), whereas $KL^{-/-}$ ovaries had no corpora lutea or

mature Graafian follicles (Figure 2-1E). Taken together, these results suggest that $KL^{-/-}$ female mice do not undergo proper pubertal initiation or progression.

Since the hypothalamus is a critical set point for regulating proper HPG axis function, we examined expression of key hypothalamic genes, including the so-called master regulator of puberty, Kiss1. Sexually mature (60 day old) WT females in diestrus express high levels of Kiss1 mRNA in the anteroventral periventricular nucleus (AVPV) and arcuate nucleus (Arc) of the hypothalamus (Figure 2-2A). However, age-matched $KL^{-/-}$ females show no signal for Kiss1 mRNA by *in situ* hybridization in the AVPV (Figure 2-2A). They do, however show comparable Kiss1 expression levels to WT in the Arc (Figure 2-2A). These expression levels are quantified by qPCR of the whole hypothalamus (including both AVPV and Arc nuclei), demonstrating that $KL^{-/-}$ females have an overall dramatically reduced expression of Kiss1 (4.4 fold) in diestrus compared to their WT littermates (Figure 2-2B).

Despite reduced Kiss1 expression, $KL^{-/-}$ females express similar levels of the Kisspeptin receptor, GPR54, to their wild-type counterparts (Figure 2-2C). Also, they show no change in mRNA expression of the downstream target of Kisspeptin, GnRH (Figure 2-2D), and immunohistochemical analysis of GnRH neurons revealed that they are intact and properly migrated in $KL^{-/-}$ females (Figure 2-2E). These measures of GnRH mRNA and protein only reflect

expression at a single timepoint, however, and do not indicate whether GnRH expression is pulsatile or tonic.

At the level of the pituitary, we observed altered expression of several genes downstream of Kiss1 in the HPG axis in $KL^{-/-}$ females at 8 weeks of age (Figure 2-3). $KL^{-/-}$ females have low mRNA expression levels of GnRH Receptor (GnRHR) and LH (Figure 2-3, A-B). Indeed, serum levels of LH are also very low in $KL^{-/-}$ females (Figure 2-3E). FSH and Cga mRNA levels and FSH levels in serum were not significantly different between $KL^{-/-}$ and WT females (Figure 2-3, C-D, F).

Since LH is a key regulator of ovarian function and therefore ovulation, we measured mRNA expression of ovarian hormone receptors, transcription factors, and steroidogenic enzymes in $KL^{-/-}$ females and their WT littermates. $KL^{-/-}$ females had no difference in expression of hormone receptors, LH Receptor (LHCGR) and FSH Receptor (FSHR), from their WT counterparts (Figure 2-4A). LH signals through its receptor LHCGR to activate the steroidogenic transcription factor SF-1, which shows decreased expression in $KL^{-/-}$ versus WT mice (Figure 2-4B). Expression of LRH-1, another key steroidogenic transcription factor in the ovary, was not changed between $KL^{-/-}$ and WT mice (Figure 2-4B). Several enzymes in the synthesis pathway for estrogen were altered in $KL^{-/-}$ ovaries. $KL^{-/-}$ females had decreased expression of steroidogenic acute regulatory protein (StAR), P450scc, P450c17, and P450arom (Figure 2-4C). These enzymes are

responsible for transporting cholesterol into the mitochondria, converting cholesterol into pregnenolone, converting pregnenolone into androstenedione, and converting androstenedione into estrone, respectively. There was no difference in expression of 17β-HSD-1 (the enzyme responsible for converting estrone into estradiol) between $KL^{-/-}$ and WT mice (Figure 2-4C).

Low P_i diet partially rescues reproductive phenotypes of $KL^{-/-}$ females.

In order to investigate the contribution of hyperphosphatemia to $KL^{-/-}$ female reproductive phenotypes, we fed $KL^{-/-}$ mice a variety of low phosphate diets. $KL^{-/-}$ females and their WT female littermates were weaned onto normal (0.35%) or low (0.02, 0.06, or 0.2%) P_i at 3 weeks of age. After 5 weeks on each diet, animals were sacrificed at a final age of 8 weeks old.

Low phosphate feeding improved phosphate balance in $KL^{-/-}$ mice. 0.02% and 0.06% P_i diets lowered serum phosphate in both $KL^{-/-}$ and WT groups (Figure 2-5A). 0.2% P_i diet did not lower serum P_i in $KL^{-/-}$ mice (Figure 2-5A); however, we believe this diet did alter phosphate balance in these mice as evidenced by improvements in other phenotypes such as body weight and gene expression (Figure 2-5, B-C, E). Low phosphate diet also improved growth phenotypes of $KL^{-/-}$ mice (Figure 2-5B). Importantly, on 0.2% P_i diet, $KL^{-/-}$ mice have no

significant difference in body weight from their WT littermates on normal chow (0.35% P_i) (Figure 2-5B).

In terms of gene expression, 0.2% P_i feeding partially restored Kiss1 expression in the hypothalamus of $KL^{-/-}$ mice (Figure 2-5C). Kiss1 expression in these mice was still not as high as WT mice on normal chow, but was significantly improved from $KL^{-/-}$ mice on normal chow. 0.06% P_i diet completely restored GnRHR mRNA expression in $KL^{-/-}$ females to WT (0.35% P_i) levels (Figure 2-5D). LH expression was also completely rescued in $KL^{-/-}$ mice fed 0.06 and 0.2% P_i diet (Figure 2-5E).

Despite these improvements in serum phosphate parameters, body weight, and hypothalamic and pituitary gene expression, $KL^{-/-}$ mice on 0.06 and 0.2% P_i diet still did not ovulate (Figure 2-5F). Notably, WT mice on these diets (0.06 and 0.2% P_i) also did not ovulate in the same experimental timeframe (data not shown). This lack of ovulation in both genotypes under conditions of low dietary phosphate is likely due to phosphate deficiency. Unlike mice fed 0.35% P_i diet, mice fed diets containing 0.2% P_i or less excreted no detectable P_i into urine (data not shown), indicating that these low P_i diets failed to meet the minimum P_i requirement of the mouse.

High P_i-fed WT female mice phenocopy $KL^{-/-}$ mice.

Because we suspect that reproductive abnormalities seen in $KL^{-/-}$ mice are due to phosphate overload and not directly due to loss of Klotho gene function (see Chapter 4), we tested the effects of high phosphate diet on HPG axis function in two strains of WT female mice, 129S1/SvImJ (129) and C57BL/6 (B6). Both strains were weaned onto control chow (0.7% P_i) or high phosphate chow (2% P_i) and maintained under these conditions for 10 weeks, at which point they were sacrificed for tissue collection.

129S1/SvImJ

Outwardly, WT 129 mice fed high P_i diet appeared normal, with a small decrease in body weight; however, they were indeed hyperphosphatemic (Figure 2-6, A-B). These mice appeared to initiate puberty appropriately, with vaginal canalization comparable to their littermates fed normal phosphate chow (data not shown). However, only leukocytes were present in vaginal smears, indicating that these mice never underwent estrus cycling (data not shown). Histological examination of ovary sections of normal chow-fed mice revealed the presence of corpora lutea (white arrowheads); however, none were observed in high P_i-fed 129 females, indicating that these mice were not ovulating (Figure 2-6E). Like $KL^{-/-}$ mice, high P_i-fed 129 animals had hypotrophic uteri and a low uterus to body weight ratio (Figure 2-6, C-D). Taken together, these results indicate, that

although puberty may have been initiated in these mice, it did not proceed properly to completion.

We next examined HPG axis gene expression in WT 129 females fed high P_i versus normal chow. Hypothalamic gene expression patterns of high P_i-fed 129 female mice phenocopy those of $KL^{-/-}$ females. Both show a 4-5 fold reduction in Kiss1 expression but no change in GnRH (Figures 2-2, B and D, and 2-7, A-B). At the level of the pituitary, high P_i-fed 129 females exhibit several differences from $KL^{-/-}$ mice. Unlike $KL^{-/-}$ females, high P_i-fed 129 animals do not have altered expression of GnRHR or LH mRNA (Figure 2-8, A-B) and have high rather than low serum LH levels (Figure 2-8D). They also have high FSH mRNA levels (while those of $KL^{-/-}$ mice are normal), but normal serum FSH levels (similar to $KL^{-/-}$) (Figure 2-8, C and E).

Ovaries of high P_i-fed WT 129 mice also show similar gene expression patterns to those of $KL^{-/-}$ mice. Both models of phosphate overload show decreased expression of StAR and P450scc and no change in expression of 17βHSD1 (Figures 2-4C and 2-9B). Unlike $KL^{-/-}$ mice, high P_i-fed 129 females do not show a decrease in expression of P450c17 or P450arom (Figure 2-9B), while they do have decreased expression of LHCGR (Figure 2-9A). Additionally, these mice have normal circulating levels of estradiol (Figure 2-9C). Similarities and differences in HPG axis parameters for all phosphate overload models are summarized in Table 2-1.

C57BL/6

Again, the B6 model of high phosphate feeding-induced phosphate overload phenocopies $KL^{-/-}$ females. B6 females fed high P_i diet exhibit growth retardation, are hyperphosphatemic, have hypotrophic uteri, low uterus/body weight ratio, and do not ovulate as evidenced by a lack of corpora lutea in ovarian sections (Figure 2-10, A-E). Like $KL^{-/-}$ mice but unlike the 129 high P_i diet model, B6 females on high P_i diet do not undergo vaginal canalization (data not shown) and thus do not appear to initiate or carry out puberty properly.

At the level of the hypothalamus, B6 mice on high P_i diet have low expression of Kiss1 mRNA but no change in GnRH just like $KL^{-/-}$ and high P_i-fed 129 females (Figure 2-11, A-B). In the pituitary, high P_i-fed B6 females have normal GnRHR expression, low LH, and high FSH compared to their littermates on normal phosphate chow (Figure 2-12, A-C). B6 females on high P_i diet have an identical ovarian phenotype to high P_i-fed 129 females. High P_i-fed WT B6 females show low expression of LHCGR, StAR and P450scc but normal expression of FSHR, P450c17, P450arom, and 17β-HSD-1 (Figure 2-13, A-B). They also exhibit normal serum estradiol levels like high P_i-fed 129 mice (Figure 2-13C). Reproductive phenotypes of high P_i-fed WT B6 females are summarized and directly compared to those of $KL^{-/-}$ and high P_i-fed WT 129 females in Table 2-1.

DISCUSSION

In this chapter we have demonstrated that two mouse models of phosphate overload, $KL^{-/-}$ females and WT females on high P_i diet, have altered HPG axis function at all levels of the axis and that this results in anovulation. We believe this anovulation to be of hypothalamic origin because mRNA levels of Kiss1 are extremely low in AVPV/rostral hypothalamus of these animals. Since Kiss1 is the most upstream point of the HPG axis that we have investigated, and since it is regarded as a gatekeeper of puberty in mice and humans, we believe its downregulation to be a central contributor to reproductive phenotypes of mouse models of phosphate overload.

Experimental mice experiencing phosphate overload do not appear to undergo proper puberty (or do not complete puberty properly in the case of WT 129 females fed high P_i diet). We believe this is due to a functional hypothalamic defect caused by low Kiss1 expression. Indeed, humans and mice that cannot carry out successful Kisspeptin signaling (due to loss of functional GPR54), do not undergo proper puberty and have hypogonadotropic hypogonadism (de Roux, Genin et al. 2003; Seminara, Messager et al. 2003). Similarly to female mouse models of phosphate overload, mice lacking a functional Kiss1 gene do not undergo estrus cycling, have thread-like uteri, do not produce mature Graafian

follicles (d'Anglemont de Tassigny, Fagg et al. 2007). These mice also have low circulating levels of gonadotropins and estradiol.

Although there are many similarities between $KL^{-/-}$ females and WT female mice on high P_i diet, there are some noted differences (see Table 2-1). It is important to point out that although these models both experience a positive phosphate balance and have elevated serum phosphate levels, they are not identical models in terms of secondary effects on phosphate homeostatic hormones. High phosphate feeding causes compensatory increases in FGF23, PTH, vitamin D, decreased serum calcium, and decreased expression of renal NaPi-IIa (Saito, Maeda et al. 2005; Tani, Sato et al. 2007). $KL^{-/-}$ mice also have elevated FGF23 and vitamin D but have increased serum calcium, decreased PTH and increased sodium-phosphate cotransporter activity (Kuro-o, Matsumura et al. 1997; Yoshida, Fujimori et al. 2002; Segawa, Yamanaka et al. 2007; Nakatani, Ohnishi et al. 2009; Brownstein, Zhang et al. 2010). As discussed in Section 1.5, $KL^{-/-}$ mice experience positive phosphate balance due to decreased renal excretion of phosphate, while WT animals on high P_i chow have increased intestinal absorption of phosphate. These differences in phosphate-regulating hormones and renal phosphate handling may exert differential effects on HPG axis function and reproductive hormone production in mice.

Additionally, differences in genetic background may explain phenotypic differences observed between 129 and B6 females on high phosphate diet (see

Table 2.1). B6 mice had less ability to thrive on high P_i chow than 129 mice under the same experimental conditions. In addition to the phenotypes described in this chapter, B6 females fed high phosphate diet had large visible ectopic calcifications of the aorta, kidneys, and skeletal muscle and several animals did not live the entire 10 week feeding period (data not shown). Therefore we believe that strain differences may greatly affect overall phosphate handling in mice and that experimenters should use caution when comparing results from different genetic backgrounds concerning effects of phosphate balance and homeostasis.

MATERIALS AND METHODS

Animal Diets and Procedures

All animals were maintained on a twelve hour light/dark cycle (lights on from 6 am to 6 pm) with *ad libitum* access to food and water. Breeders were fed a commercially available standard rodent chow (Teklad Global 16% Protein Rodent Diet, Harlan Laboratories, Indianapolis, IN). Experimental animals were weaned between 19-21 days of age and placed on either the standard chow diet or custom diets (Harlan Laboratories, Indianapolis, IN) to control phosphate intake. Mineral composition of each diet is as follows: standard chow (0.35% P_i), normal phosphate diet (0.7% P_i), low phosphate diet (0.02, 0.06, or 0.2% P_i), high

phosphate diet (2% P_i). All animal studies were conducted in accordance with standards of ethical and humane care as described in the National Institutes of Health Guide for the Care and Use of Laboratory Animals and using protocols approved by the Institutional Animal Care and Use Committee at University of Texas Southwestern Medical Center (Committee for the Update of the Guide for the Care and Use of Laboratory Animals 2011).

$KL^{-/-}$ mice and their WT littermates were maintained on a congenic 129S1/SvImJ genetic background and obtained through heterozygous breeding. For high phosphate feeding experiments, WT 129S1/SvImJ mice taken from the Klotho colony were bred to maintain the 129S1/SvImJ WT line. WT C57BL/6 breeders were purchased from the Mouse Breeding Core Facility at University of Texas Southwestern Medical Center, and their progeny were used for high phosphate feeding experiments.

For experiments using tissue RNA, animals were anesthetized with Avertin (200 μL/10 g body weight) and sacrificed by cervical dislocation. Tissues were snap frozen in liquid nitrogen and stored at -80^{o}C until RNA isolation. For H&E staining, animals were sacrificed using the same method as described above, and tissues were fixed in 10% neutral buffered formalin (NBF). For immunohistochemistry and *in situ* hybridization, animals were anesthetized as described above and subsequently fixed by intracardiac perfusion with an RNase free saline solution (150 mM NaCl) until the liver was blanched followed by

fixation with RNase-free 10% NBF until the liver was firm. Brains were post-fixed in RNase-free 10% NBF overnight and placed in 20% sucrose (dissolved in diethyl pyrocarbonate (DEPC)-treated water) the following morning for 24 hours. The next day, 30 μm coronal sections were cut into 5 series on a freezing microtome. Sections were stored at -20^{o}C in a cryoprotectant solution (50% DEPC-PBS, 30% ethylene glycol and 20% glycerol) until further use.

Estrus Cycle Analysis

Estrus cycle stage was determined by vaginal cytology (Caligioni 2009). Vaginal smears were collected by flushing the vagina 3 times with 30 μL of PBS. The final flush was collected and allowed to dry on a glass slide. Slides were stained with Giemsa for 5 minutes and then rinsed with tap water. Estrus cycle stages were defined as follows: diestrus- predominantly leukocytes; proestrus- predominantly nucleated epithelial cells; estrus- predominantly cornified, non-nucleated epithelial cells; metestrus- a mixture of cell types including leukocytes, nucleated epithelial cells, and cornified cells. Experimental animals that could be staged (those with a vaginal opening) were all sacrificed in diestrus.

***In situ* Hybridization**

Animals were perfused and brain sections were prepared as described in Animal Diets and Procedures (Section 2.4.1). Prior to the following *in situ* hybridization procedure, brain sections were sorted in DEPC-PBS and mounted onto Superfrost Plus slides (Fisher Scientific, Hampton, NH).

Pretreatment

Slides were pretreated under RNase-free conditions. First, slides were fixed in 4% paraformaldehyde for 20 minutes and then dehydrated in an ethanol series. Next, slides were incubated in xylene for 15 minutes, followed by rehydration. Slides were subsequently incubated in boiling sodium citrate buffer (0.01 M, pH 6) for 10 minutes, followed by dehydration in an ethanol series. Slides were thoroughly dried and stored with desiccators at -20^{o}C until further use.

In vitro Transcription and Hybridization of Probes

Probe sequences used for Kiss1 have been previously validated and published (Donato, Silva et al. 2009). ^{35}S-labeled riboprobes were synthesized using an *in vitro* transcription kit (Ambion, Austin, TX). 200-300 ng of template cDNA were reverse transcribed in each reaction, using ^{35}S-UTP for radioactive incorporation. After synthesis, probes were incubated with RNase inhibitor (SUPERase-In) and DNase for 10 min at 37^{o}C to break up the remaining cDNA

template. The probes were purified from unincorporated ^{35}S-UTP by passing them through illustra ProbeQuant columns (GE Healthcare Life Sciences, Piscataway, NJ).

^{35}S-labeled riboprobes were diluted to 10^6 cpm/mL in hybridization buffer and 120 μL of this mixture was added to each slide. Slides were coverslipped with HybriSlips (Sigma-Aldrich, St. Louis, MO). Slides were allowed to incubate in a humidified oven at 57^{o}C overnight.

Post-hybridization

Hybridization coverslips were removed and slides were incubated with 0.002% RNAse A (Roche Applied Science, Penzberg, Germany) for 30 minutes at RT. Next, slides and tissues were subjected to a series of high stringency washes, followed by tissue dehydration in 70% ethanol for 10 minutes. Slides were allowed to air dry and then placed in an autoradiography cassette. *In situ* hybridization signals were detected using autoradiography film.

Quantitative Real-time PCR

Total RNA was isolated with Trizol (Invitrogen, Carlsbad, CA) following a modified version of the manufacturer's protocol. Hypothalamic and pituitary tissues were homogenized in 800 μL of Trizol by passing the tissue through a 23

gauge needle 8 times. Ovaries were homogenized first with a pellet pestle (Kimble Kontes, Sigma-Aldrich, St. Louis, MO) and then by passing through a needle. 160 μL of chloroform was added to each Trizol/tissue solution, and each sample was centrifuged for 15 minutes at 12,000 rpm at 4^{o}C. The aqueous phase was transferred to a new tube, and total RNA was precipitated by adding an equal volume (~400 μL) 70% ethanol. The RNA solution was then immediately applied to an RNeasy mini-column (Qiagen, Germantown, MD) for further purification according to a modified version of the manufacturer's protocol. Briefly, once bound to the column, the RNA was washed 3 times and eluted with 40 μL RNase-free water. Total purified RNA concentration was measured on a NanoDrop (Thermo Scientific, Waltham, MA).

To remove any contaminating DNA, 0.5 μg of total RNA was treated with 0.1 U/μL of RQ1 RNase-free DNase (Promega, Madison, WI) in a 20 μL reaction. The DNase-treated RNA was reverse transcribed into first-strand cDNA with SuperScript III Reverse Transcriptase (Invitrogen, Carlsbad, CA). Each qPCR reaction contained 6.25 ng of cDNA and was performed in triplicate using SYBR Green (Invitrogen, Carlsbad, CA) as a fluorophore. Primers used for qPCR analysis are listed in Table 2-2. Primers were validated using methods described by Bookout et al., and qPCR data was analyzed following the comparative cycle threshold method (Bookout, Cummins et al. 2006).

Histology

GnRH Immunohistochemistry

Animals were perfused and brains were prepared and sectioned as described in Animal Diets and Procedures (Section 2.4.1). A standard immunoperoxidase staining protocol was employed, with the following steps performed on an orbital shaker. Free-floating brain sections were rinsed 3x in 0.1M phosphate buffered saline (PBS) (10' each), blocked with 0.3% hydrogen peroxide (H_2O_2) (30'), and rinsed again 3x in 0.1M PBS (10' each). Sections were then blocked for 1 hour in 1M PBS/0.25% Triton X-100 (PBT) containing 3% normal donkey serum. Brain sections were incubated with primary antibody (rabbit-anti-GnRH (ImmunoStar, Hudson, WI), 1:5000 in PBT) for one hour at room temperature (RT), followed by washing 3x in PBT (10' each). Sections were incubated in secondary antibody (biotinylated donkey-anti-rabbit, 1:1000 in PBT) for 1 hour at RT, followed by washing 4x in PBT (10' each). Sections were then allowed to react with streptavidin-conjugated 3,3'-diaminobenzidine (DAB) and H_2O_2 until sufficient color development was observed.

Hematoxylin and Eosin Staining

Tissues were prepared as described in Animal Diets and Procedures (Section 2.2.1), and fixed for an additional period of one week-one month in 10%

NBF before histological preparation. Tissues were submitted to the Richardson Molecular Pathology Core at University of Texas Southwestern Medical center, where they were embedded in paraffin blocks, sectioned, and stained with H&E according to standard protocols.

Serum Chemistry and Hormone Measurements

While fully anesthetized, blood was collected by retro-orbital bleeding. Blood was allowed to clot at room temperature for 1-1.5 hours and then centrifuged at 5000 revolutions per minute (RPM) for 10 minutes at 4^{o}C. Serum supernatant was transferred to a new tube and snap frozen in liquid nitrogen, followed by long-term storage at -80^{o}C.

Serum phosphate was measured at the Mouse Metabolic Phenotyping Core at UT Southwestern Medical Center on a Vitros 250 Chemistry System. Serum LH and FSH were measured at the University of Virginia Center for Research in Reproduction Ligand Assay and Analysis Core. LH was measured using a sandwich immunoradiometric assay (IRMA), and FSH was measured by radioimmunoassay (RIA). Estradiol was measured by enzyme-linked immunosorbent assay (ELISA) (Calbiotech, Spring Valley, CA).

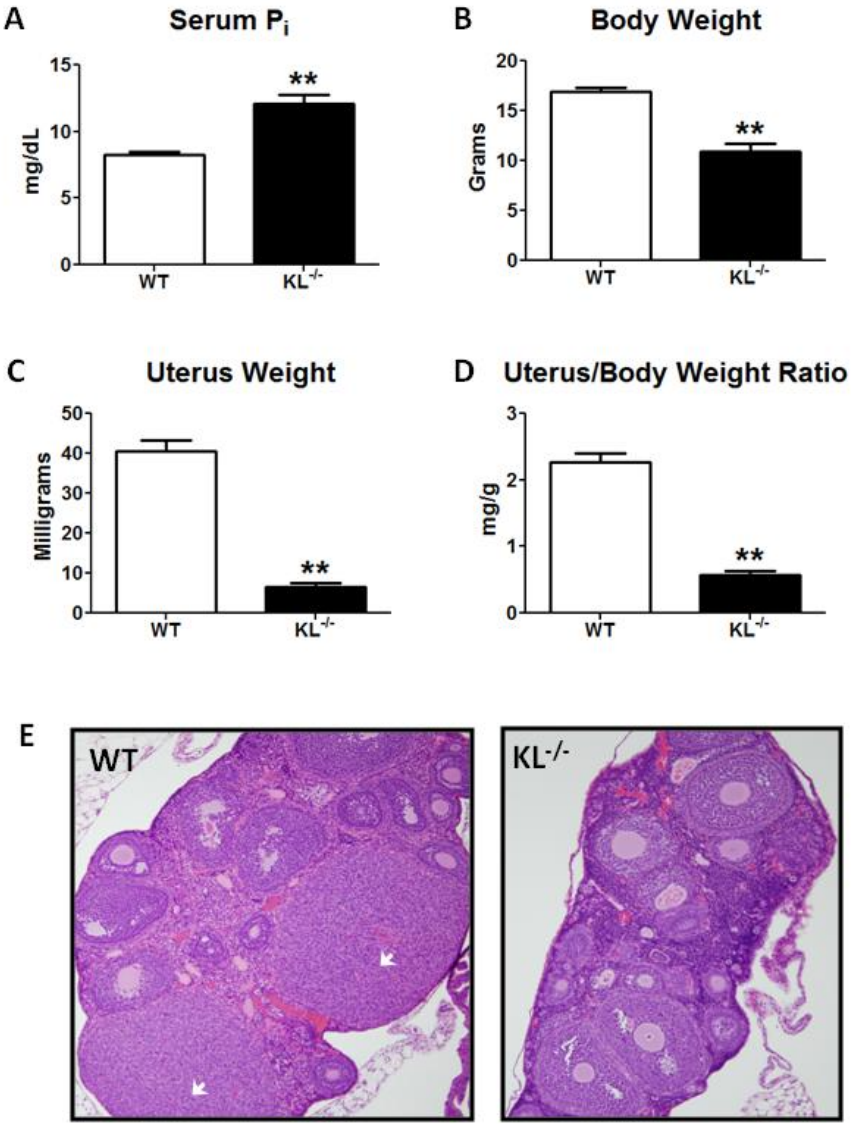

Figure 2-1. $KL^{-/-}$ females have hypotrophic uteri and do not ovulate. $KL^{-/-}$ females and their WT littermates were sacrificed at 8 weeks of age for the following measurements. (A) Serum phosphate levels. (B) Body weight. (C) Uterus weight (wet). (D) Uterus to body weight ratio. Double asterisk indicates $p<0.005$ (Student's t-test). (E) Histological sections of WT and $KL^{-/-}$ ovary stained with H&E. White arrowheads indicate corpora lutea.

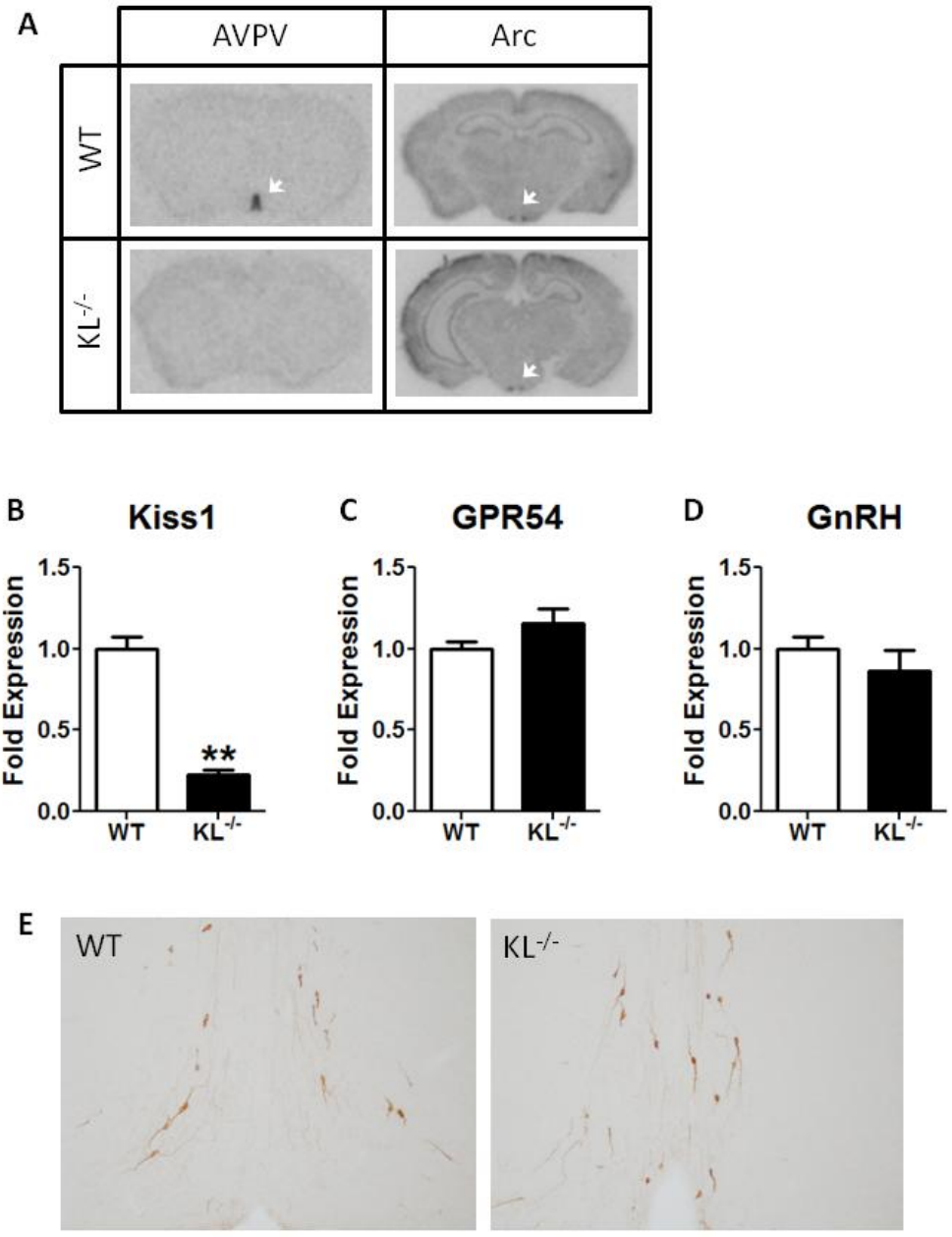

Figure 2-2. KL$^{-/-}$ females have low expression of Kiss1 in the AVPV. (A) Kiss1 *in situ* hybridization in brains from 60 day old WT and KL$^{-/-}$ females in diestrus. White arrowheads denote Kiss1 expression in AVPV and Arc nuclei. (B-D) qPCR of whole hypothalamus from 8 week old WT and KL$^{-/-}$ females. Double asterisk indicates $p<0.005$ (Student's t-test). (E) GnRH immunohistochemistry using the same brain samples as in (A).

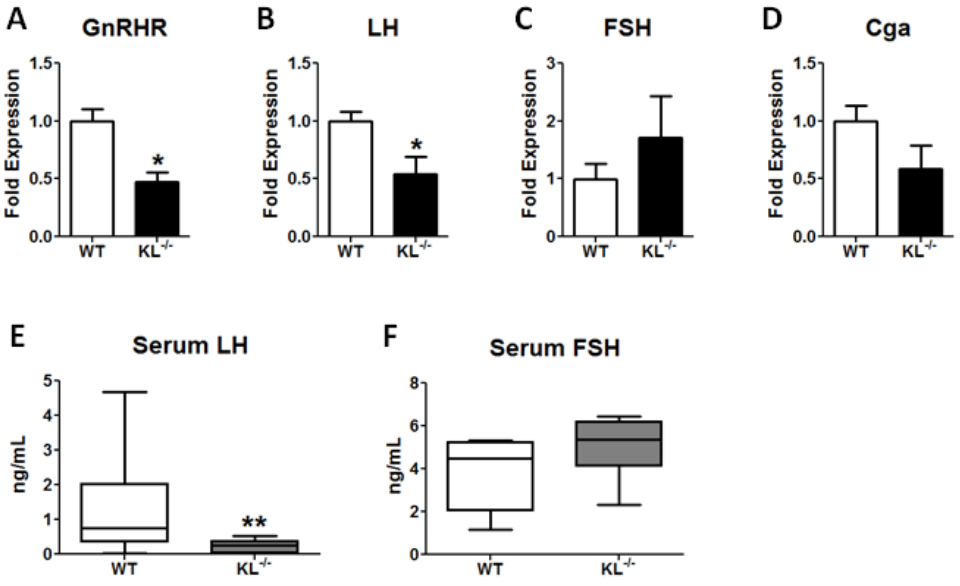

Figure 2-3. $KL^{-/-}$ females have low GnRHR and LH levels. $KL^{-/-}$ females and their WT female littermates were sacrificed at 8 weeks of age. (A-D) Pituitary gene expression was measured by qPCR. Single asterisk indicates $p<0.05$ (Student's t-test). (E-F) Serum hormone levels were measured, and their range is graphed in a box-and-whisker plot. Double asterisk indicates a significant difference in variance with $p<0.005$ (F-test for variance).

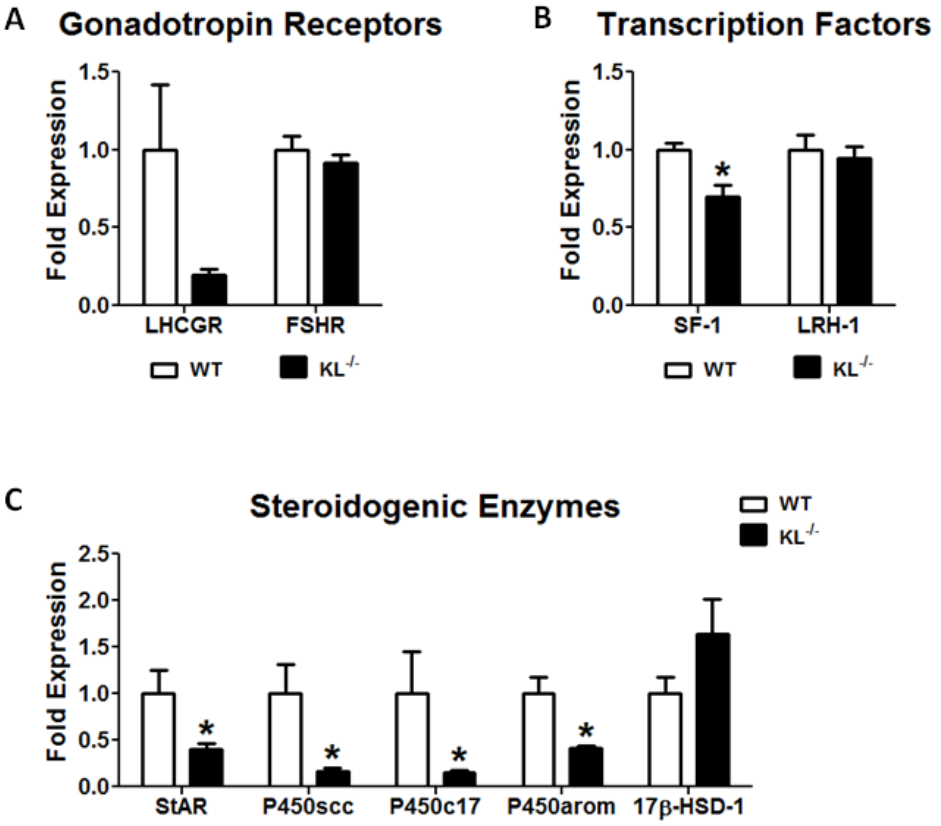

Figure 2-4. $KL^{-/-}$ females show altered expression of steroidogenic enzyme mRNAs in the ovaries. $KL^{-/-}$ females and their WT female littermates were sacrificed at 8 weeks of age. Ovarian gene expression was measured by qPCR. Single asterisk indicates $p<0.05$ (Student's t-test). (A) mRNA expression of gonadotropin receptors LHCGR and FSHR. (B) mRNA expression of ovarian transcription factors SF-1 and LRH-1. (C) mRNA expression of ovarian steroidogenic enzymes StAR, P450scc, P450c17, P450arom, and 17β-HSD-1.

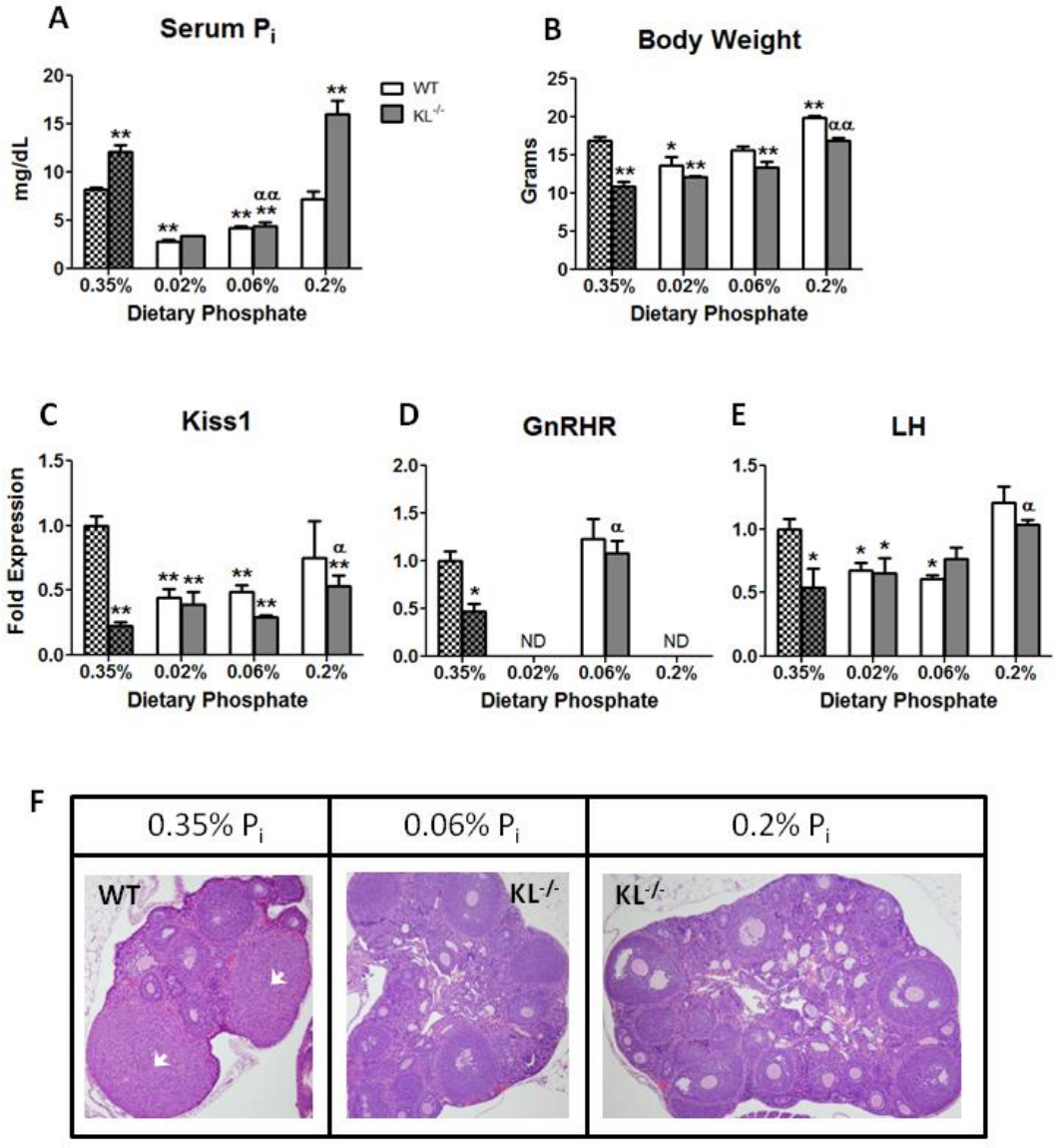
A
Serum P_i
mg/dL
WT
KL-/-
0.35%
0.02%
0.06%
0.2%
Dietary Phosphate
B
Body Weight
Grams
C
Kiss1
Fold Expression
D
GnRHR
ND
E
LH
F
0.35% P_i
0.06% P_i
0.2% P_i
WT
KL-/-

Figure 2-5. Low phosphate diet partially rescues $KL^{-/-}$ female reproductive phenotypes. $KL^{-/-}$ females and their WT littermates were weaned onto normal chow (0.35% P_i) or low P_i diet (0.02%, 0.06%, or 0.2%). Animals were sacrificed at 8 weeks of age (after 5 weeks on each diet). (A-E) White bars indicate WT and grey bars indicate $KL^{-/-}$. Hatched bars indicate WT and $KL^{-/-}$ animals on normal chow. (A) Serum phosphate. Statistics could not be calculated for $KL^{-/-}$ (0.02% P_i) group because only one serum sample was available. (B) Body weight. (C) qPCR measurement of Kiss1 mRNA expression in whole hypothalamus. (D) qPCR measurement of GnRHR mRNA expression in the pituitary gland. (E) qPCR measurement of LH mRNA expression in the pituitary gland. Single asterisk indicates a significant difference from WT (0.35% P_i) with $p<0.05$ (Student's t-test). Double asterisk indicates a significant difference from WT (0.35% P_i) with $p<0.005$ (Student's t-test). Alpha indicates a significant difference from $KL^{-/-}$ (0.35% P_i) with $p<0.05$ (Student's t-test). Double alpha indicates a significant difference from $KL^{-/-}$ (0.35% P_i) with $p<0.005$ (Student's t-test). "ND" indicates no data for these groups. (F) Histological sections of WT and $KL^{-/-}$ ovaries under different dietary phosphate conditions stained with H&E. White arrowheads indicate corpora lutea.

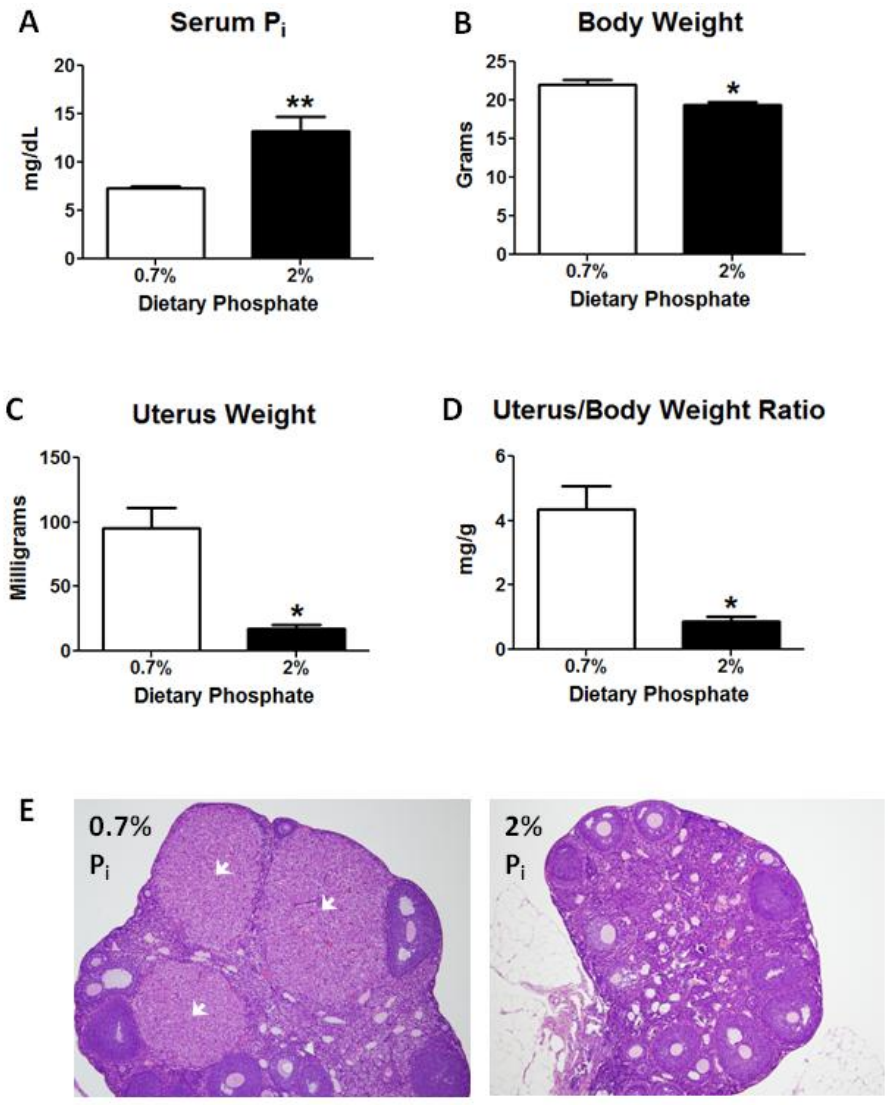

Figure 2-6. WT 129 females on high phosphate diet phenocopy KL$^{-/-}$ females. WT 129 females were weaned onto normal P_i (0.7%) or high P_i (2%) chow at 3 weeks of age. Animals were sacrificed at 13 weeks of age after 10 weeks of high phosphate feeding. (A) Serum phosphate. Double asterisk indicates $p<0.005$ (Student's t-test). (B) Body weight. Single asterisk indicates $p<0.05$ (Student's t-test). (C) Uterus weight (wet). (D) Uterus to body weight ratio. (E) Histological sections of the ovary stained with H&E. White arrowheads indicate corpora lutea.

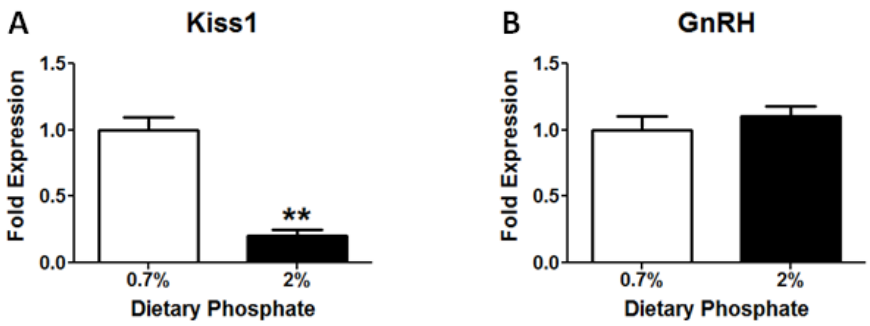

Figure 2-7. WT 129 females on high phosphate chow have low expression of Kiss1 mRNA in the hypothalamus. WT 129 females were weaned onto normal P_i (0.7%) or high P_i (2%) chow at 3 weeks of age. Animals were sacrificed at 13 weeks of age after 10 weeks of high phosphate feeding. Hypothalami were dissected into rostral and caudal blocks, and gene expression in the rostral block was measured by qPCR. (A) mRNA expression of Kiss1. Double asterisk indicates $p<0.005$ (Student's t-test). (B) mRNA expression of GnRH.

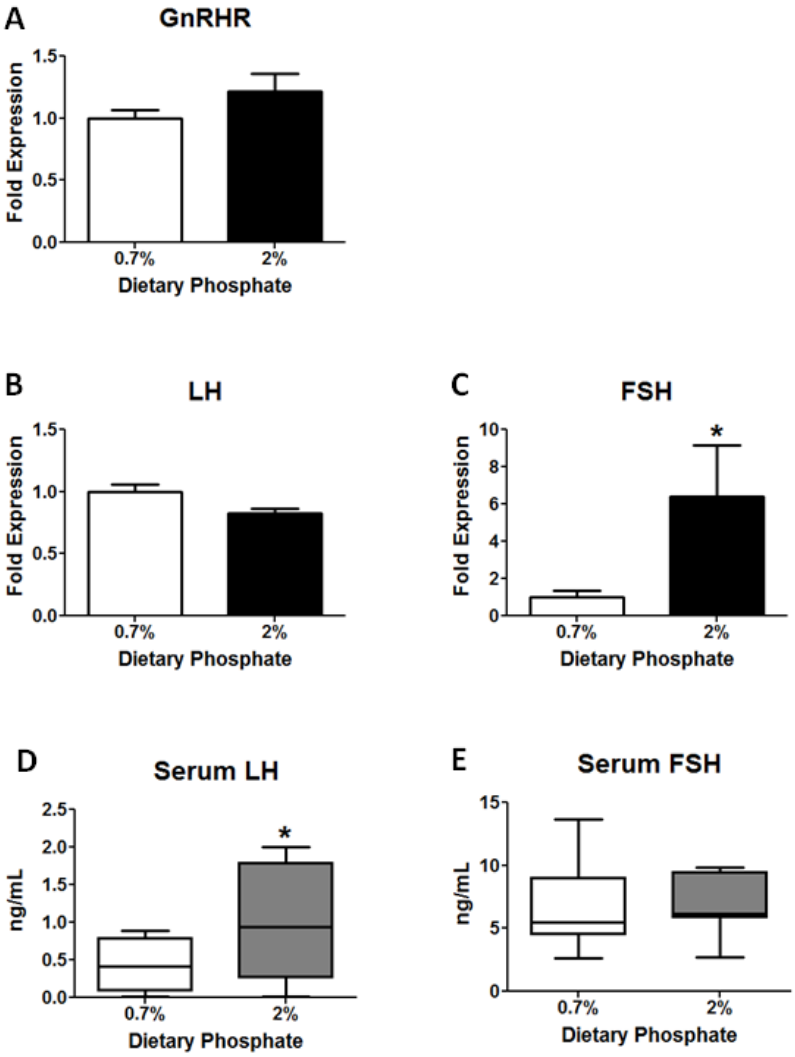

Figure 2-8. WT 129 females on high phosphate diet have aberrant pituitary hormone levels. WT 129 females were weaned onto normal P_i (0.7%) or high P_i (2%) chow at 3 weeks of age. Animals were sacrificed at 13 weeks of age after 10 weeks of high phosphate feeding. (A-C) Pituitary gene expression of GnRHR (A), LH (B), and FSH (C) was measured by qPCR. Single asterisk indicates $p<0.05$ (Student's t-test). (D-E) Serum hormone levels of LH (D) and FSH (E) were measured, and their ranges are graphed in box-and-whisker plots. Single asterisk indicates a significant difference in variance with $p<0.05$ (F-test for variance).

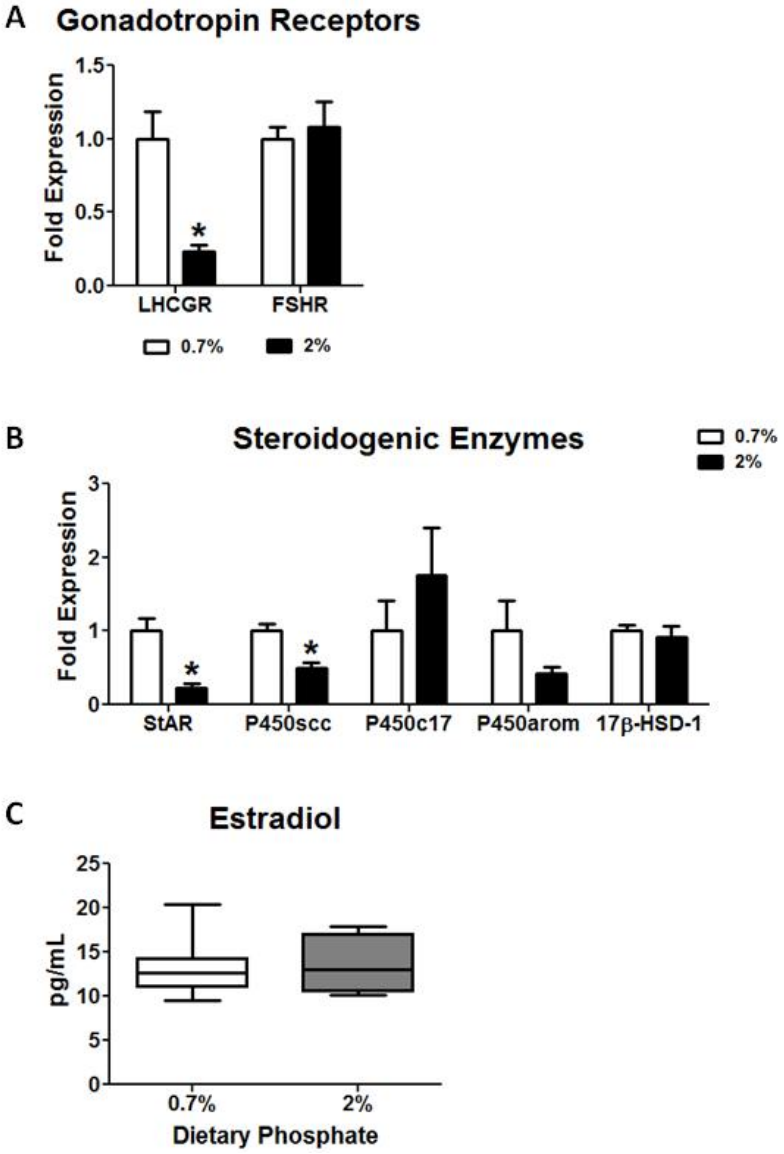

Figure 2-9. WT 129 females on high P_i chow have low expression of LHCGR, StAR, and P450scc in the ovaries. WT 129 females were weaned onto normal P_i (0.7%) or high P_i (2%) chow at 3 weeks of age. Animals were sacrificed at 13 weeks of age after 10 weeks of high phosphate feeding. (A-B) mRNA levels of gonadotropin receptors (A) and steroidogenic enzymes (B) in the ovaries were measured by qPCR. Single asterisks indicate $p<0.05$ (Student's t-test). (C) Serum estradiol levels were measured, and their ranges are graphed in a box-and-whisker plot.

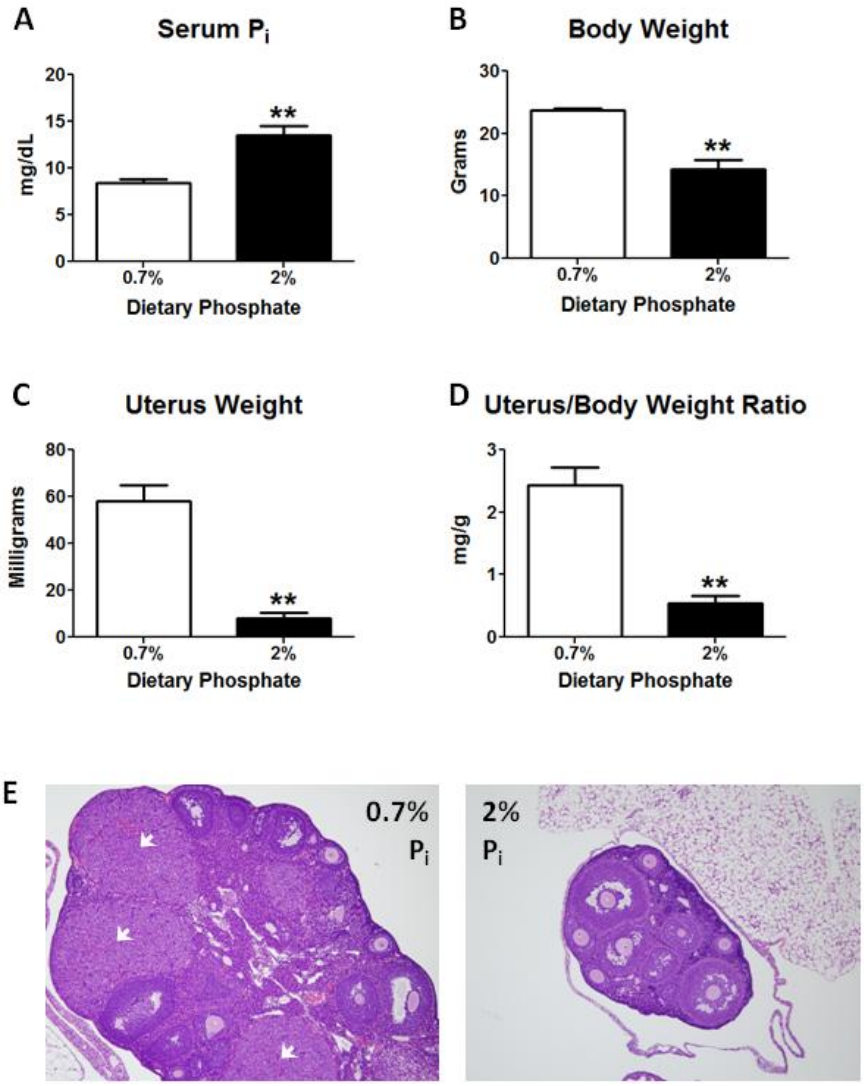

Figure 2-10. WT B6 females on high phosphate diet also phenocopy $KL^{-/-}$ females. WT B6 females were weaned onto normal P_i (0.7%) or high P_i (2%) chow at 3 weeks of age. Animals were sacrificed at 13 weeks of age after 10 weeks of high phosphate feeding. (A) Serum phosphate. Double asterisk indicates $p<0.005$ (Student's t-test). (B) Body weight. (C) Uterus weight (wet). (D) Uterus to body weight ratio. (E) Histological sections of the ovary stained with H&E. White arrowheads indicate corpora lutea.

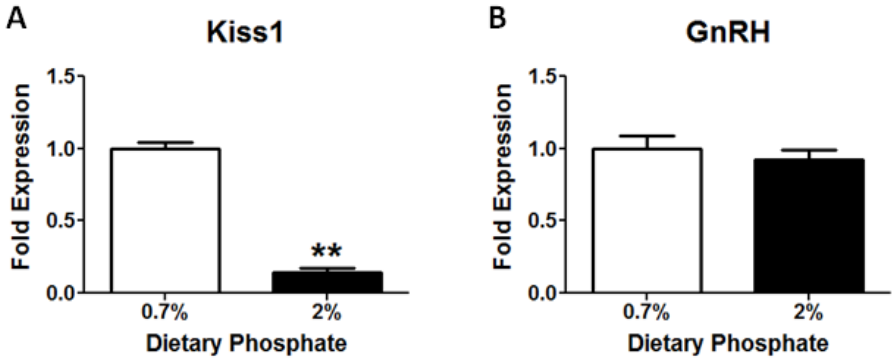

Figure 2-11. WT B6 females on high phosphate diet have low expression of Kiss1 mRNA in the hypothalamus. WT B6 females were weaned onto normal P_i (0.7%) or high P_i (2%) chow at 3 weeks of age. Animals were sacrificed at 13 weeks of age after 10 weeks of high phosphate feeding. Hypothalami were dissected into rostral and caudal blocks, and gene expression in the rostral block was measured by qPCR. (A) mRNA expression of Kiss1. Double asterisk indicates $p<0.005$ (Student's t-test). (B) mRNA expression of GnRH.

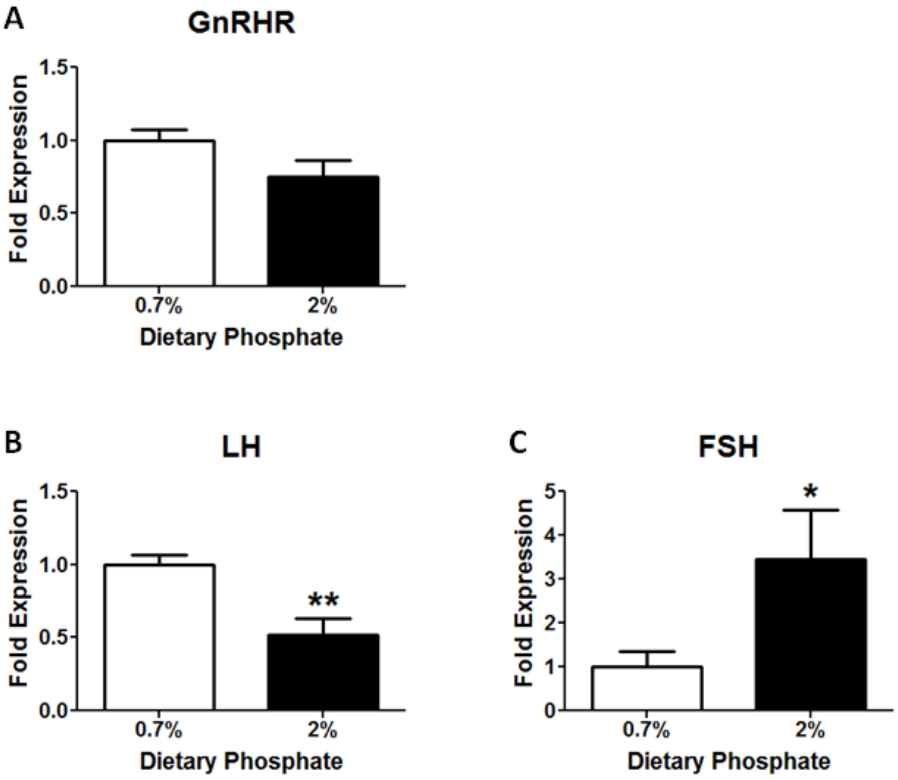

Figure 2-12. WT B6 females on high P_i diet have aberrant pituitary hormone gene expression. WT B6 females were weaned onto normal P_i (0.7%) or high P_i (2%) chow at 3 weeks of age. Animals were sacrificed at 13 weeks of age after 10 weeks of high phosphate feeding. (A-C) Pituitary gene expression of GnRHR (A), LH (B), and FSH (C) was measured by qPCR. Double asterisk indicates $p<0.005$ (Student's t-test). Single asterisk indicates $p<0.05$ (Student's t-test).

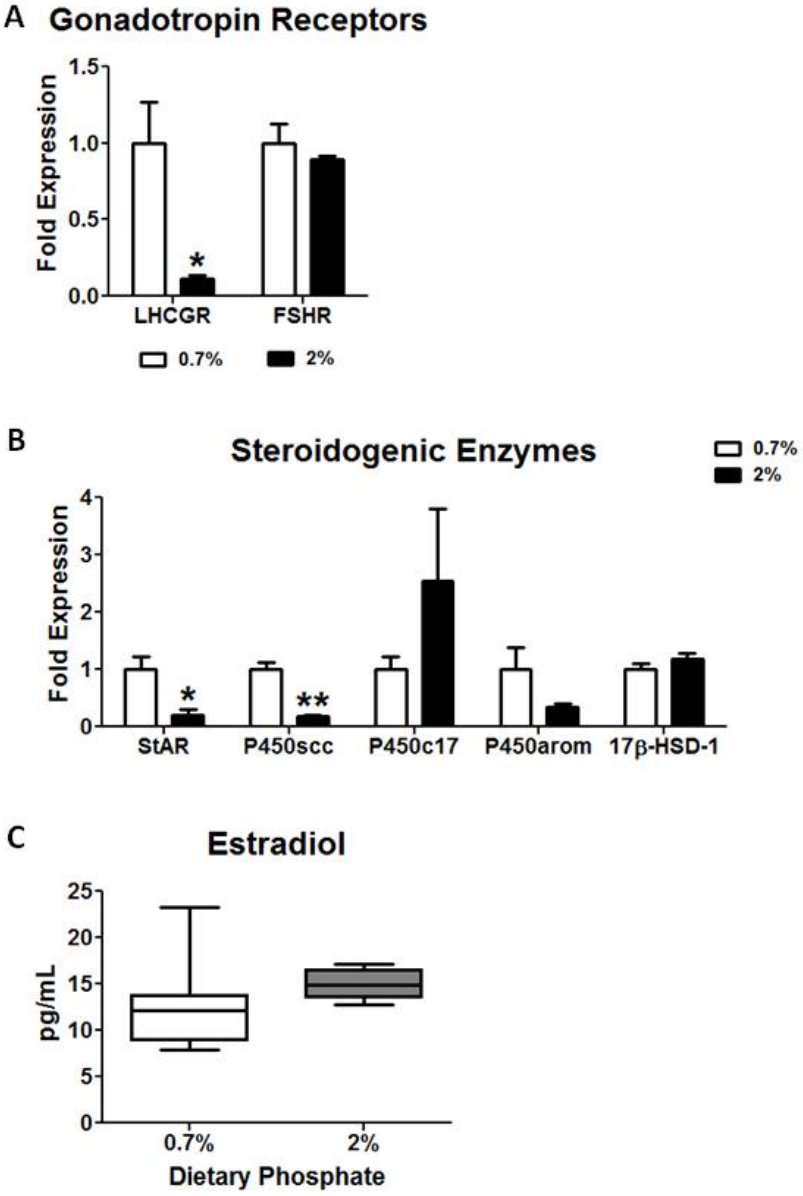

Figure 2-13. WT B6 females on high P_i chow have low expression of LHCGR, StAR, and P450scc in the ovaries. WT B6 females were weaned onto normal P_i (0.7%) or high P_i (2%) chow at 3 weeks of age. Animals were sacrificed at 13 weeks of age after 10 weeks of high phosphate feeding. (A-B) mRNA levels of gonadotropin receptors (A) and steroidogenic enzymes (B) in the ovaries were measured by qPCR. Single asterisks indicate $p<0.05$ (Student's t-test). Double asterisk indicates $p<0.005$ (Student's t-test). (C) Serum estradiol was measured by ELISA.

Table 2-1. Phenotypic summary of female mouse models of phosphate overload.

	KL$^{-/-}$	**129 (High P_i Diet)**	**B6 (High P_i Diet)**
Serum P_i	↑	↑	↑
Body Weight (BW)	↓	↓	↓
Uterus Weight	↓	↓	↓
Uterus/BW Ratio	↓	↓	↓
Vaginal Canalization	None	Present	None
Corpora Lutea in Ovary	None	None	None
Kiss1	↓	↓	↓
GnRHR	↓	↔	↔
LH	↓	↔	↓
FSH	↔	↑	↑
Serum LH	↓	↑	ND
Serum FSH	↔	↔	ND
LHCGR	↔	↓	↓
SF-1	↓	ND	ND
LRH-1	↔	ND	ND
StAR	↓	↓	↓
P450scc	↓	↓	↓
P450c17	↓	↔	↔
P450arom	↓	↔	↔
Serum Estradiol	ND	↔	↔

↓: Decreased versus control.
↑: Increased versus control.
↔: No change versus control.
ND: Not measured.
Highlighted: Similar phenotypes among all three groups.

Table 2-2. Mouse primer sets used for qPCR.

Gene	Forward Primer (5'-3')	Reverse Primer (5'-3')
CyclophilinA	GGCCGATGACGAGCCC	TGTCTTTGGAACTTTGTCTGCAA
Kiss1	TGCTGCTTCTCCTCTGTGTC	CTCTCTGCATACCGCGATTC
GPR54	GTTATCTGCCGCCACAAGC	CCGAGACCTGCTGGATGTAG
GnRH	ACTGTGTGTTTGGAAGGCTGC	TTCCAGAGCTCCTCGCAGATC
GnRHR	TTCATCAAGACCCACGCAAA	GAGGTAGCGAATGCGACTGTC
LH	TGTCAACGCAACTCTGGCC	GGCAGTACTCGGACCATGCT
FSH	GACTGCACAGGACGTAGCTGTTTA	CTGAGATGGTGATGTTGGTCAATT
Cga	GACTTTATTATTCAGGGTTGCCCA	AGAAGCAACAGCCCATACACTG
LHCGR	GAAAGCACAGTTAGAGAAACAAAT	TAATCCCAGCCACTGAGTTCA
FSHR	TTCAACGGAACCCAGCTAGA	GAAAACATCATCAGGCAATTCTTC
SF-1	CCCTTATCCGGCTGAGAATT	CCAGGTCCTCGTCGTACGA
LRH-1	TGGGAAGGAAGGGACAATCTT	CGAGACTCAGGAGGTTGTTGAA
StAR	CGGAGCAGAGTGGTGTCATC	TGAGTTTAGTCTTGGAGGGACTTC
P450scc	TGAATGACCTGGTGCTTCGT	GGCAAAGCTAGCCACCTGTA
P450c17	GGCTTTCCTGGTGCACAAT	ACATACTGGTCAATCTCCTTTTGG
P450arom	CCGAGCCTTTGGAGAACAA	AGGGCCCGTCAGAGCTT
17β-HSD-1	ACTGTGCCAGCAAGTTTGCG	AAGCGGTTCGTGGAGAAGTAG

CHAPTER THREE
Exploring the Mechanism of Phosphate Overload-Induced Female Infertility

INTRODUCTION AND RATIONALE

In this chapter, we will explore the mechanisms underlying the HPG axis dysfunction that we have observed in two female mouse models of phosphate overload. As described in Chapter 2, these mice have aberrant HPG axis function at all levels of the axis, typified by decreased expression of Kiss1 in the hypothalamus, aberrant LH in the pituitary, and decreased expression of steroidogenic genes in the ovaries resulting in anovulation (see Table 2.1 for summary). Therefore, in this chapter, we will examine each of these nodes along the HPG axis in greater detail in order to pinpoint the source of dysfunction in this axis in female mice undergoing phosphate overload.

To test the functionality of the hypothalamus and specifically the ability of the hypothalamus to express and regulate Kiss1, we have employed an estradiol replacement procedure. It has been well documented that Kiss1 expression is subject to feedback control from gonadal steroids, and specifically estradiol stimulates Kiss1 expression in the AVPV while inhibiting Kiss1 expression in the Arc (see Oakley, Clifton et al. 2009 for review). We created a procedure based on several published protocols to test the ability of estradiol to exert positive and

negative regulation of Kiss1 expression in female mice undergoing phosphate overload (Yoshizawa, Handa et al. 1997; Kinuta, Tanaka et al. 2000; Frasor, Barnett et al. 2003; Navarro, Castellano et al. 2004). This procedure is usually performed in ovariectomized mice to reduce interference from endogenous estradiol production. However, since female mouse models of phosphate overload experience blunted ovary function and do not undergo estrus cycling, we felt that ovariectomy was unnecessary for our purpose.

To test the functionality of the pituitary gland in female mice undergoing phosphate overload, we tested the ability of acute Kisspeptin administration to elicit an LH surge in these animals. Kisspeptin's ability to potently stimulate LH secretion has been very well documented in rodents (Roa, Castellano et al. 2009). Based on references detailed in this review and based on several other published findings, we established a protocol for acute Kisspeptin-10 administration in female mouse models of phosphate overload (Castellano, Navarro et al. 2005; Navarro, Castellano et al. 2005; Thompson, Murphy et al. 2006; d'Anglemont de Tassigny, Fagg et al. 2008; Roa, Castellano et al. 2009).

Toyama et al. have already examined the functionality and responsiveness of $KL^{-/-}$ mouse ovaries (Toyama, Fujimori et al. 2006). They have shown that $KL^{-/-}$ ovaries are capable of full function in the proper environment since transfer of $KL^{-/-}$ ovaries to WT animals and subsequent mating allowed recipient animals to become pregnant and give birth to pups. Additionally, even in $KL^{-/-}$ mice,

ovaries are capable of responding to proper hormonal cues because gonadotropin administration in these animals resulted in successful (although reduced compared to WT) ovulation of eggs. We have similarly tested the responsiveness of ovaries of mice undergoing dietary phosphate overload to gonadotropin administration and have measured ovulation events in these mice. This novel data will be presented herein.

In this chapter, we will also investigate alternate causes of reduced HPG axis function and reduced Kiss1 expression such as hyperprolactinemia, elevated stress hormones, low leptin levels, and direct toxicity of phosphate to Kiss1 neurons (Kronenberg, Melmed et al. 2008). Indeed these factors have been/may be implicated in reproductive dysfunction associated with CKD as well (Handelsman 1985; Holley 2004).

Hyperprolactinemia is known to cause sexual dysfunction and is very common in men and women and is very common in CKD (Handelsman 1985; Kronenberg, Melmed et al. 2008). In CKD, high serum levels of prolactin may occur due to increased pituitary production or decreased renal clearance (Holley 2004; Anantharaman and Schmidt 2007). Additionally elevation of stress hormones and hypothyroidism, which are also comorbid with CKD, are known to cause hyperprolactinemia (Handelsman 1985; Kronenberg, Melmed et al. 2008). High levels of prolactin have been shown to inhibit gonadotropin pulsatility through inhibiting GnRH pulsatility (Sauder, Frager et al. 1984; Cohen-Becker,

Selmanoff et al. 1986; Milenkovic, D'Angelo et al. 1994). Additionally, prolactin may directly regulate Kiss1 neurons (Crampton 2011). In this chapter, we will investigate whether hyperprolactinemia contributes to reproductive phenotypes in female mouse models of phosphate overload.

Chronic activation of the hypothalamic-pituitary-adrenal (HPA) axis and elevated levels of stress hormones can inhibit reproductive axes. This condition is associated with increased levels of corticotropin releasing hormone (CRH), adrenocorticotropic hormone (ACTH), cortisol, prolactin and other factors (Kronenberg, Melmed et al. 2008). It has been demonstrated that elevated CRH can inhibit GnRH pulsatility (Rivier and Vale 1984; Gambacciani, Yen et al. 1986; Xiao, Luckhaus et al. 1989), and that ACTH can inhibit pituitary responsiveness to GnRH (Matteri, Moberg et al. 1986; Kamel and Kubajak 1987). Furthermore, CRH and corticosterone have been shown to decrease Kiss1 expression in female rats (Kinsey-Jones, Li et al. 2009). Therefore, we will investigate the contribution of elevated stress hormones to reproductive phenotypes in female mouse models of phosphate overload.

Leptin is a hormone secreted from white adipose tissue that signals to the body that it has sufficient energy stores (Kronenberg, Melmed et al. 2008). Leptin deficiency is associated with hypogonadotropic hypogonadism, and it has been well established that leptin is required for puberty onset, although the precise role of leptin in puberty initiation remains unknown (Gueorguiev, Goth et al.

2001). It has been hypothesized that leptin functions to modulate puberty by acting on Kiss1 neurons, although this idea has recently been challenged (Donato, Cravo et al. 2011; Elias 2012). Leptin levels are actually high in patients with CKD, and this is thought to play a role in uremic anorexia in these patients although it is not known how leptin may contribute to this pathophysiology (Heimburger, Lonnqvist et al. 1997; Stenvinkel, Lindholm et al. 2000; Yamamoto, Carrero et al. 2009). We will present our findings on leptin levels in $KL^{-/-}$ mice in this chapter.

Lastly, in this chapter we will investigate whether high phosphate can cause acute changes directly in Kiss1 neurons. It has long been known that addition of phosphate to cell culture media induces intracellular signaling cascades such as ERK1/2 phosphorylation and induction of c-Fos and osteopontin (Khoshniat, Bourgine et al. 2011; Sage, Lu et al. 2011). More recently, it has been appreciated that phosphate mediates these effects in the form of calcium-phosphate nanoparticles (Ewence, Bootman et al. 2008). In a recent publication, calcium-phosphate nanoparticles were shown to be directly toxic to human granulosa cells (Liu, Qin et al. 2010). Since we believe Kiss1 to be a key target for mediating reproductive phenotypes in mice undergoing phosphate overload, we will investigate direct effects of high phosphate media on Kiss1 neurons using a single-cell electrophysiological recording technique.

RESULTS

Investigating HPG Axis Functionality

Estradiol administration shows proper feedback control of Kiss1 expression under conditions of phosphate overload.

In order to investigate hypothalamic functionality in female mice undergoing phosphate overload, we specifically examined responsiveness of Kiss1-expressing brain areas to chronic peripheral estradiol administration. After undergoing 10 weeks of high P_i (2%) feeding, WT 129 and B6 animals were given an estradiol replacement protocol, consisting of daily administration of vehicle or estradiol at 10 am for 4 days. As a positive control for estradiol action, we measured uterine weight gain and pituitary prolactin (PRL) gene expression.

Both 129 and B6 mice on high P_i diet responded to estradiol administration by inducing uterine growth (Figure 3-1, A and E), indicating to us that our estradiol dosing and administration protocol worked well. 129 animals also upregulated PRL mRNA in the pituitary in response to estradiol treatment (another positive control), and B6 animals had a tendency for PRL upregulation, but this change did not reach statistical significance (Figure 3-1, B and F). Based on these results, we assumed that our estradiol replacement protocol was appropriate.

We next measured hypothalamic expression of Kiss1 in response to chronic estradiol administration. When we sacrificed our animals, we dissected the hypothalami into rostral and caudal blocks containing the AVPV and Arc nuclei, respectively, allowing us to measure Kiss1 expression separately in these areas. Both 129 and B6 WT females fed high P_i chow responded to the estradiol replacement protocol by upregulating Kiss1 expression in the rostral hypothalamus (containing the AVPV) and downregulating Kiss1 expression in the caudal hypothalamus (containing the Arc) (Figure 3-1, C-D, G-H). We interpret these results to mean that the hypothalamus of animals undergoing phosphate overload (at least at the level of Kiss1 producing cells) is functional if given the proper input cues. We therefore reason that necessary hormonal cues may be lacking in conditions of phosphate overload.

Kisspeptin-10 administration elicits LH surging in models of phosphate overload.

Since the hypothalamus appears functional in female mice undergoing phosphate overload, we next investigated the functionality of the pituitary gland in these mice. We sought to investigate the quality of the Kiss1-GnRH-LH axis in $KL^{-/-}$ and WT 129 females fed a high P_i diet by observing whether acute administration of Kisspeptin-10 could elicit an LH surge in these animals. Peripubertal $KL^{-/-}$ females and their WT littermates responded to Kisspeptin-10 injections by secreting LH in a dose-dependent manner (Figure 3-2A). When

divided by baseline LH secretion in these animals, KL-/- mice actually responded more robustly to Kisspeptin-10 than their WT female littermates (Figure 3-2B). Perhaps low levels of Kiss1 expression in these mice have resulted in a priming effect to sensitize these animals to Kisspeptin.

Since the 300 nmol/kg dose of Kisspeptin-10 most potently stimulated LH secretion in $KL^{-/-}$ and WT mice, we chose this single dose to inject into WT 129 females on high P_i chow. Like, KL-/- females, WT females undergoing dietary phosphate overload are capable of responding to Kisspeptin-10 injection by producing a robust LH surge (Figure 3-2C). These data indicate to us that the Kiss1-GnRH-LH axis is intact in both models of phosphate overload and that given the proper cues, pituitary gonadotrophs do respond normally. This may suggest that proper Kisspeptin cues are absent in these mouse models of phosphate overload resulting in abnormal regulation of LH.

Gonadotropin administration induces ovulation in high phosphate diet-fed mice.

It has been well established that gonadotropin treatment in mice induces ovulation, and standard protocols have been developed for this purpose (Fowler and Edwards 1957; Vergara, Irwin et al. 1997). Toyama et al. have demonstrated that $KL^{-/-}$ females are capable of responding to this superovulation procedure, which includes administration of pregnant mare's serum gonadotropin (PMSG) followed by administration of human chorionic gonadotropin (hCG), by inducing

follicle maturation and a small number of ovulation events (Toyama, Fujimori et al. 2006). We have investigated whether WT 129 mice on high phosphate diet, which never normally ovulate (see Figure 2-6), are capable of producing a similar response to gonadotropin administration.

We treated 13 week old WT 129 females (those that had undergone high phosphate feeding for 10 weeks) and their littermates on normal phosphate chow with PMSG and hCG as described in Section 3.4.2. Normal chow-fed animals responded to this treatment with an average ovulation of 42 eggs. High P_i-fed females ovulated less eggs (19 on average), but nonetheless were capable of responding properly to gonadotropin treatment (Figure 3-3). This indicates that the pituitary-gonadal arm of the HPG axis is intact in both models of phosphate overload, again suggesting that there may be a lack of proper cues (in this case serum gonadotropins) under conditions of phosphate overload.

Alternate contributors to HPG axis dysfunction in mouse models of phosphate overload.

Taken together, our data presented in Figures 3-1 – 3-3 suggests that although we have observed derangements at all levels of the HPG axis in $KL^{-/-}$ females and WT females fed high phosphate diet, it appears that the hypothalamus, pituitary gland, and ovaries are functional in these animals. These

three organs responded properly to upstream hormonal cues, suggesting female mice undergoing phosphate overload may lack proper hormonal cues necessary to initiate successful HPG axis function. Therefore, we have investigated alternative factors that may impinge upon proper HPG axis function (possibly at the level of Kiss1 expression) in these mice.

Female mice undergoing phosphate overload are hypoprolactinemic.

We investigated whether female mice undergoing phosphate overload are hyperprolactinemic since hyperprolactinemia is known to cause reproductive dysfunction and since humans with hyperphosphatemia (i.e. CKD patients) often have hyperprolactinemia (references). However, $KL^{-/-}$ mice and WT 129 and B6 females on high P_i chow have low prolactin mRNA levels in the pituitary and low circulating prolactin protein (Figure 3-4, A-E). Thus hyperprolactinemia is not responsible for reproductive deficits in these mice.

Female mice undergoing phosphate overload may have elevated stress axes.

We have evaluated whether HPA axis genes are upregulated in female mouse models of phosphate overload. $KL^{-/-}$ mice have elevated CRH expression in the hypothalamus and also upregulated expression of corticotropin releasing hormone receptor 1 (CRHR1) in the pituitary gland (Figure 3-5, A-B). They do not however have upregulated expression of the downstream target of CRH,

ACTH, in the pituitary (Figure 3-5C). Additionally, WT 129 and B6 females on high P_i chow also have normal expression of ACTH compared to their normal chow-fed littermates (Figure 3-5, D-E). Downstream of ACTH, we measured expression of steroidogenic enzyme mRNAs (StAR, CYP11A1, CYP17, CYP21A1, CYP11B1, and CYP11B2) that are responsible to synthesis of corticosteroids in the adrenal gland. WT 129 animals on high P_i chow did not have elevated mRNA levels (Figure 3-6A); however, high P_i fed B6 animals had elevated expression of all enzymes except CYP21A1 (Figure 3-6B). These results may be due to genetic background differences between these two mouse strains. Taken together, these results may suggest elevated HPA axis function in mice undergoing phosphate overload, but this does not fully explain dysfunction of the HPG axis caused by phosphate overload.

Decreased leptin levels in $KL^{-/-}$ females are rescued by low phosphate feeding.

We have also investigated the contribution of leptin to reproductive dysfunction in $KL^{-/-}$ females. As expected because of their low body weight and decreased amount of white adipose tissue (Figure 2-1 and data not shown), $KL^{-/-}$ mice have low circulating leptin levels compared to their WT littermates (Figure 3-7). Low phosphate feeding (0.2% Pi diet) induces leptin secretion in WT and $KL^{-/-}$ mice to levels above those in WT mice on normal chow. Although some reproductive phenotypes of $KL^{-/-}$ females are rescued by 0.2% Pi feeding, these

mice still do not ovulate (see Figure 2-5). These results indicate that low leptin levels do not explain anovulation in $KL^{-/-}$ mice.

High P_i treatment does not acutely alter electrophysiological properties of Kiss1 neurons.

Since it is known that high extracellular phosphate can acutely induce changes in intracellular signaling (Khoshniat, Bourgine et al. 2011), we hypothesized that high P_i in serum and CSF may directly impact Kiss1 neurons in an acute timeframe. To identify Kiss1 neurons in the preoptic area (including the AVPV and PeN), mice expressing Cre-recombinase driven by *Kiss1* regulatory elements (Cravo, Margatho et al. 2011) were crossed to reporter mice carrying Cre-inducible R26-GFP (Jax mice®). Kiss1-Cre/GFP neurons in the preoptic area were targeted using epifluorescence and Nomarski (i.e., IR-DIC) illumination (Figure 3-8, A-B). Kiss1-Cre neurons were identified by enhanced green fluorescent protein (eGFP) signal under a fluorescent microscope (Figure 3-8C). Alexa Fluor 594 hydrazide was added to the intracellular pipette solution for real-time confirmation that eGFP-positive neurons were targeted for recording (Figure 3-8, D-E).

AVPV/PeN Kiss1-Cre/GFP neurons were recorded under conditions of zero current injection (I=0) in whole-cell patch-clamp configuration. In current-clamp mode, the average resting membrane potential (RMP) of all AVPV/PeN

Kiss1 neurons recorded from females in diestrus was -72.8 ± 2.5 mV (range -59 mV to -81 mV, n=8). Similar to previously reported data (Frazão *et al.*, submitted) most AVPV/PeN Kiss1 neurons were quiescent (7 out of 8). To determine whether high phosphate levels acutely modulate activity of AVPV/PeN Kiss1 neurons, we first examined the acute changes of the RMP using artificial cerebrospinal fluid (ACSF) solution contained elevated NaH_2PO_4 (2.5 mM). (Normal ASCF contains 1.25 mM NaH_2PO_4.) Increased phosphate levels did not induced changes in RMP of the AVPV/PeN Kiss1 neurons (RMP before: 75.7mV ± 1.7mV, RMP after: 77.7mV ± 1.5mV, n=3, Figure 3-8F) or input resistance (input resistance before: 0.3 ± 0.0 MΩ, input resistance after 0.3 ± 0.0 MΩ, n=3). These data suggest that phosphate levels do not acutely modulate activity in AVPV/PeN Kiss1 neurons. As previous demonstrated, tolbutamide (200 μM), an ATP-sensitive potassium channel blocker, depolarizes AVPV/PeN Kiss1 neurons (Frazao *et al*., submitted) and was used as a positive control (n=6, RMP after tolbutamide: -50.7 ± 1.2 mV; Figure 3-8H).

DISCUSSION

In this chapter, we have shown that $KL^{-/-}$ females and WT females undergoing dietary phosphate overload have a functional HPG axis that is capable of responding properly to regulatory hormonal inputs. However, despite this,

these mice experience hormonal aberrations at all levels of the HPG axis under normal conditions (see Chapter 2), suggesting that necessary hormonal cues to initiate proper HPG axis function are lacking in these mice. Thus these mice are experiencing hypogonadotropic hypogonadism. We would argue that low Kiss1 expression observed in $KL^{-/-}$ females and WT females on high phosphate diet is the critical missing set-point in these mice.

Since there appeared to be no obvious defects in the functionality of the HPG axis itself in female mouse models of phosphate overload, we next investigated potential hormonal aberrations in other endocrine systems in these mice that may impinge upon HPG axis function. Hyperprolactinemia is not apparent in female mice undergoing phosphate overload, so we do not suspect it to be a contributor to reproductive phenotypes of these mice. Our investigation of elevated HPA axis activation in mice with genetic or dietary phosphate overload did not appear to be a striking candidate for affecting HPG axis function in these mice. Finally, low phosphate diet rescued leptin levels in $KL^{-/-}$ females but failed to induce puberty initiation in these animals, suggesting that leptin may not solely contribute to reproductive dysfunction in these mice either.

Based on this evidence, we conclude that $KL^{-/-}$ females and WT female mice on high P_i diet are suffering from "functional hypothalamic anovulation" due to lack of appropriate cues to activate the HPG axis (hormonal or otherwise). Actually our experimental animals have a reproductive phenotype that is nearly

identical to female patients presenting with functional hypothalamic anovulation. In both cases, low levels of LH lead to a poorly estrogenized vagina and uterine atrophy/hypoplasia (Kronenberg, Melmed et al. 2008). Additionally, patients with functional hypothalamic anovulation appear to have fully functional and responsive pituitary glands, and pulsatile intravenous administration of GnRH can rescue low LH levels in these patients (Kronenberg, Melmed et al. 2008).

$KL^{-/-}$ mice were originally described as a mouse model of human premature aging syndromes that exhibited infertility as one of the manifestations of these aging-like phenotypes (Kuro-o, Matsumura et al. 1997). Recent studies have demonstrated that mice with premature aging syndromes due to genotoxic stress (accumulation of DNA damage or dysfunctional telomeres) shift the metabolic state from growth and reproduction to somatic maintenance (Schumacher, van der Pluijm et al. 2008). Specifically, these mice attenuate the somatotroph endocrine axis (growth hormone- IGF-1 axis) and trigger metabolic responses resembling those to caloric restriction. Notably, attenuation of the somatotroph endocrine axis and caloric restriction are established interventions that suppress aging and extend life span when applied to animals without genotoxic stress (Masoro 2005; van der Pluijm, Garinis et al. 2007). Thus, these changes observed in premature aging syndromes are regarded as a survival response to maximize longevity under genotoxic stress. We have observed similar

changes in mice under "phosphotoxic stress." $KL^{-/-}$ females and WT females on high P_i diet have decreased body weight and smaller (or absent in the case of $KL^{-/-}$) white adipose depots (see Chapter 2 and data not shown). Unpublished data from our lab indicate that mice fed high P_i diet exhibit changes in hepatic gene expression resembling those seen in mice under caloric restriction. Thus, suppression of reproduction may be regarded as one of the survival responses to pro-aging pressure caused by phosphotoxic stress.

MATERIALS AND METHODS

Animals Diets and Procedures

Animal diets and procedures for $KL^{-/-}$ mice and their WT littermates and for WT 129 and B6 animals are described in Section 2.4.1. For Kiss1-Cre/GFP mice the following protocols were employed. Female mice on diestrus (estrus cycle monitored by vaginal cytology, n=4, (8-10 weeks old) expressing enhanced green fluorescent protein (eGFP) under the transcriptional control of Cre-recombinase were used (Cravo, Margatho et al. 2011). All mice used in this study were housed in the University of Texas Southwestern Medical Center Animal Resource Center, in a light (12 h on/12 h off) and temperature (21–23 °C) controlled environment. They were fed standard chow diet (Harlan Teklad Global

Diet, Harlan Laboratories Inc., Indianapolis, IN) and had free access to water. All experiments were carried out in accordance with the guidelines established by the National Institute of Health Guide for the Care and Use of Laboratory Animals, as well as with those established by the University of Texas Institutional Animal Care and Use Committee.

Quantitative Real-time PCR

Procedures employed for RNA isolation and qPCR analysis are described in Section 2.4.4. Mouse primers used for qPCR experiments in this chapter are listed in Table 3-1. Primers for CyclophilinA, Kiss1, StAR, CYP11A1 (P450scc), and CYP17 (P450c17) are listed in Table 2-2.

Estradiol Administration

WT 129 and B6 females underwent high phosphate feeding for 10 weeks after weaning (as described in Section 2.4.1) prior to the start of estradiol replacement. At 13 weeks of age, WT 129 and B6 females underwent an estradiol replacement protocol. We based our methods on several previously published protocols (Yoshizawa, Handa et al. 1997; Kinuta, Tanaka et al. 2000; Frasor, Barnett et al. 2003; Navarro, Castellano et al. 2004). Mice received IP injections

of 40 μg/kg 17β-estradiol (E2) (Sigma-Aldrich, St. Louis, MO) or vehicle (corn oil) at 10 am every day, for 4 days. On the fourth day, mice were anesthetized with Avertin (200mL/kg body weight) and sacrificed by cervical dislocation at 2 pm (6 hours after the morning injection).

For qPCR analysis of rostral versus caudal hypothalamic gene expression, hypothalami were dissected from the brain with the following limits: anterior limit- 1mm anterior to the optic chiasm, posterior limit- immediately posterior to the mammillary bodies, lateral limits- 2 mm to either side of the third ventricle (limits of the optic tract), dorsal limit- immediately dorsal to the thalamus (some thalamic contamination may have occurred but was purposefully avoided), ventral limit- the ventral-most portion of the third ventricle. Each hypothalamus was then coronally bisected between the optic chiasm and the third ventricle to produce rostral and caudal hypothalamic blocks.

Kisspeptin-10 Administration

$KL^{-/-}$ Females

Mouse Kiss1 (110-119) amide (Kisspeptin-10) (Phoenix Pharmaceuticals, Burlingame, CA) or vehicle (150 mM NaCl) was acutely administered to 25 day old $KL^{-/-}$ female mice via intraperitoneal (IP) injection at the following doses: 0, 3, 10, 30, 100, and 300 nmol/kg. Approximately 18 minutes after the injection,

mice were anesthetized with Avertin (200 mL/10 kg body weight). Blood was subsequently collected 20 minutes post-Kisspeptin-10 injection by retro-orbital bleeding. Blood was then allowed to clot for 1-1.5 hours at room temperature, followed by centrifugation for at 5000 RPM for 10 minutes at 4^{o}C. Serum supernatant was collected and stored at -80^{o}C. Serum samples were sent to the University of Virginia Center for Research in Reproduction for LH measurements by sandwich IRMA.

WT 129S1/SvImJ Females

Kisspeptin-10 or saline vehicle was also injected into WT 129 females, but only at the 300 nmol/kg dose. Mice were weaned onto 2% high phosphate diet (see Section 2.4.1), and maintained under this condition for 10 weeks. At the end of 10 weeks of high P_i feeding, Kisspeptin-10 was administered and serum was collected using the same procedure as described for $KL^{-/-}$ mice (Section 3.4.1).

Gonadotropin Administration

WT 129 females were weaned onto normal or high phosphate diet (see Section 2.4.1), and maintained under these conditions for 10 weeks. After 10 weeks on each diet, mice received gonadotropin treatments to induce ovulation, following a standard superovulation protocol (Fowler and Edwards 1957;

Vergara, Irwin et al. 1997). On day 1 at noon, mice received an IP injection of 5 IU of pregnant mare serum gonadotropin (PMSG) (Sigma-Aldrich, St. Louis, MO). 48 hours later, at noon on day 3, mice received an IP injection of 5 IU of human chorionic gonadotropin (hCG) (Sigma-Aldrich, St. Louis, MO). 24 hours later, at noon on day 4, mice were anesthetized with Avertin (200 mL/kg body weight) and sacrificed by cervical dislocation. Each ovary was dissected and connections to each oviduct and uterine horn were maintained. Tissue was examined under a dissecting microscope and the enlarged, cystic area of the oviduct containing ovulated eggs was identified and severed with fine-tipped forceps. Eggs were then collected (in a bunch with surrounding cumulus cells) and counted under the dissecting microscope.

Serum Hormone Measurements

Serum prolactin was measured by enzyme-linked immunosorbent assay (ELISA) (Calbiotech, Spring Valley, CA). Circulating leptin was measured using a mouse leptin ELISA kit (Millipore, Billerica, MA).

Whole-cell Recordings

Whole-cell patch-clamp recordings were performed in Kiss1 neurons expressed in the preoptic area (AVPV/PeN). During the recordings, neurons were maintained in hypothalamic slice preparations and data analyses were performed as previously described (Hill, Williams et al. 2008; Williams, Margatho et al. 2010). Mice were decapitated and the entire brain was removed. After removal, brains were immediately submerged in ice-cold, carbogen-saturated (95% O_2 and 5% CO_2) ACSF (126 mM NaCl, 2.8 mM KCl, 1.2 mM $MgCl_2$, 2.5 mM $CaCl_2$, 1.25 mM NaH_2PO_4, 26 mM $NaHCO_3$, and 5mM glucose). Coronal sections from a hypothalamic block (250µM) were cut with a Leica VT1000S Vibratome and then incubated in oxygenated ACSF at room temperature for at least 1h before recording. Slices were transferred to the recording chamber and allowed to equilibrate for 10–20 min before recording. The slices were bathed in oxygenated ACSF (32°C–34°C) at a flow rate of ≅ 2 mL/min. The pipette solution for whole-cell recording was modified to include an intracellular dye (Alexa Fluor 594) for whole-cell recording: 120 mM K-gluconate, 10mM KCl, 10mM HEPES, 5mM EGTA, 1 mM CaCl2, 1 mM MgCl2, 2mM (Mg)-ATP, and 0.03mM Alexa Fluor 594 hydrazide dye, pH 7.3. Epifluorescence was briefly used to target fluorescent cells, at which time the light source was switched to infrared differential interference contrast imaging to obtain the whole-cell recording (Nikon Eclipse FN1 equipped with a fixed stage and a QuantEM:512SC electron-multiplying charge-coupled device camera). Electrophysiological signals were recorded using

an Axopatch 700B amplifier (Molecular Devices), low-pass filtered at 2–5 kHz, digitized at 88 kHz (Neuro-corder; Cygnus Technology), and analyzed offline on a PC with pCLAMP programs (Molecular Devices). Recording electrodes had resistances of 2.5–5 MΩ when filled with the K-gluconate internal solution. Input resistance was assessed by measuring voltage deflection at the end of the response to a hyperpolarizing rectangular current pulse (500 ms of –10 to -50 pA). For some experiments measuring voltage, the K-gluconate was replaced by equimolar Cs-gluconate. Membrane potential values were compensated to account for junction potential (-8 mV).

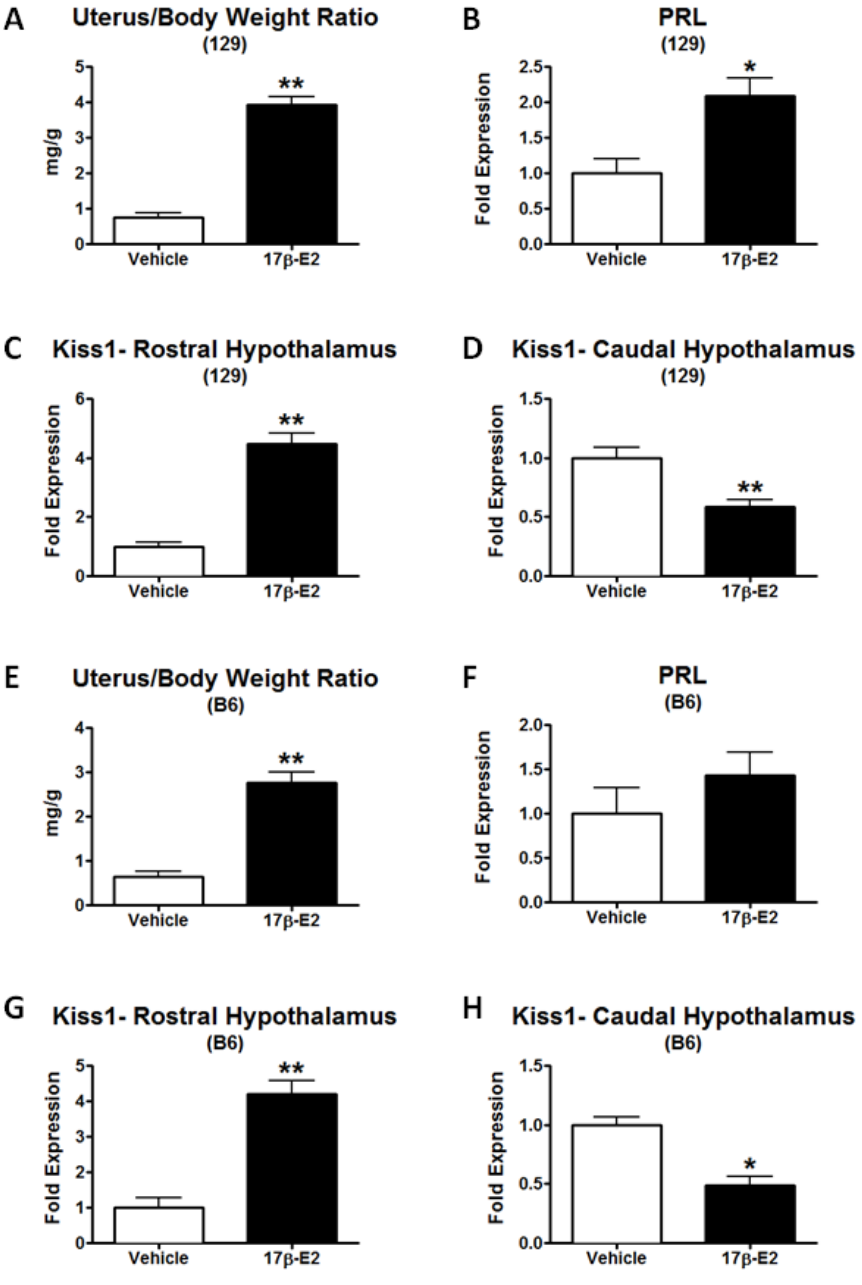
A
Uterus/Body Weight Ratio
(129)
mg/g
**
Vehicle
17β-E2
B
PRL
(129)
Fold Expression
*
Vehicle
17β-E2
C
Kiss1- Rostral Hypothalamus
(129)
Fold Expression
**
Vehicle
17β-E2
D
Kiss1- Caudal Hypothalamus
(129)
Fold Expression
**
Vehicle
17β-E2
E
Uterus/Body Weight Ratio
(B6)
mg/g
**
Vehicle
17β-E2
F
PRL
(B6)
Fold Expression
Vehicle
17β-E2
G
Kiss1- Rostral Hypothalamus
(B6)
Fold Expression
**
Vehicle
17β-E2
H
Kiss1- Caudal Hypothalamus
(B6)
Fold Expression
*
Vehicle
17β-E2

Figure 3-1. WT 129 and B6 females on high P_i diet show proper hypothalamic responses to estradiol administration. WT 129 (A-D) and B6 (E-H) females were weaned onto high P_i (2%) chow at 3 weeks of age. At 13 weeks of age (after 10 weeks of high phosphate feeding), animals underwent an estradiol replacement protocol for 4 days. Animals were injected with vehicle or 17β-estradiol (17β-E2) each day at 10 am and were sacrificed 6 hours post-injection on day 4. (A, E) Uterus to body weight ratio. (B, F) Prolactin (PRL) mRNA was measured in the pituitary gland by qPCR. (C, D, G, H) Hypothalami were dissected into rostral (C, G) and caudal (D, H) blocks, and Kiss1 mRNA was measured by qPCR. Single asterisk indicates $p<0.05$, and double asterisk indicates $p<0.005$ (Student's t-test).

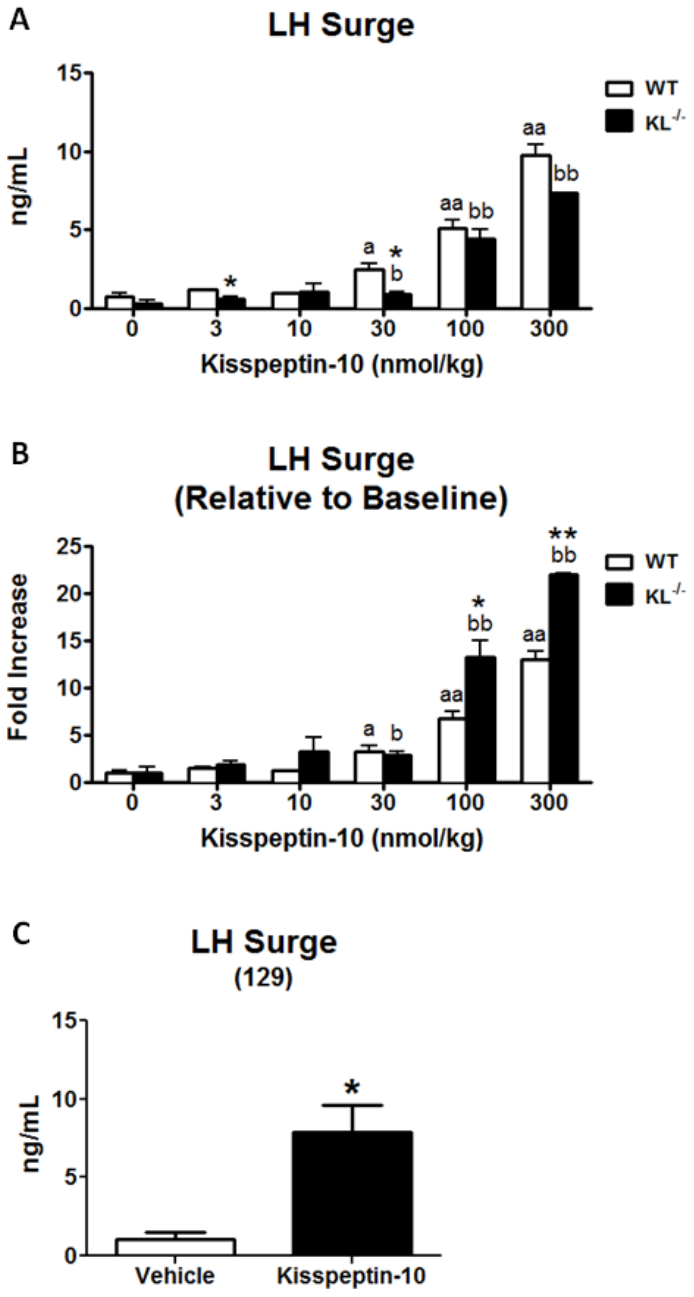
A
LH Surge
ng/mL
15
10
5
0
WT
KL-/-
aa
bb
a
b
*
0
3
10
30
100
300
Kisspeptin-10 (nmol/kg)
B
LH Surge
(Relative to Baseline)
Fold Increase
25
20
15
10
5
0
**
*
aa
bb
a
b
WT
KL-/-
Kisspeptin-10 (nmol/kg)
C
LH Surge
(129)
ng/mL
15
10
5
0
*
Vehicle
Kisspeptin-10

Figure 3-2. Both $KL^{-/-}$ and WT females on high Pi diet elicit an LH surge in response to acute Kisspeptin-10 administration. (A-B) Peripubertal (25 day old) $KL^{-/-}$ females and their WT female littermates were injected with recombinant vehicle or Kisspeptin-10 at the indicated doses. Animals were sacrificed and serum was harvested 20 minutes post injection. (A) Serum LH surge (ng/mL) in response to Kisspeptin-10 administration. (B) Relative LH response. LH surge was divided by baseline serum LH (LH levels after vehicle administration). "a" ($p<0.05$, Student's t-test) and "aa" ($p<0.005$, Student's t-test) denote a significant difference between WT (Kisspeptin-10-injected) and WT (vehicle-injected). "b" ($p<0.05$, Student's t-test) and "bb" ($p<0.005$, Student's t-test) denote a significant difference between $KL^{-/-}$ (Kisspeptin-10-injected) and $KL^{-/-}$ (vehicle-injected). Single asterisk ($p<0.05$, Student's t-test) and double asterisk ($p<0.005$, Student's t-test) denote a significant difference between $KL^{-/-}$ and WT within the same treatment group. (C) WT 129 females were weaned onto high phosphate diet (2%) at 3 weeks of age. At 13 weeks of age (after 10 weeks on high P_i chow), animals received vehicle or Kisspeptin-10 injections and were sacrificed 20 minutes post-injection. Serum LH surge was measured. Single asterisk indicates $p<0.05$ (Student's t-test).

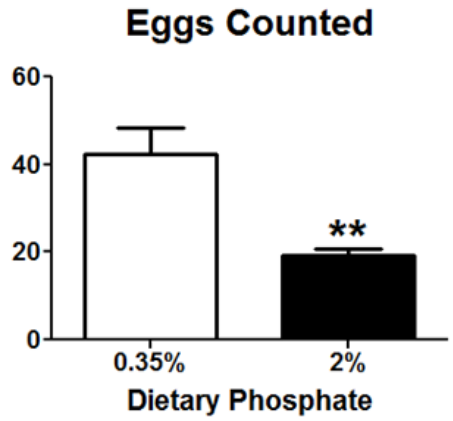

Figure 3-3. WT 129 females on high phosphate diet ovulate in response to gonadotropin administration. WT 129 females were weaned onto normal (0.35%) or high P_i (2%) chow at 3 weeks of age. At 13 weeks of age (after 10 weeks on each diet), animals received a standard superovulation procedure. Intact oviducts were harvested and ruptured under a dissecting microscope so that ovulated eggs could be counted. Double asterisk indicates a statistical difference of $p<0.005$ (Student's t-test).

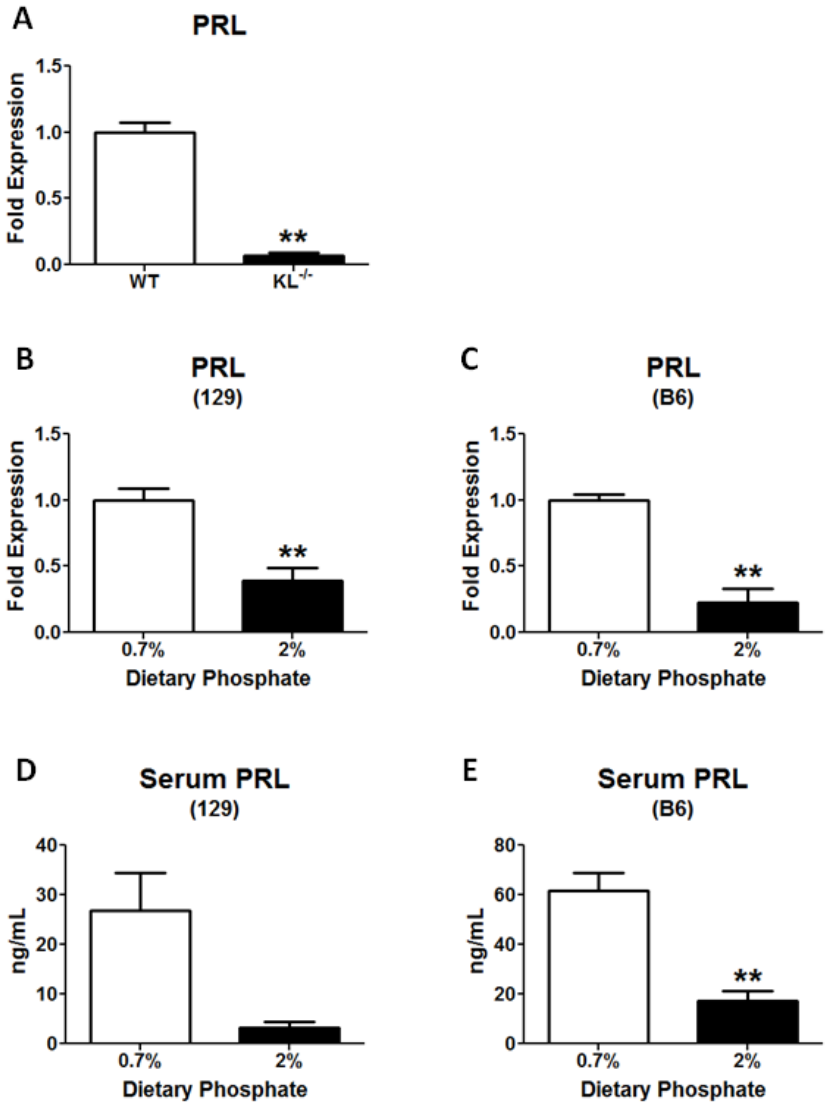

Figure 3-4. Female mice undergoing phosphate overload have hypoprolactinemia. (A) WT and $KL^{-/-}$ females were sacrificed at 8 weeks of age, and prolactin (PRL) mRNA levels in the pituitary gland were measured by qPCR. Double asterisk indicates $p<0.005$ (Student's t-test). (B-E) WT 129 (B, D) and B6 (C, F) females were weaned onto normal (0.7%) or high phosphate (2%) chow at 3 weeks of age. Mice were sacrificed at 13 weeks of age (after 10 weeks on each diet). PRL mRNA in the pituitary gland was measured by qPCR (B-C), and serum PRL was measured by ELISA (D-E).

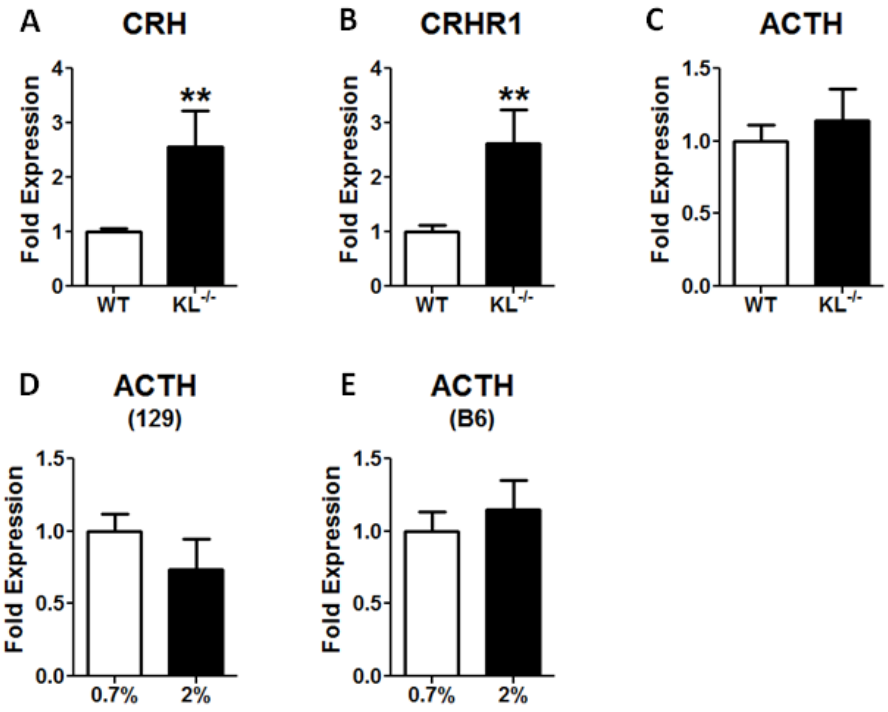

Figure 3-5. $KL^{-/-}$ females have elevated CRH and CRHR1 mRNA expression. (A-C) WT and $KL^{-/-}$ females were sacrificed at 8 weeks of age. mRNA expression of CRH, CRHR1, and ACTH were measured by qPCR. Double asterisk indicates $p<0.005$ (Student's t-test). (D-E) WT 129 (D) and B6 (E) females were weaned onto normal (0.7%) or high phosphate (2%) chow at 3 weeks of age. Mice were sacrificed at 13 weeks of age (after 10 weeks on each diet). ACTH mRNA in the pituitary gland was measured by qPCR.

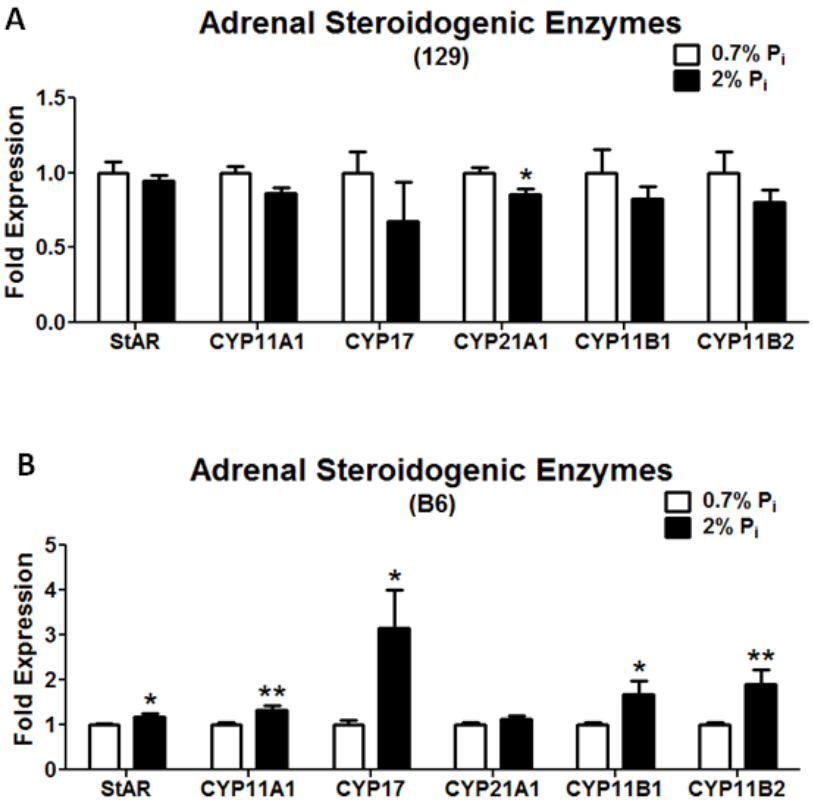

Figure 3-6. WT B6 females on high phosphate diet display increased expression of adrenal steroidogenic enzymes. (A-B) WT 129 (A) and B6 (B) females were weaned onto normal (0.7%) or high phosphate (2%) chow at 3 weeks of age. Mice were sacrificed at 13 weeks of age (after 10 weeks on each diet). StAR, CYP11A1, CYP17, CYP21A1, CYP11B1, and CYP11B2 mRNA in the adrenal gland was measured by qPCR. Single asterisk indicates $p<0.05$ (Student's t-test). Double asterisk indicates $p<0.005$ (Student's t-test).

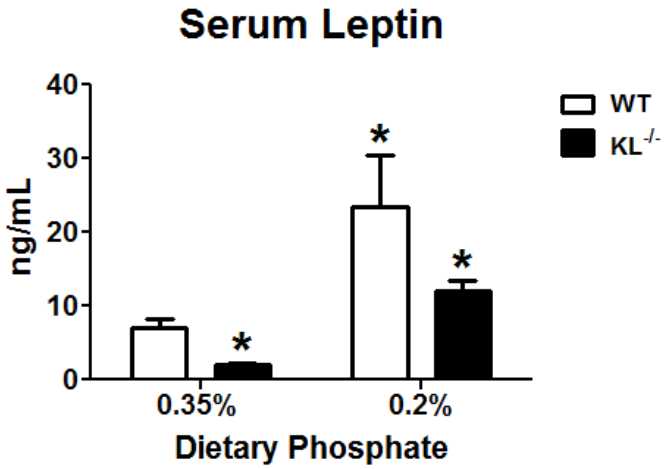

Figure 3-7. Low phosphate diet rescues low leptin levels in $KL^{-/-}$ females. $KL^{-/-}$ females and their WT female littermates were weaned onto normal (0.35%) or low phosphate (0.2%) chow at 3 weeks of age. Animals were maintained under these dietary conditions for 5 weeks and sacrificed at a final age of 8 weeks old. Serum leptin levels were measured by ELISA. Asterisks indicate a significant difference from WT (0.35% P_i) with $p<0.05$ (Student's t-test).

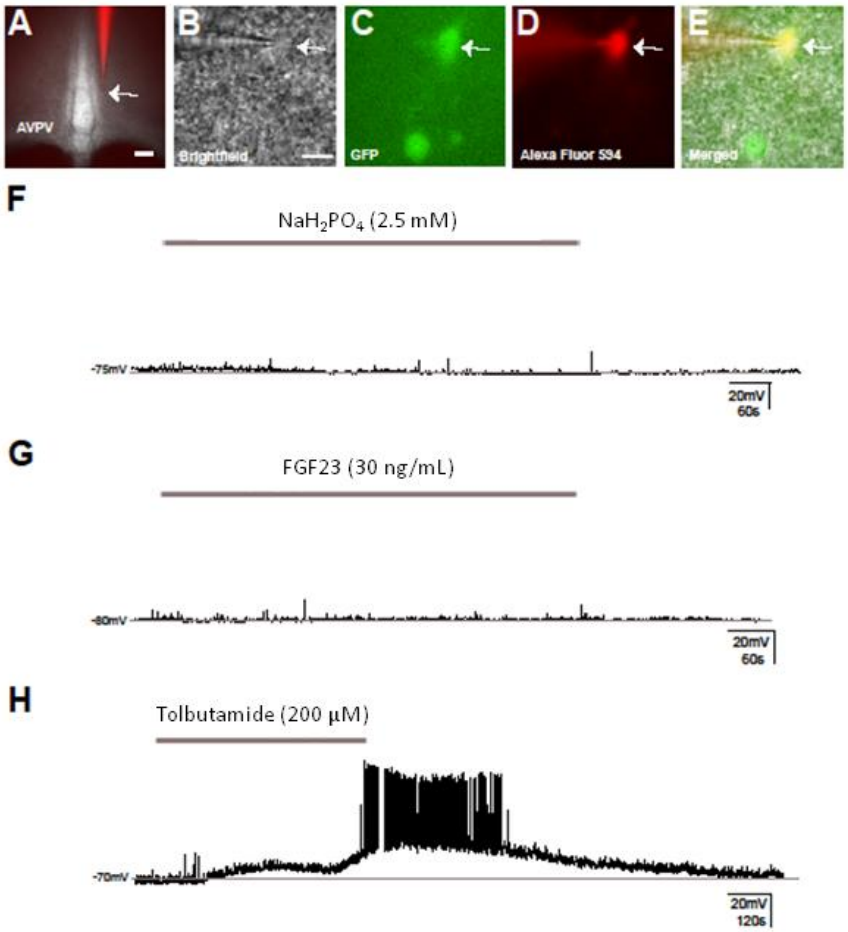

Figure 3-8. High phosphate does not acutely modulate AVPV Kiss1 neurons activity. (A-F) Identification of Kiss1-Cre/GFP cells for whole-cell patch-clamp recordings. (A) Low magnification for anatomical reference. (B) Brightfield illumination showing a targeted neuron. (C) The same neuron under fluorescent (FITC) illumination. (D) Complete dialysis of Alexa Fluor 594 from the intracellular pipette at the end of the recording. (E) Colocalization of Alexa Fluor 594 and GFP. (F-G) Current-clamp recording demonstrates that increased (2.5mM) or FGF23 (30ng/ml) has no acute effect on AVPV/PeN Kiss1 neurons resting membrane potential. (H) Current-clamp recording demonstrates that tolbutamide (200µM) depolarizes AVPV/PeN Kiss1 neurons. Scale bar: A= 100 µm, B-E= 10 µm.

Table 3-1. Mouse primer sets used for qPCR.

Gene	Forward Primer (5'-3')	Reverse Primer (5'-3')
Prolactin	TAATTAGCCAGGCCTATCCTGAA	GATGGAAGTTGTGACCAAACAAAG
CRH	TCTGGATCTCACCTTCCACCT	CCATCAGTTTCCTGTTGCTGT
CRHR1	AGGGCTTCTTCGTGTCTGTG	CTGATGGAGTGCTTGTCCTG
ACTH	GAGGCCTTTCCCCTAGAGTT	CACCGTAACGCTTGTCCTT
CYP21A1	TGCCTCACTTTTGGAGACAAG	GTCCTGGACACAGTCGTGAAG
CYP11B1	TTTCCGGCCTGTCAGCTA	GGCTGGTGGCGACTAGGA
CYP11B2	CTGGCAGCCTGAAGTTTATCC	GAGCTGTGAGGTGGACTTGAA

CHAPTER FOUR
Investigating Extrarenal FGF23 Signaling

INTRODUCTION AND RATIONALE

In this chapter, we will investigate the potential of the phosphaturic hormone FGF23 to signal in other tissues besides the kidney, such as the brain, pituitary gland, and ovaries. Our lab has previously shown that FGF23 can bind *in vitro* to Klotho protein that is in complex with FGFR1, FGFR3, and FGFR4 (Kurosu, Ogawa et al. 2006); however, it appears that FGF23 signaling *in vitro* and, more importantly, *in vivo* may only be supported by the Klotho-FGFR1 complex (Urakawa, Yamazaki et al. 2006; Liu, Vierthaler et al. 2008; Gattineni, Bates et al. 2009). Downstream of Klotho and FGFR1, FGF23 induces phosphorylation of FGF receptor substrate-2α (FRS2α) and p44/42 mitogen-activated protein (MAP) kinase (ERK1/2) (Kurosu, Ogawa et al. 2006), and further downstream it upregulates early growth response 1 (Egr-1) transcription factor mRNA and c-Fos transcription factor mRNA (Urakawa, Yamazaki et al. 2006; Farrow, Summers et al. 2010).

Klotho and FGFR1 expression are not limited to the kidney (Kuro-o, Matsumura et al. 1997; Fon Tacer, Bookout et al. 2010), so this begs the question of whether FGF23 can also signal in extrarenal tissues that express both Klotho

and FGFR1. Indeed, FGF23 was recently demonstrated to signal in the parathyroid gland by inducing ERK1/2 phosphorylation and upregulating Egr-1 mRNA to inhibit PTH synthesis and secretion (Ben-Dov, Galitzer et al. 2007). When the Klotho gene was originally characterized, its expression was found to be highest in the kidney, but significant expression was also detected in the brain, pituitary gland, and ovaries (Kuro-o, Matsumura et al. 1997). FGFR1 expression is nearly ubiquitous and is also expressed in these tissues (Fon Tacer, Bookout et al. 2010). Since these are the very organs that are responsible for the reproductive phenotypes of $KL^{-/-}$ females, we reasoned that loss of Klotho (and therefore loss of FGF23 signaling) in these tissues may be directly responsible for infertility in these animals. Furthermore, unpublished data from our lab suggests that high phosphate feeding significantly reduces Klotho expression in the kidney. Therefore, we will also examine the effects of high P_i diet on Klotho expression in the HPG axis in WT mice, and the potential contribution of reduced Klotho expression (and thus reduced FGF23 signaling) to the reproductive phenotypes of these mice.

As described in Section 1.1.2, FGF23 is produced in and secreted from the bone. Actually, the original identification of FGF23 showed preferential expression of FGF23 in the ventrolateral thalamic nucleus of the brain (Yamashita, Yoshioka et al. 2000). However, our lab and others have not been able to replicate this finding and have been unable to detect FGF23 expression in

the brain (data not shown) (Fon Tacer, Bookout et al. 2010). FGF23 secreted from the bone enters the circulation and functions as an endocrine hormone that could exert signaling in extrarenal, Klotho-expressing tissues such as the pituitary gland and ovaries; however, in order for bone-derived FGF23 to signal in the brain, it must be able to cross the blood-brain barrier (BBB). Another endocrine FGF, Fibroblast Growth Factor 21 (FGF21), has been shown to cross the BBB (Hsuchou, Pan et al. 2007), so we will investigate the ability of FGF23 to cross the BBB and elicit downstream signaling in the brain in this chapter.

RESULTS

Klotho is expressed in the hypothalamus and pituitary gland but not the ovaries.

Like previous reports (Kuro-o, Matsumura et al. 1997; Fon Tacer, Bookout et al. 2010), we detected Klotho mRNA expression by qPCR in the whole hypothalamus, pituitary gland, and the ovaries; however, expression in the ovaries was not different between WT and $KL^{-/-}$ females, so we interpret this to mean that the ovaries do not in fact express significant Klotho mRNA (Figure 4-1A). Consistent with previous reports (Kuro-o, Matsumura et al. 1997; Fon

Tacer, Bookout et al. 2010), extrarenal Klotho expression was highest in the pituitary gland.

Although Klotho mRNA was detected in the hypothalamus and pituitary gland, this does not guarantee protein expression. Therefore, we performed a Western blot to determine if organs in the HPG axis indeed express Klotho protein. Confirming our gene expression data, we observed Klotho expression in the whole hypothalamus and the pituitary gland but not the ovaries, and expression was highest in the pituitary gland (although still significantly lower than that of the kidney) (Figure 4-1B). Since we observed no Klotho mRNA or protein expression in the ovaries, we conclude that the female gonads are not likely a target of FGF23 hormonal signaling.

Supporting our qPCR and Western blotting data, we also observed Klotho expression by *in situ* hybridization in many areas throughout the brain including the hypothalamus and also in the anterior lobe of the pituitary gland (Figure 4-2A). Like previous reports, we observed Klotho expression in the brain to be highest in the choroid plexus (Figure 4-2A) (Kuro-o, Matsumura et al. 1997; Ohyama, Kurabayashi et al. 1998; Li, Watanabe et al. 2004; German, Khobahy et al. 2012). Specifically, Klotho was expressed in the AVPV and the Arc, the two hypothalamic nuclei responsible for KISS1 expression (Figure 4-2A). Although this data suggests that Klotho may be expressed in Kisspeptin-producing cells, we employed an additional technique to more definitively demonstrate Klotho

expression in these cells. We used fluorescence-activated cell sorting (FACS) to sort green fluorescent protein-positive (GFP+) cells from Kiss1-Cre/GFP reporter mice (Cravo, Margatho et al. 2011). GFP+ cells isolated from AVPV and Arc nuclei expressed both Klotho and FGFR1 mRNA in addition to KISS1 (Figure 4-2, B-C). These results suggest that FGF23 may be able to exert signaling in these cells because its co-receptor complex is present.

Since unpublished results from our lab suggest that high phosphate diet inhibits Klotho expression in the kidneys (data not shown), we also measured Klotho expression in the pituitary gland after 10 weeks of high phosphate feeding. Indeed, in 129 and B6 strains, high phosphate diet decreased Klotho mRNA in the pituitary gland by approximately 50% (Figure 4-3, A-B). Since WT females fed high phosphate chow practically phenocopy $KL^{-/-}$ females (see Chapter 2), we reasoned that this decrease in Klotho expression in both models could directly contribute to their reproductive phenotypes by reducing FGF23 signaling in the HPG axis.

FGF23 does not signal in the hypothalamus and does not enter the brain.

Since we observed Klotho expression in the hypothalamus and specifically the very neurons responsible for Kiss1 expression, we tested to see whether FGF23 could elicit downstream signaling in the whole hypothalamus and in

individual Kiss1 neurons. We chose to inject FGF23 peripherally (via acute IP injection) because we believe the major source of FGF23 to be peripheral from the bone. However, peripherally injected FGF23 did not upregulate Egr-1 mRNA in a WT or even FGF23-null background at doses more than sufficient to elicit signaling in the kidney (Figure 4-4, A-B). Additionally, we employed two techniques to reduce endogenous FGF23 levels in WT mice (a 24 hour fast prior to FGF23 injection or 7 days of low phosphate feeding) in an attempt to sensitize them to exogenous FGF23, but FGF23 also did not elicit downstream signaling in the whole hypothalamus in those conditions (Figure 4-4B).

In addition, we tried a more chronic FGF23 administration paradigm in which animals received 3 IP FGF23 injections, each 12 hours apart, and were perfused 2 hours after the last injection. Subsequent immunohistochemical analysis of serial brain sections did not reveal induction of c-Fos protein in any brain regions, including the AVPV (Figure 4-4C).

Since peripherally administered FGF23 did not induce downstream signaling in the hypothalamus despite expression of both Klotho and FGFR1, we tested whether FGF23 protein could cross the BBB. Following several published protocols, we labeled FGF23 protein with ^{125}I to allow us to trace its biodistribution after IP administration into WT mice (Kastin, Akerstrom et al. 2001; Boje 2002; Hsuchou, Pan et al. 2007). We evaluated the activity of ^{125}I-FGF23 by testing its ability to upregulate Egr-1 mRNA in the kidney, and

observed no change in FGF23 functionality after iodine labeling (Figure 4-5A). Within 30 minutes post-IP injection, ^{125}I-FGF23 accumulated in the kidney, but did not accumulate in the hypothalamus or other brain regions tested (Figure 4-5B). Taken together, we interpret these results to mean that FGF23 cannot elicit signaling in the hypothalamus because it cannot cross the BBB.

In a final effort to rule out FGF23 action in Kiss1 neurons, we performed whole-cell electrophysiological recordings of GFP+ cells from brain slices from Kiss1-Cre/GFP mice. Since FGF23 induces FRS2α and ERK1/2 phosphorylation within minutes (data not shown), we reasoned that addition of FGF23 to the cell recording bath could alter electrophysiological properties of the cell within a similar time frame. However, treatment with FGF23 (30ng/mL) had no effect on the RMP or input resistance of AVPV/PeN Kiss1 neurons from female mice in diestrus (RMP before: 71.2mV ± 2.8mV, RMP after: 73.4mV ± 2.6mV; input resistance before: 0.6 ± 0.1 MΩ, input resistance after 0.3 ± 0.1 MΩ, n=5, Figure 3-8G). This data suggests that even when circumventing the BBB using this in vitro cell recording technique, FGF23 does not acutely modulate activity in AVPV/PeN Kiss1 neurons.

Taken together, although we can detect Klotho and FGFR1 expression in the hypothalamus, specifically the AVPV and Arc nuclei, we have not been able to demonstrate an ability of FGF23 to elicit signaling in these tissues/cells. Thus, lack of Klotho expression/lowered Klotho expression in the hypothalamus of mice

undergoing phosphate overload may not directly contribute to their reproductive phenotypes.

FGF23 upregulates Egr-1 but does not induce downstream signaling in the pituitary gland.

Since Klotho is expressed at a relatively high level in the pituitary gland, and since we know FGFR1 is expressed in the pituitary as well (Fon Tacer, Bookout et al. 2010), we conducted similar experiments to those we conducted in the hypothalamus to observe whether FGF23 can elicit downstream signaling in the pituitary gland. Since $KL^{-/-}$ females and WT females on a high P_i diet have altered pituitary gene expression (See Figures 2-3, 2-11, and 2-15), perhaps FGF23 regulates the HPG axis at this level. Interestingly, Urakawa et al. have demonstrated that intravenous injection of FGF23 into rats can upregulate Egr-1 mRNA in the pituitary gland (Urakawa, Yamazaki et al. 2006).

For an acute administration paradigm, FGF23 was injected IP and the pituitary gland was harvested 30 minutes post-injection. Contrary to the study by Urakawa et al., this FGF23 treatment did not upregulate Egr-1 mRNA in WT mice under normal feeding conditions (0.35% Pi diet, administered *ad libitum*) (Figure 4-6A). However, in two FGF23-reduced backgrounds (24 hour pre-fast treatment and 7 day pre-treatment on low P_i diet), FGF23 administration

upregulated Egr-1 mRNA in the pituitary (Figure 4-6A). This data suggests that perhaps FGF23 can signal in the pituitary gland in mice, but only under certain conditions when endogenous FGF23 concentration is low (perhaps in situations such as phosphate deprivation, starvation, or malnutrition).

Since we observed Egr-1 upregulation after acute FGF23 administration in a reduced-FGF23 background, we repeated this experiment with a longer FGF23 treatment (6 hours) to see whether or not this treatment would induce changes in pituitary hormone gene expression downstream of Egr-1. After a 24 hour fasting pre-treatment, FGF23 failed to induce any significant gene expression changes in GnRHR, LH, FSH, Cga, thyrotropin-releasing hormone receptor (TRHR), or thyroid-stimulating hormone (TSH) (Figure 4-6B). As a positive control, we measured the expression of CYP24A1 (the major vitamin D-degrading enzyme) in the kidney, and this was induced by our FGF23 treatment (Figure 4-6C). These data indicate to us that FGF23-induced upregulation of Egr-1 in the pituitary under FGF23-reduced conditions may not be relevant to pituitary function, since we could not observe any changes in downstream gene expression in pituitary genes. Furthermore, when we employed the same chronic injection paradigm as described for the hypothalamus, we again did not observe an induction of c-Fos protein after repeated FGF23 administration (Figure 4-6D).

Therefore, despite Klotho and FGFR1 expression in the pituitary gland, our data indicates that FGF23 signaling in the pituitary may not occur under

normal physiological conditions and may not contribute to the reproductive phenotypes of $KL^{-/-}$ and high P_i-fed WT females.

DISCUSSION

In Chapter 2, we demonstrated that conditions of phosphate overload inhibit female reproductive axes in two mouse models ($KL^{-/-}$ females and WT females on high P_i chow). We specifically observed a reduction in Kiss1 mRNA in the hypothalamus and a reduction in LH mRNA in the pituitary of these animals (Figures 2-2, 2-3, 2-7, 2-8, 2-11, and 2-12). In this chapter, we have shown that Klotho mRNA and protein are expressed in the hypothalamus and pituitary gland (Figure 4-1). This led us to hypothesize that loss of Klotho in these organs may directly contribute to reproductive phenotypes of mice undergoing phosphate overload. Since we know that FGFR1 is also expressed in these tissues (Figure 4-1) (Fon Tacer, Bookout et al. 2010), we reasoned that FGF23 may signal in the hypothalamus and pituitary gland to promote female fertility. Additionally, we observed decreased Klotho expression in the pituitary gland under conditions of high P_i feeding (Figure 4-3), so we could logically extend a pathological role for reduced FGF23 signaling in both models.

However, we have shown in this chapter that, contrary to our hypothesis, peripherally-derived FGF23 does not exert signaling in the hypothalamus or

pituitary gland (Figures 4-4, 4-6, and 4-7). We did observe an upregulation of Egr-1 mRNA in the pituitary in response to acute FGF23 treatment, but only under conditions of reduced endogenous FGF23 levels (24 hour fast pretreatment or 7 day low P_i diet pretreatment) (Figure 4-7A). Furthermore, we could not observe changes in expression of key pituitary hormones and receptors after a longer FGF23 treatment (Figure 4-7B). Hence, we believe that FGF23 signaling in the pituitary may not be physiologically relevant. It is also possible that the conditions we employed to reduce FGF23 background had an effect of increasing Klotho expression, thereby increasing the ability of FGF23 to signal in the pituitary under those conditions. However, we have not yet directly tested this possibility.

Recently, another group published a study that corroborates our findings. Ohnishi et al. demonstrated that restoring proper phosphate balance in $KL^{-/-}$ mice by crossing them to $NaPi2a^{-/-}$ mice (generating $NaPi2a^{-/-}/KL^{-/-}$ double-knockout mice) restores fertility in these mice (Ohnishi and Razzaque 2010). This study clearly demonstrates that Klotho itself is not directly necessary for female fertility, but that phosphate overload is the likely contributor to reproductive deficits in $KL^{-/-}$ females. Additionally, when the authors fed the double-knockout mice a high P_i diet, their aging-like phenotypes and infertility returned (Ohnishi and Razzaque 2010), indicating that phosphate toxicity alone is enough to cause these phenotypes. Taken together with our data, we believe that phosphate

overload itself and not direct loss of FGF23/Klotho signaling is responsible for inhibiting female fertility in mice.

From an evolutionary standpoint, it may make sense for FGF23 only to signal in the kidneys and the parathyroid gland. By and large, the main physiological role of FGF23 is to regulate phosphate homeostasis by decreasing P_i reabsorption in the kidneys. Supporting this role, FGF23 also inhibits the production of active vitamin D by the kidneys. Therefore, it logically follows that FGF23 would also signal outside the kidney in other phosphate-regulating organs such as the parathyroid gland, but perhaps not in organs unrelated to phosphate homeostasis such as the hypothalamus and pituitary gland.

Proper skeletal development and bone growth/maturation are required to carry out successful pregnancy. Therefore it makes sense for there to be an endocrine circuit linking the bone (via FGF23) to reproduction (via hormone production by the hypothalamus and pituitary gland). However, our data did not support this idea, at least not in the form of HPG axis regulation by FGF23. In males, the bone-derived hormone osteocalcin is secreted and acts on the testes to stimulate testosterone production (Oury, Sumara et al. 2011). Perhaps a similar, as of yet undiscovered, mechanism has evolved to link the skeleton to reproductive capacity and hormone production in females.

Since Klotho protein in the hypothalamus and pituitary gland may not function as an FGF23 co-receptor in these tissues, the question still remains as to

its role in these extrarenal organs. In addition to its role as a hormone receptor, the extracellular domain of Klotho protein can be shed from the plasma membrane and can function as a hormone itself to inhibit insulin and insulin-like growth factor 1 (IGF-1) signaling (Kurosu, Yamamoto et al. 2005). Shed Klotho can also regulate cell surface retention and activity of transient receptor potential cation channel subfamily V member 5 (TRPV5) and potassium inwardly-rectifying channel subfamily J member 1 (ROMK1) ion channels through its activity as a sialidase enzyme (Cha, Ortega et al. 2008; Cha, Hu et al. 2009). Full-length and shed Klotho binds to and inhibits Wnt signaling (Liu, Fergusson et al. 2007). Additionally, shed Klotho binds the type-II TGF-β receptor and inhibits TGF-β1 signaling and TGF-β1-induced epithelial to mesenchymal cell transitions (Doi, Zou et al. 2011). Since shed Klotho exerts this multitude of additional activities, it is entirely conceivable that Klotho protein in the hypothalamus and pituitary gland acts in its shed form instead of as a co-receptor for FGF23. Of note, shed Klotho protein can be detected in cerebrospinal fluid (CSF) (Imura, Iwano et al. 2004). This strongly suggests a role for shed Klotho protein in the brain; however, this hypothesis has yet to be tested.

MATERIALS AND METHODS

Animal Diets and Procedures

General descriptions regarding animal housing and diets and conditions for sacrifice and tissue storage/processing are described in Section 2.4.1. Acute and chronic FGF23 injections were performed on 8 week old WT male C57BL6 mice obtained from the UT Southwestern Medical Center Mouse Breeding Core Facility. For the chronic FGF23 administration paradigm, mice were conditioned for two weeks prior to the start of the experiment with gentle handling at 2 pm daily. Unless otherwise noted, mice were *ad libitum* fed a standard rodent chow (Teklad Global 16% Protein Rodent Diet, Harlan Laboratories, Indianapolis, IN). Mice that received phosphate-restricted diet (Sections 4.2.2 and 4.2.3) were *ad libitum* fed a custom research diet (0.02% P_i, 1% Ca^{2+}, Harlan Laboratories, Indianapolis, IN) for 7 days.

Experiments conducted in $FGF23^{-/-}$ mice were performed by members of Beate Lanske's laboratory at Harvard School of Dental Medicine in Boston, MA. Kiss1-Cre/GFP mice were generated in the laboratory of Carol Elias at UT Southwestern Medical Center in Dallas, TX (Cravo, Margatho et al. 2011), and FACS sorting and qPCR analysis of GFP+ neurons from these mice was performed by Stan Atkin and Roberta Cravo at UT Southwestern Medical Center in Dallas, TX. These mice were also used for whole-cell electrophysiological recordings, and these experiments were performed by Renata Frazão at UT Southwestern Medical Center in Dallas, TX.

All animal studies were conducted in accordance with standards of ethical and humane care as described in the National Institutes of Health Guide for the Care and Use of Laboratory Animals and using protocols approved by the Institutional Animal Care and Use Committee at University of Texas Southwestern Medical Center (Committee for the Update of the Guide for the Care and Use of Laboratory Animals 2011).

Quantitative Real-time PCR

The procedures employed for RNA isolation, cDNA synthesis, and qPCR analysis are described in Section 2.4.4. The following primers were used for qPCR (listed 5' to 3'): mouse c-Fos, forward CCCACGGTGACAGCCATCTCCA, reverse CTGCGCTCTGCCTCCTGACACG (Kurumaji, Ito et al. 2008); mouse Cyclophilin A, forward GGCCGATGACGAGCCC, reverse TGTCTTTGGAACTTTGTCTGCAA (Trogan, Choudhury et al. 2002); mouse Egr-1, forward CCTATGAGCACCTGACCACA, reverse TCGTTTGGCTGGGATAACTC (Gehrig, Langmann et al. 2007); mouse Klotho, forward AATTATGTGAATGAGGCTCTGAAAG, reverse TACGCAAAGTAGCCACAAAGG.

Klotho *in situ* Hybridization

A detailed procedure for *in situ* hybridization is described in Section 2.4.3. ^{35}S-labeled Klotho antisense and sense riboprobes were prepared from a previously described cDNA construct (Kuro-o, Matsumura et al. 1997).

FACS Cell Sorting and PCR Amplification

FACS sorting and qPCR gene expression analysis of GFP+ neurons from Kiss-Cre/GFP mice was performed by Stan Atkin and Roberta Cravo at UT Southwestern Medical Center in Dallas, TX, according to a published protocol by Cravo et al. (Cravo, Margatho et al. 2011). Primers used for qPCR analysis are listed as follows (listed 5' to 3'): mouse Cyclophilin A, forward GGAGATGGCACAGGAGGAA, reverse GCCCGTAGTGCTTCAGCTT; mouse FGFR1, forward TGTTTGACCGGATCTACACACA, reverse CTCCCACAAGAGCACTCCAA; mouse Kiss1, forward GGCAAAAGTGAAGCCTGGAT, reverse GATTCCTTTTCCCAGGCATT. Mouse Klotho primers are listed above in Section 4.4.2. cDNA content in each reaction was normalized to CyclophilinA.

Western Blotting

Flash-frozen tissues were homogenized by sonication in a standard tissue lysis buffer containing protease and phosphatase inhibitor cocktails. After lysis, samples were centrifuged for 12 minutes at 14,000 RPM at 4^{o}C to remove any insoluble material. Supernatants were collected, and protein concentration of each sample was measured by Micro BCA Protein Assay (Pierce, Waltham, MA). 4X sodium dodecyl sulfate (SDS) loading buffer was added to the sample, and they were boiled for 5 minutes. 30 μg of protein per sample was subjected to SDS-polyacrylamide gel electrophoresis (SDS-PAGE). Proteins were transferred via overnight wet transfer to a Hybond-C Extra nitrocellulose membrane (Amersham Biosciences, Piscataway, NJ).

For immunoblotting, membranes were blocked for 30 minutes at RT in a 5% milk solution. Membranes were incubated with primary antibody for 1 hour at RT. Primary antibodies consisted of anti-Klotho rat monoclonal antibody (KM2119) (Kato, Arakawa et al. 2000) or anti-GAPDH rabbit polyclonal antibody (ab9485, Abcam, Cambridge, UK). Membranes were then washed 3X for 10 minutes each in TBST. Secondary antibody was added and incubated with each membrane for 1 hour at RT. Secondary antibodies consisted of anti-rat antibody conjugated to horseradish peroxidase (HRP) or anti-rabbit-HRP. Membranes were again washed 4X for 10 minutes each in TBST. Membranes were reacted for 1 minute with SuperSignal West Dura Chemiluminescent

Substrate (Thermo Scientific, Waltham, MA), and enhanced chemiluminescence (ECL) signals were captured on autoradiography film.

Peripheral FGF23 Administration

Non-degradable recombinant human FGF23 (R179Q) was generously provided by Moosa Mohammadi (New York University Langone Medical Center, New York, NY), and synthesized as previously described (Plotnikov, Hubbard et al. 2000).

Acute Paradigm

8 week old male C57BL6 mice were IP injected with vehicle (150mM saline) or human FGF23 (R179Q) at a dose of 0.3 mg/kg. At 25 minutes post injection, animals were anesthetized with Avertin (200 μL/10 g body weight). At 30 minutes post injection, animals were sacrificed by cervical dislocation and tissues were harvested and snap frozen in liquid nitrogen and stored at -80^{o}C until further use.

Chronic Paradigm

8 week old male C57BL6 mice were conditioned for two weeks with gentle handling at 2 pm daily prior to the start of the experiment. These animals

then received 3 IP injections of either vehicle (150 mM saline) or human FGF23 (R179Q) (1 mg/kg dose). Injections were given at 2 pm on day one, and again at 2 am and 2 pm on the following day. Two hours after the final injection mice were anesthetized with Avertin (200 μL/10g body weight) and perfused as described in Section 2.4.1. Brain sections were also prepared and stored as described in Section 2.4.1.

c-Fos Immunohistochemistry

Brains and pituitary glands from animals receiving the chronic FGF23 treatment paradigm (Section 4.4.5) were processed and analyzed for c-Fos immunoreactivity. Animals were perfused and brains were processed as described in Section 2.4.1. Perfusion was performed by Charlotte Lee, and brain sectioning and staining were performed by Danielle Lauzon and Matthew Harper at UT Southwestern Medical Center, Dallas, TX. Immunohistochemistry was performed as previously described (Donato, Cavalcante et al. 2010), using an anti-c-Fos rabbit polyclonal antibody (PC38, Calbiochem, Gibbstown, NJ).

Fixed pituitary glands were frozen in Tissue-Tek OCT Compound (Sakura, The Netherlands) at -20^{o}C. 5 μm pituitary sections were prepared on a freezing microtome and mounted onto Superfrost Plus microscope slides (Fisher Scientific, Waltham, MA). The following steps were performed on an orbital

shaker. Slides were blocked in 0.3% hydrogen peroxide (H_2O_2) for 30 minutes and then washed 3X in PBS for 10 minutes each. Slides received an additional block in PBT with 3% normal donkey serum for 30 minutes. Slides were then incubated with anti-c-Fos rabbit polyclonal antibody (PC38, Calbiochem, Gibbstown, NJ) overnight at 4^{o}C. The next day, slides were washed 3X with PBS for 10 minutes each. Slides were then incubated with secondary antibody (biotinylated-anti-rabbit) for 1 hour at RT. Sides were again washed 3X in PBS for 10 minutes each. Slides were next incubated with Avidin Biotin Complex (in which biotinylated HRP was allowed to complex with Avidin), for 1 hour. Again, slides were washed 3X in PBS for 10 minutes each. Next, slides were reacted with nickel-enhanced DAB solution for 4-6 minutes until sufficient color developed. Slides were then rinsed with tap water to stop the reaction. Once the slides were dry, coverslips were mounted with Permount mounting medium (Fisher Scientific, Waltham, MA).

FGF23 ^{125}I Labeling and Quantification of Tissue Incorporation

Recombinant human FGF23 (R179Q) was provided by Moosa Mohammadi (New York University Langone Medical Center, New York, NY), and prepared as described in Section 4.5.5. FGF23 was labeled with ^{125}I using Pre-coated Iodination Tubes (Pierce, Waltham, MA) following the Chizzonite

Indirect Iodination Method, as described by the manufacturer. $Na^{125}I$ was purchased from Perkin Elmer (Waltham, MA). Specific activity of ^{125}I-FGF23 was determined using a standard trichloroacetic acid (TCA) precipitation protocol.

We followed several published protocols for measurement of BBB permeability and tissue incorporation of IP injected ^{125}I-FGF23 (Kastin, Akerstrom et al. 2001; Boje 2002; Hsuchou, Pan et al. 2007). Animals were sacrificed 3, 5, 10, 30, 60, 120, and 240 minutes post-injection by decapitation. Approximately 2 minutes before decapitation, each mouse was anesthetized with Avertin (200 μL/10 g body weight). Whole blood and tissues were collected, weighed, and placed in scintillation vials into which scintillation fluid (3a70B Complete Counting Cocktail, Research Products International Corp, Mount Prospect, IL) was added. Brains were dissected into cerebellum, hypothalamus, cortex, and sub-cortical regions. Scintillation counts per minute (cpm) were measured using a liquid scintillation counter. Data is expressed as a ratio of (cpm)/g (tissue):cpm/g (blood). When tissue/blood ratio is plotted versus time, a positive slope indicates tissue incorporation of ^{125}I-FGF23, a negative slope indicates clearance of ^{125}I-FGF23, and a slope of zero indicates no tissue incorporation of ^{125}I-FGF23.

Whole-cell Recordings

A detailed protocol for whole-cell recordings using Kiss1-Cre/GFP mice is described in Section 3.4.7. Recombinant human FGF23 (R179Q) used in this experiment was generously provided through collaboration with Genzyme (Cambridge, MA).

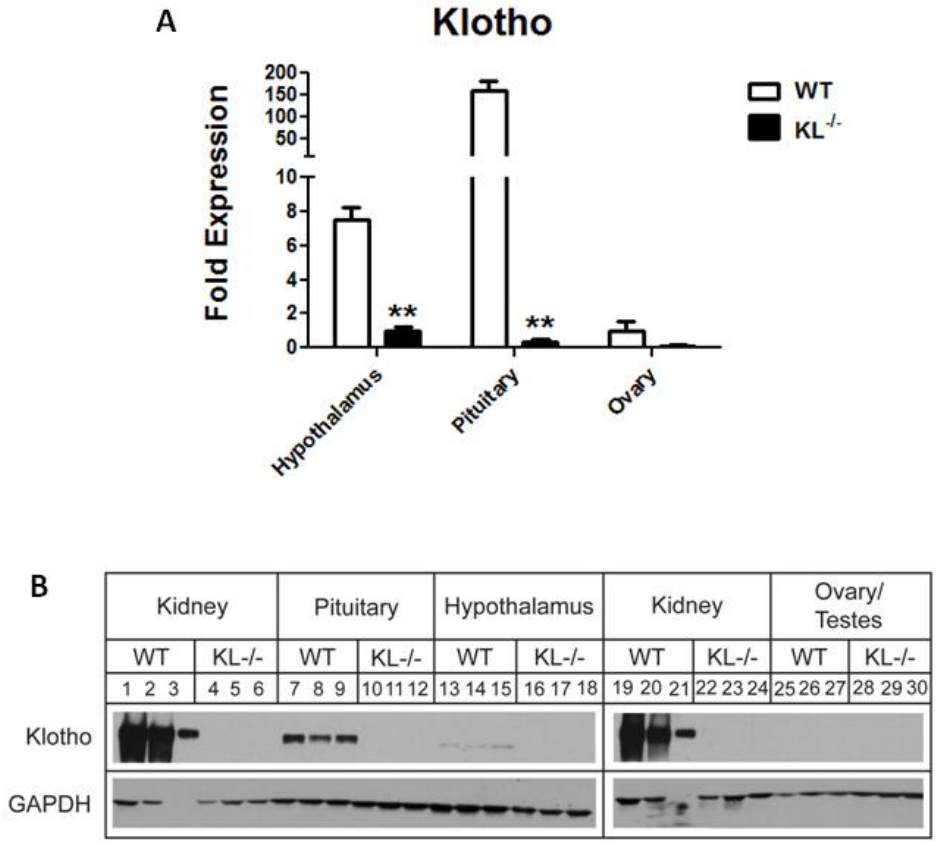

Figure 4-1. Klotho is expressed in the kidneys, pituitary gland, and the hypothalamus, but not the ovaries. (A) Klotho mRNA expression was measured by qPCR in wild-type (WT) versus Klotho knockout ($KL^{-/-}$) females at 8 weeks of age. Data are plotted as fold expression relative to WT ovary. Double asterisk indicates statistical significance between WT and $KL^{-/-}$ within the same tissue ($p<0.005$, Student's t-test). (B) Klotho protein expression was detected via Western Blotting. Protein in lanes 1-28 was isolated from 8 week old females. Protein in lanes 3 and 21 was diluted 1:10. Each lane represents one mouse (i.e. protein expression was measured in triplicate, except for $KL^{-/-}$ ovary which was only measured in singlet (lane 28). Protein in lanes 29 and 30 is from testes from two 8 week old $KL^{-/-}$ males.

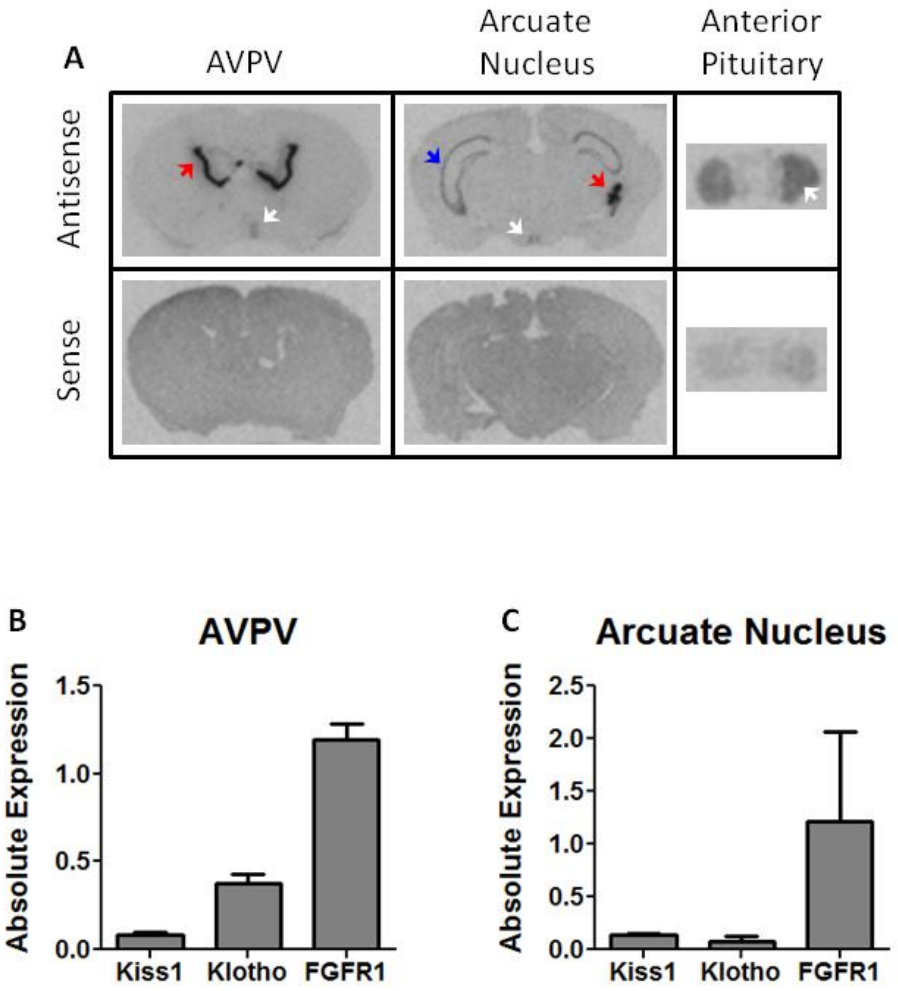

Figure 4-2. Klotho is preferentially expressed in the AVPV and arcuate nucleus of the hypothalamus. (A) Klotho *in situ* hybridization was performed on serial brain and pituitary sections from 60 day old WT female mice in diestrus. Sections were incubated with antisense and sense probes. White arrowheads indicate Klotho mRNA expression in the AVPV, Arc, and the anterior pituitary gland. Red arrowheads indicate Klotho expression in the choroid plexus. The blue arrowhead indicates Klotho expression in the hippocampus. (B) AVPV and Arc nuclei were dissected from Kiss1-Cre/GFP mice, and GFP+ cells were FACS sorted from these neuronal populations. cDNA was amplified from the GFP+ cell population, and mRNA expression of Kiss1, Klotho, and FGFR1 was determined by qPCR analysis.

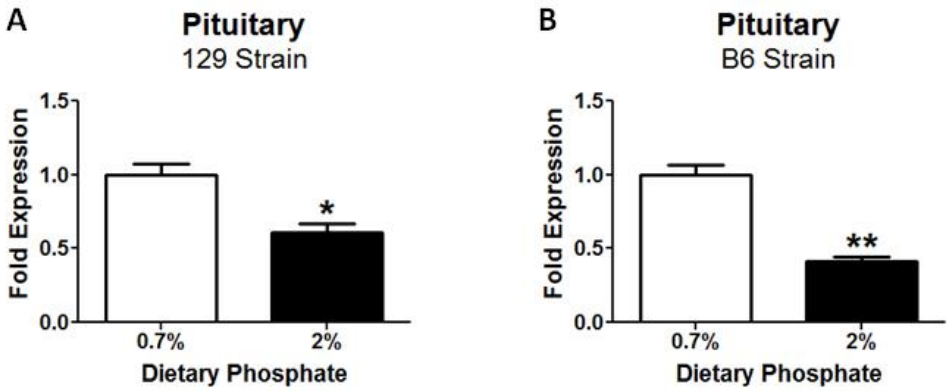

Figure 4-3. Klotho expression in the pituitary gland is decreased by high phosphate feeding. Klotho mRNA expression was measured by qPCR in mice weaned onto normal chow (0.7% Pi) or high phosphate chow (2% Pi) and maintained on each diet for 10 weeks. Experiments were conducted in WT 129 females (A) or WT B6 females (B). Single asterisk indicates $p<0.05$, and double asterisk indicates $p<0.005$ (Student's t-test).

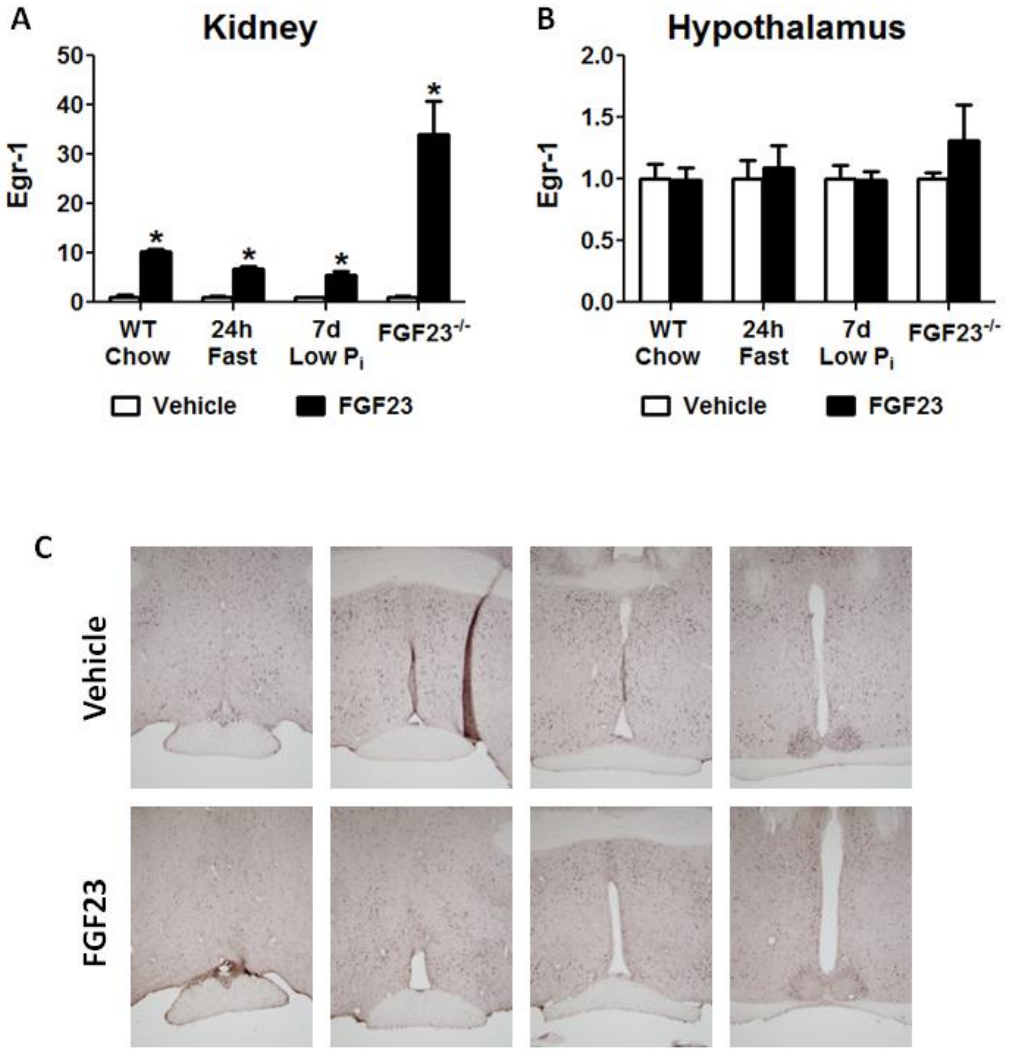

Figure 4-4. Peripherally-injected FGF23 does not induce Egr-1 mRNA or c-Fos protein upregulation in the hypothalamus. (A-B) Vehicle or 0.3 mg/kg FGF23 was IP injected into mice, which were sacrificed 30 minutes post-injection (acute injection paradigm). mRNA expression in kidney (A) and hypothalamus (B) was measured by qPCR. WT Chow: WT animals on normal chow diet; 24h Fast: WT animals were fasted for 24 hours prior to FGF23 injection; 7d Low P_i: WT animals on 0.02% Pi chow for 7 days prior to FGF23 injection; $FGF23^{-/-}$: FGF23 knockout animals on normal chow diet. Asterisk indicates $p<0.05$ (Student's t-test). (C) FGF23 chronic injection paradigm. WT animals received 3 IP injections of vehicle or 1 mg/kg FGF23 (each 12 hours apart). Animals were sacrificed 2 hours after the last injection and brains were stained for c-Fos immunoreactivity. AVPV sections are presented rostral to caudal (left to right).

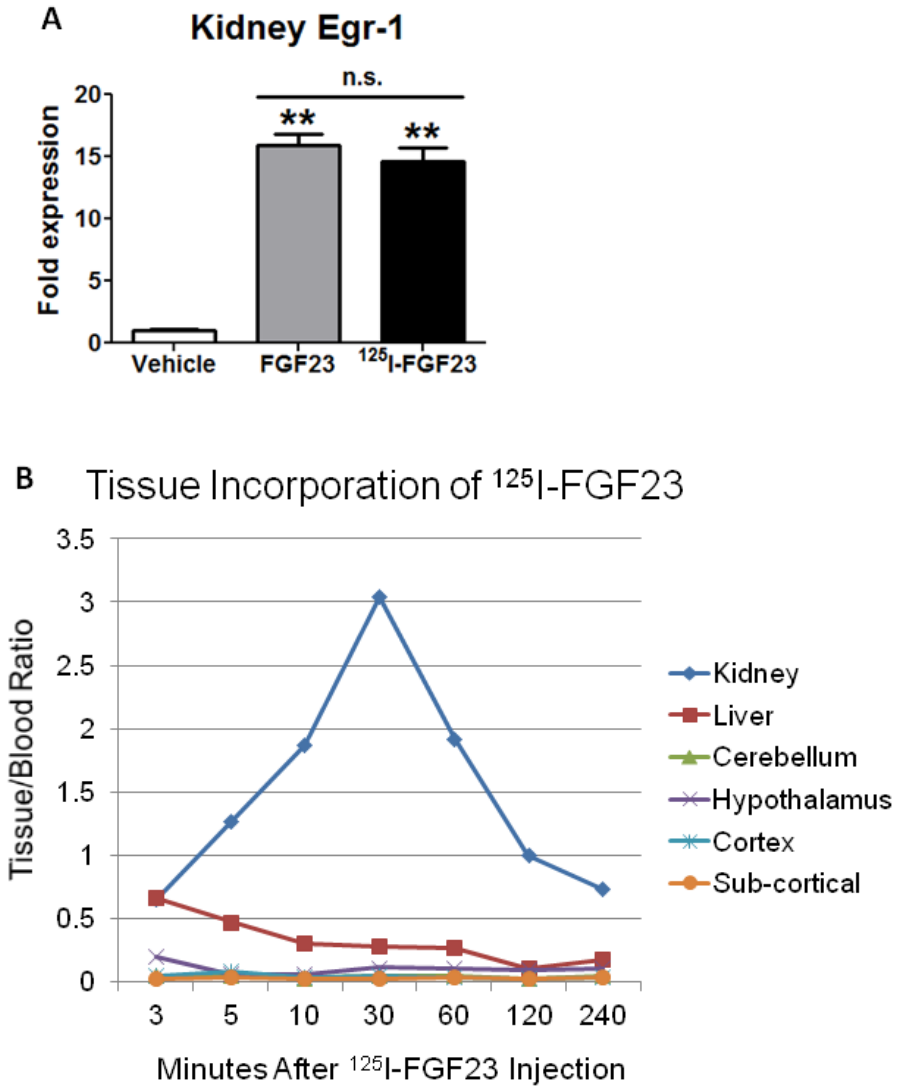

Figure 4-5. FGF23 does not cross the BBB. FGF23 was labeled with ^{125}I and IP injected into WT B6 mice. (A) Mice were sacrificed 30 minutes post-injection, and Egr-1 expression in kidney was measured by qPCR. Double asterisk indicates significant difference from vehicle with $p<0.005$ (Student's t-test). "n.s." indicates no significant difference between FGF23 and ^{125}I-FGF23 groups. (B) Mice were sacrificed at indicated timepoints and tissue incorporation of ^{125}I-FGF23 was measured by scintillation counting. Data are expressed as a ratio of cpm/g tissue: cpm/g blood. Tissue incorporation is indicated by a positive slope and a tissue/blood ratio>0.1.

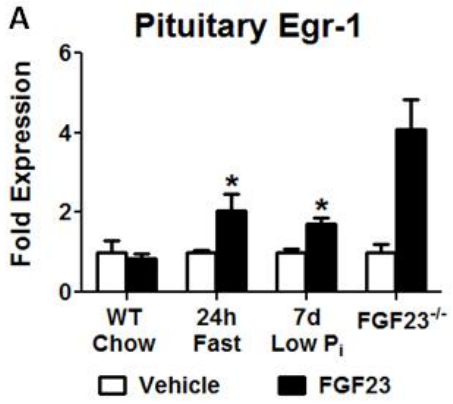
A
Pituitary Egr-1
Fold Expression
6
4
2
0
*
*
WT Chow
24h Fast
7d Low Pi
FGF23-/-
Vehicle
FGF23

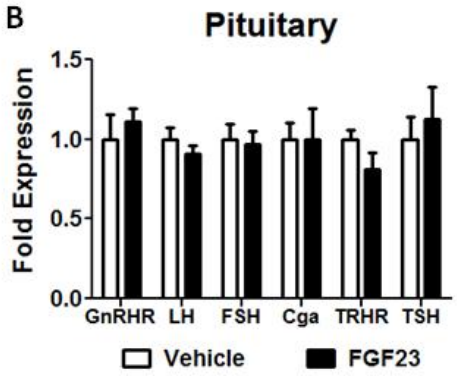
B
Pituitary
Fold Expression
1.5
1.0
0.5
0.0
GnRHR
LH
FSH
Cga
TRHR
TSH
Vehicle
FGF23

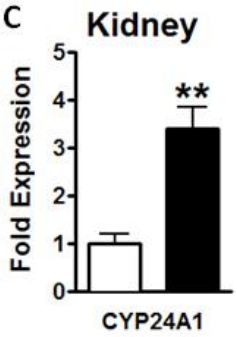
C
Kidney
Fold Expression
5
4
3
2
1
0
**
CYP24A1

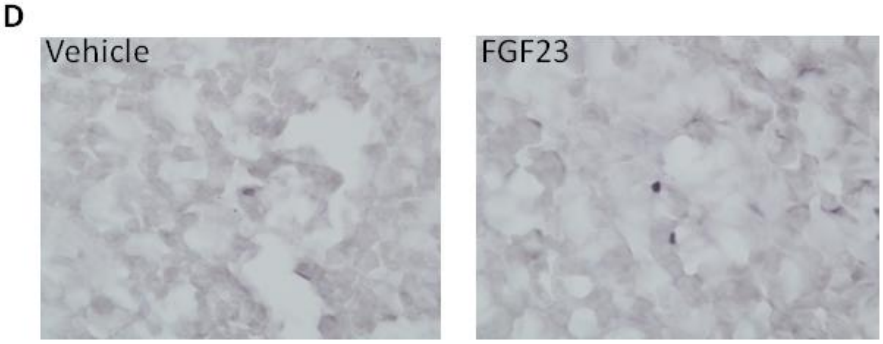
D
Vehicle
FGF23

Figure 4-6. FGF23 upregulates Egr-1 in the pituitary but only under altered physiological conditions, and does not induce changes in downstream gene expression. (A) FGF23 acute injection paradigm. Vehicle or 0.3 mg/kg FGF23 was IP injected into mice, which were sacrificed 30 minutes post-injection. Egr-1 expression in the pituitary gland was measured by qPCR. WT Chow: WT animals on normal chow diet; 24h Fast: WT animals were fasted for 24 hours prior to FGF23 injection; 7d Low P_i: WT animals on 0.02% Pi chow for 7 days prior to FGF23 injection; $FGF23^{-/-}$: FGF23 knockout animals on normal chow diet. Asterisk indicates $p<0.05$ (Student's t-test). (B-C) Animals were injected with vehicle or 0.3 mg/kg FGF23 and sacrificed 6 hours later. Downstream gene expression was measured in the pituitary (B) and the kidney (C) by qPCR. Double asterisk indicates $p<0.05$ (Student's t-test). (D) FGF23 chronic injection paradigm. WT animals received 3 IP injections of vehicle or 1 mg/kg FGF23 (each 12 hours apart). Animals were sacrificed 2 hours after the last injection and pituitary glands were stained for c-Fos immunoreactivity.

CHAPTER FIVE
Concluding Remarks and Future Directions

A NOVEL MOUSE MODEL FOR REPRODUCTIVE DYSFUNCTION IN CHRONIC KIDNEY DISEASE

Chronic kidney disease (CKD) is defined as a state of impaired renal function over for 3 months or longer. CKD can be caused not only by kidney diseases such as polycystic kidney and glomerulonephritis but also by any diseases that affect kidney, most notably hypertension and diabetes. CKD affects more than 10% of the total population in many countries and is recognized as a global public health problem (Stevens, Li et al. 2010). Hyperphosphatemia is observed universally in CKD patients and is identified as a potent mortality risk factor (Tonelli, Sacks et al. 2005). The vast majority of CKD patients die from early onset of age-related conditions such as cardiovascular disease, cancer, or infection, resulting in significant increases in all-cause mortality. CKD patients exhibit low renal Klotho expression and high blood FGF23 levels (i.e. resistance to FGF23) and suffer many complications reminiscent of $KL^{-/-}$ mice, including hyperphosphatemia, osteopenia, vascular calcification, cardiac hypertrophy, and hypogonadism. Furthermore, like $KL^{-/-}$ mice, P_i restriction (low P_i diet and P_i binders) improves clinical outcome of CKD patients (Ibels, Alfrey et al. 1978; Martin and Gonzalez 2011), indicating that dietary P_i overload that exceeds renal

capacity of P_i excretion contributes to pathophysiology of CKD. Thus, our current studies may have relevance to CKD.

Juvenile CKD

In this dissertation, we have shown that female mice undergoing phosphate overload (both $KL^{-/-}$ and WT mice fed high phosphate chow) exhibit reproductive dysfunction. These mice fail to initiate and carry our proper puberty and exhibit a state of hypogonadotropic hypogonadism. This failed pubertal progression leads to hypothalamic anovulation in these mice. We presume these effects to be largely due to a loss of proper Kiss1 expression in the hypothalamus of these animals.

In our model, $KL^{-/-}$ and WT females fed high phosphate diet develop a positive phosphate balance before puberty has begun. $KL^{-/-}$ mice have already developed hyperphosphatemia at after weaning and WT mice develop hyperphosphatemia within days of beginning a high phosphate diet (unpublished observations). Since our WT mice are weaned onto high Pi chow, they also experience phosphate overload shortly after weaning. Thus, our female mouse models of phosphate overload may mimic what is seen in juvenile CKD but may be distinct from adult CKD that develops after puberty. Juvenile CKD patients experience a loss of kidney function and subsequent positive phosphate balance

before puberty initiation (Lane 2005). Thus pubertal delay and blunted hormone production in these patients may result from a prior state of phosphate overload.

According to William's Textbook of Endocrinology, "There has been little research of sexual function in women with renal disease" (Kronenberg, Melmed et al. 2008). From our comprehensive review of the available literature there is considerably much less research concerning reproductive function in children with renal disease and all available studies have been conducted in humans. Thus our model represents a novel rodent system in which to study the effects of positive phosphate balance on puberty. We suggest that $KL^{-/-}$ mice and WT mice on high phosphate diet may present an invaluable tool for gathering *in vivo* mechanistic insight into failed or blunted puberty associated with juvenile CKD.

If our mouse models of phosphate overload are indeed a good model for juvenile CKD, they would suggest that Kiss1 expression and thus Kisspeptin secretion may be altered in children with renal failure. Since we believe low levels of Kiss1 to be the primary cause of infertility in female mouse models of phosphate overload, we would therefore like to measure Kisspeptin levels in serum of juvenile CKD patients.

Adult CKD

We believe that our model of phosphate overload in WT female mice could easily be extended to become a model for adult CKD. Adult female CKD patients develop a positive phosphate balance after pubertal completion and achievement of full fertility. Yet these patients suffer from reproductive dysfunction commonly including disrupted menstrual cycling, aberrant gonadotropin regulation, anovulation, and infertility (Holley 2004).

Thus, we would like to establish a new model of phosphate overload in WT female mice and CKD model mice by beginning high phosphate diet after full achievement of puberty and sexual maturity. We would like to investigate estrus cycling, ovulation, HPG axis hormone levels, and fertility in these adult once they have sustained a positive phosphate balance. Our results could provide a novel rodent model for infertility phenotypes associated with CKD and could generate further mechanistic insight into the underlying causes of reproductive dysfunction in adult CKD.

Furthermore, we would also like to measure Kisspeptin levels in women with CKD. No our knowledge, no such investigation has been made to date. If Kisspeptin levels are altered in women with CKD, this could represent a novel treatment target for sexual dysfunction in women with renal failure.

Treatment Recommendations for Sexual Dysfunction Associated with CKD

Current treatments for female sexual dysfunction in CKD are aimed at restoring normal hormone levels and cyclicity with hormone replacement therapy. These treatments usually include oral progesterone and estradiol administration. Testosterone therapy may also be used to treat hypoactive sexual desire disorder in women with CKD. However, these treatments are not effective in all patients and do not address the underlying cause of the hormonal aberrations in these patients (Anantharaman and Schmidt 2007; Taal, Chertow et al. 2011).

Based on evidence from our mouse models, we would suggest therapy aimed at reducing phosphate load in these patients. Phosphate-restricted diet and phosphate binders may be effective at relieving some symptoms associated with reproductive dysfunction in women with CKD. It is important to note that we believe these treatments should be administered to patients before overt hyperphosphatemia is observed. Positive phosphate balance occurs before hyperphosphatemia in disease progression and can be recognized by elevated serum FGF23 and PTH (Taal, Chertow et al. 2011).

FUTURE EXPERIMENTS

Understanding the Mechanism of Phosphate Overload-induced Female Infertility

In Chapter 2, we investigated the acute effects of high phosphate treatment on electrophysiological properties of AVPV/PeN Kiss1 neurons. It may not be surprising that phosphate treatment did not elicit a change in RMP or input resistance of these cells because there are no known phosphate-sensitive ion channels in neurons. However, we still believe this whole-cell recording system will be useful for us in future experiments.

Frazão et al. have demonstrated that AVPV/PeN Kiss1 neurons in prepubertal females have strikingly different electrophysiological properties from those observed in sexually mature females (Frazão et al., submitted). We would like to measure electrophysiological properties of AVPV/PeN Kiss1 neurons in female Kiss1-Cre/GFP mice that have undergone high phosphate feeding. We suspect that even though these animals will be of reproductive age, they may exhibit electrophysiological properties similar to those observed in prepubertal animals. This data would indicate to us that phosphate overload may perturb Kiss1 neuronal function at the level of the neuron itself. However, this does not address whether sustained levels of high serum phosphate are directly toxic to Kiss1 neurons or whether an intermediary factor upregulated by positive phosphate balance acts on Kiss1 neurons to mediate these effects.

Effects of Phosphate Overload on Male Fertility

In this dissertation, we have only examined the effects of phosphate overload on female fertility. However, we believe it will be worthwhile to extend our current models to investigate the effects of phosphate overload on male fertility. Indeed, $KL^{-/-}$ males are infertile and are completely deficient in sperm production (Kuro-o, Matsumura et al. 1997), which can be rescued by low P_i diet (data not shown). Furthermore, men and adolescent males with CKD suffer from sexual dysfunction and perturbed puberty, respectively (Holley 2004; Lane 2005; Anantharaman and Schmidt 2007).

High phosphate feeding in normal WT adult male mice (beginning at 12 weeks of age) does not inhibit sperm production in these mice (unpublished data from our laboratory). Therefore, dietary phosphate overload in adult male mice may not be a good model for male sexual dysfunction associated with adult CKD. However, we have not measured pituitary or gonadal hormone production by these mice, which could be abnormal even though sperm are still produced.

However, we believe that $KL^{-/-}$ males and WT males fed high phosphate diet from weaning may prove to be a valuable model for investigating the mechanisms of perturbed puberty associated with juvenile CKD. Unlike female mice undergoing phosphate overload, infertility in $KL^{-/-}$ males may not be due to perturbed Kiss1 regulation because Kiss1 mRNA levels were normal in these mice as measured by qPCR and *in situ* hybridization (data not shown). This may not be surprising because it has been well documented that Kiss1 expression is

sexually dimorphic and is markedly higher in the AVPV of females than males (Clarkson and Herbison 2006; Kauffman, Gottsch et al. 2007). In rodents the AVPV is a sexually differentiated structure that is much more prominent in females versus males, and AVPV is thought to modulate the preovulatory GnRH/LH surge, which is absent in males (Oakley, Clifton et al. 2009). Therefore, an alternate system may mediate phosphate overload-induced infertility in $KL^{-/-}$ males.

A CAUTION AGAINST EXCESS PHOSPHATE CONSUMPTION

Our model of dietary phosphate overload in female mice does not include a dramatic increase in phosphate consumption. Mice are fed less than 3 fold more phosphate on high P_i diet than control diet. Yet, this increase in phosphate consumption is enough to result in significant changes in reproductive health in WT animals. Furthermore, unpublished data from our laboratory suggests that high phosphate feeding in WT mice also affects multiple organ systems besides the HPG axis including most notably the kidneys, liver, skeletal muscle, and heart (data not shown).

Although humans and rodents may handle excess dietary phosphate differently, our results and others' suggest that high phosphate consumption in otherwise healthy individuals may be detrimental to health (Bell, Draper et al.

1977). Some level of phosphate consumption is unavoidable and altogether necessary for survival. However, we would caution against excess consumption of highly processed foods containing phosphate-derived preservatives. Such additives are now estimated to increase phosphorus intake by as much as 1.0 g/day (Uribarri 2009). Furthermore, we would suggest that the USDA change their policies for nutrient measurement to include food preservatives and not just vitamin fortifications and additives. This would allow for greater knowledge and control of true levels of dietary phosphate consumption in humans and would be very valuable for CKD patients who are prescribed a phosphate-restricted diet.

BIBLIOGRAPHY

ADHR Consortium (2000). "Autosomal dominant hypophosphataemic rickets is associated with mutations in FGF23." Nat Genet **26**(3): 345-348.

Anantharaman, P. and R. J. Schmidt (2007). "Sexual function in chronic kidney disease." Adv Chronic Kidney Dis **14**(2): 119-125.

Ardissino, G., V. Dacco, et al. (2003). "Epidemiology of chronic renal failure in children: data from the ItalKid project." Pediatrics **111**(4 Pt 1): e382-387.

Beck, L., A. C. Karaplis, et al. (1998). "Targeted inactivation of Npt2 in mice leads to severe renal phosphate wasting, hypercalciuria, and skeletal abnormalities." Proc Natl Acad Sci U S A **95**(9): 5372-5377.

Bell, R. R., H. H. Draper, et al. (1977). "Physiological responses of human adults to foods containing phosphate additives." J Nutr **107**(1): 42-50.

Ben-Dov, I. Z., H. Galitzer, et al. (2007). "The parathyroid is a target organ for FGF23 in rats." J Clin Invest **117**(12): 4003-4008.

Benet-Pages, A., P. Orlik, et al. (2005). "An FGF23 missense mutation causes familial tumoral calcinosis with hyperphosphatemia." Hum Mol Genet **14**(3): 385-390.

Bergwitz, C. and H. Juppner (2010). "Regulation of phosphate homeostasis by PTH, vitamin D, and FGF23." Annu Rev Med **61**: 91-104.

Bianchetti, L., C. Oudet, et al. (2002). "M13 endopeptidases: New conserved motifs correlated with structure, and simultaneous phylogenetic occurrence of PHEX and the bony fish." Proteins **47**(4): 481-488.

Bogovich, K. and J. S. Richards (1982). "Androgen biosynthesis in developing ovarian follicles: evidence that luteinizing hormone regulates thecal 17 alpha-hydroxylase and C17-20-lyase activities." Endocrinology **111**(4): 1201-1208.

Boje, K. M. (2002). "In vivo measurement of blood-brain barrier permeability." Curr Protoc Pharmacol **Chapter 7**: Unit 7 4.

Bookout, A. L., C. L. Cummins, et al. (2006). "High-throughput real-time quantitative reverse transcription PCR." Curr Protoc Mol Biol **Chapter 15**: Unit 15 18.

Boyar, R. M., R. S. Rosenfeld, et al. (1974). "Human puberty. Simultaneous augmented secretion of luteinizing hormone and testosterone during sleep." J Clin Invest **54**(3): 609-618.

Brown, E. M. and R. J. MacLeod (2001). "Extracellular calcium sensing and extracellular calcium signaling." Physiol Rev **81**(1): 239-297.

Brownstein, C. A., J. Zhang, et al. (2010). "Increased bone volume and correction of HYP mouse hypophosphatemia in the Klotho/HYP mouse." Endocrinology **151**(2): 492-501.

Caligioni, C. S. (2009). "Assessing reproductive status/stages in mice." Curr Protoc Neurosci **Appendix 4**: Appendix 4I.

Calvo, M. S. and Y. K. Park (1996). "Changing phosphorus content of the U.S. diet: potential for adverse effects on bone." J Nutr **126**(4 Suppl): 1168S-1180S.

Camalier, C. E., M. R. Young, et al. (2010). "Elevated phosphate activates N-ras and promotes cell transformation and skin tumorigenesis." Cancer Prev Res (Phila) **3**(3): 359-370.

Cariboni, A. and R. Maggi (2006). "Kallmann's syndrome, a neuronal migration defect." Cell Mol Life Sci **63**(21): 2512-2526.

Castellano, J. M., V. M. Navarro, et al. (2005). "Changes in hypothalamic KiSS-1 system and restoration of pubertal activation of the reproductive axis by kisspeptin in undernutrition." Endocrinology **146**(9): 3917-3925.

Cha, S. K., M. C. Hu, et al. (2009). "Regulation of renal outer medullary potassium channel and renal K(+) excretion by Klotho." Mol Pharmacol **76**(1): 38-46.

Cha, S. K., B. Ortega, et al. (2008). "Removal of sialic acid involving Klotho causes cell-surface retention of TRPV5 channel via binding to galectin-1." Proc Natl Acad Sci U S A **105**(28): 9805-9810.

Chen, C. D., S. Podvin, et al. (2007). "Insulin stimulates the cleavage and release of the extracellular domain of Klotho by ADAM10 and ADAM17." Proc Natl Acad Sci U S A **104**(50): 19796-19801.

Clarkson, J., X. d'Anglemont de Tassigny, et al. (2009). "Distribution of kisspeptin neurones in the adult female mouse brain." J Neuroendocrinol **21**(8): 673-682.

Clarkson, J. and A. E. Herbison (2006). "Postnatal development of kisspeptin neurons in mouse hypothalamus; sexual dimorphism and projections to gonadotropin-releasing hormone neurons." Endocrinology **147**(12): 5817-5825.

Cohen-Becker, I. R., M. Selmanoff, et al. (1986). "Hyperprolactinemia alters the frequency and amplitude of pulsatile luteinizing hormone secretion in the ovariectomized rat." Neuroendocrinology **42**(4): 328-333.

Collins, M. T., J. R. Lindsay, et al. (2005). "Fibroblast growth factor-23 is regulated by 1alpha,25-dihydroxyvitamin D." J Bone Miner Res **20**(11): 1944-1950.

Committee for the Update of the Guide for the Care and Use of Laboratory Animals (2011). Guide for the Care and Use of Laboratory Animals. Washington, D.C., The National Academies Press.

Crampton, J. R. (2011). Prolactin Regulation of Kisspeptin Neurons. Bachelor of Medical Science with Honours, University of Otago.

Craver, L., M. P. Marco, et al. (2007). "Mineral metabolism parameters throughout chronic kidney disease stages 1-5--achievement of K/DOQI target ranges." Nephrol Dial Transplant **22**(4): 1171-1176.

Cravo, R. M., L. O. Margatho, et al. (2011). "Characterization of Kiss1 neurons using transgenic mouse models." Neuroscience **173**: 37-56.

Cravo, R. M., L. O. Margatho, et al. (2011). "Characterization of Kiss1 neurons using transgenic mouse models." Neuroscience **173**: 37-56.

d'Anglemont de Tassigny, X., L. A. Fagg, et al. (2008). "Kisspeptin can stimulate gonadotropin-releasing hormone (GnRH) release by a direct action at GnRH nerve terminals." Endocrinology **149**(8): 3926-3932.

d'Anglemont de Tassigny, X., L. A. Fagg, et al. (2007). "Hypogonadotropic hypogonadism in mice lacking a functional Kiss1 gene." Proc Natl Acad Sci U S A **104**(25): 10714-10719.

de Roux, N., E. Genin, et al. (2003). "Hypogonadotropic hypogonadism due to loss of function of the KiSS1-derived peptide receptor GPR54." Proc Natl Acad Sci U S A **100**(19): 10972-10976.

Doi, S., Y. Zou, et al. (2011). "Klotho inhibits transforming growth factor-beta1 (TGF-beta1) signaling and suppresses renal fibrosis and cancer metastasis in mice." J Biol Chem **286**(10): 8655-8665.

Donato, J., Jr., J. C. Cavalcante, et al. (2010). "Male and female odors induce Fos expression in chemically defined neuronal population." Physiol Behav **99**(1): 67-77.

Donato, J., Jr., R. M. Cravo, et al. (2011). "Leptin's effect on puberty in mice is relayed by the ventral premammillary nucleus and does not require signaling in Kiss1 neurons." J Clin Invest **121**(1): 355-368.

Donato, J., Jr., R. J. Silva, et al. (2009). "The ventral premammillary nucleus links fasting-induced changes in leptin levels and coordinated luteinizing hormone secretion." J Neurosci **29**(16): 5240-5250.

Dorrington, J. H., Y. S. Moon, et al. (1975). "Estradiol-17beta biosynthesis in cultured granulosa cells from hypophysectomized immature rats; stimulation by follicle-stimulating hormone." Endocrinology **97**(5): 1328-1331.

El-Abbadi, M. M., A. S. Pai, et al. (2009). "Phosphate feeding induces arterial medial calcification in uremic mice: role of serum phosphorus, fibroblast growth factor-23, and osteopontin." Kidney Int **75**(12): 1297-1307.

Elias, C. F. (2012). "Leptin action in pubertal development: recent advances and unanswered questions." Trends Endocrinol Metab **23**(1): 9-15.

Ewence, A. E., M. Bootman, et al. (2008). "Calcium phosphate crystals induce cell death in human vascular smooth muscle cells: a potential mechanism in atherosclerotic plaque destabilization." Circ Res **103**(5): e28-34.

Falender, A. E., R. Lanz, et al. (2003). "Differential expression of steroidogenic factor-1 and FTF/LRH-1 in the rodent ovary." Endocrinology **144**(8): 3598-3610.

Farrow, E. G., L. J. Summers, et al. (2010). "Altered renal FGF23-mediated activity involving MAPK and Wnt: effects of the Hyp mutation." J Endocrinol **207**(1): 67-75.

Feild, J. A., L. Zhang, et al. (1999). "Cloning and functional characterization of a sodium-dependent phosphate transporter expressed in human lung and small intestine." Biochem Biophys Res Commun **258**(3): 578-582.

Feng, J. Q., L. M. Ward, et al. (2006). "Loss of DMP1 causes rickets and osteomalacia and identifies a role for osteocytes in mineral metabolism." Nat Genet **38**(11): 1310-1315.

Foley, R. N., P. S. Parfrey, et al. (1998). "Epidemiology of cardiovascular disease in chronic renal disease." J Am Soc Nephrol **9**(12 Suppl): S16-23.

Fon Tacer, K., A. L. Bookout, et al. (2010). "Research resource: Comprehensive expression atlas of the fibroblast growth factor system in adult mouse." Mol Endocrinol **24**(10): 2050-2064.

Forster, R. E., P. W. Jurutka, et al. (2011). "Vitamin D receptor controls expression of the anti-aging klotho gene in mouse and human renal cells." Biochem Biophys Res Commun **414**(3): 557-562.

Fowler, R. E. and R. G. Edwards (1957). "Induction of superovulation and pregnancy in mature mice by gonadotrophins." J Endocrinol **15**(4): 374-384.

Frasor, J., D. H. Barnett, et al. (2003). "Response-specific and ligand dose-dependent modulation of estrogen receptor (ER) alpha activity by ERbeta in the uterus." Endocrinology **144**(7): 3159-3166.

Frishberg, Y., N. Ito, et al. (2007). "Hyperostosis-hyperphosphatemia syndrome: a congenital disorder of O-glycosylation associated with augmented processing of fibroblast growth factor 23." J Bone Miner Res **22**(2): 235-242.

Frishberg, Y., O. Topaz, et al. (2005). "Identification of a recurrent mutation in GALNT3 demonstrates that hyperostosis-hyperphosphatemia syndrome and familial tumoral calcinosis are allelic disorders." J Mol Med (Berl) **83**(1): 33-38.

Fukumoto, S. (2009). "The role of bone in phosphate metabolism." Mol Cell Endocrinol **310**(1-2): 63-70.

Funes, S., J. A. Hedrick, et al. (2003). "The KiSS-1 receptor GPR54 is essential for the development of the murine reproductive system." Biochem Biophys Res Commun **312**(4): 1357-1363.

Gambacciani, M., S. S. Yen, et al. (1986). "GnRH release from the mediobasal hypothalamus: in vitro inhibition by corticotropin-releasing factor." Neuroendocrinology **43**(4): 533-536.

Gattineni, J., C. Bates, et al. (2009). "FGF23 decreases renal NaPi-2a and NaPi-2c expression and induces hypophosphatemia in vivo predominantly via FGF receptor 1." Am J Physiol Renal Physiol **297**(2): F282-291.

Gehrig, A., T. Langmann, et al. (2007). "Genome-wide expression profiling of the retinoschisin-deficient retina in early postnatal mouse development." Invest Ophthalmol Vis Sci **48**(2): 891-900.

German, D. C., I. Khobahy, et al. (2012). "Nuclear localization of Klotho in brain: an anti-aging protein." Neurobiol Aging.

Gerrior, S., L. Bente, et al. (2004). Nutrient content of the U.S. food supply, 1909-2000. U.S. Center for Nutrition Policy and Promotion. Washington, D.C., U.S. Dept. of Agriculture Center for Nutrition Policy and Promotion.

Ghazizadeh, S. and M. Lessan-Pezeshki (2007). "Reproduction in women with end-stage renal disease and effect of kidney transplantation." Iran J Kidney Dis **1**(1): 12-15.

Go, A. S., G. M. Chertow, et al. (2004). "Chronic kidney disease and the risks of death, cardiovascular events, and hospitalization." N Engl J Med **351**(13): 1296-1305.

Gottsch, M. L., M. J. Cunningham, et al. (2004). "A role for kisspeptins in the regulation of gonadotropin secretion in the mouse." Endocrinology **145**(9): 4073-4077.

Gueorguiev, M., M. L. Goth, et al. (2001). "Leptin and puberty: a review." Pituitary **4**(1-2): 79-86.

Gutierrez, O., T. Isakova, et al. (2005). "Fibroblast growth factor-23 mitigates hyperphosphatemia but accentuates calcitriol deficiency in chronic kidney disease." J Am Soc Nephrol **16**(7): 2205-2215.

Haisenleder, D. J., A. C. Dalkin, et al. (1991). "A pulsatile gonadotropin-releasing hormone stimulus is required to increase transcription of the gonadotropin subunit genes: evidence for differential regulation of transcription by pulse frequency in vivo." Endocrinology **128**(1): 509-517.

Han, S. K., M. L. Gottsch, et al. (2005). "Activation of gonadotropin-releasing hormone neurons by kisspeptin as a neuroendocrine switch for the onset of puberty." J Neurosci **25**(49): 11349-11356.

Handelsman, D. J. (1985). "Hypothalamic-pituitary gonadal dysfunction in renal failure, dialysis and renal transplantation." Endocr Rev **6**(2): 151-182.

Hanley, N. A., Y. Ikeda, et al. (2000). "Steroidogenic factor 1 (SF-1) is essential for ovarian development and function." Mol Cell Endocrinol **163**(1-2): 27-32.

Heimburger, O., F. Lonnqvist, et al. (1997). "Serum immunoreactive leptin concentration and its relation to the body fat content in chronic renal failure." J Am Soc Nephrol **8**(9): 1423-1430.

Hilfiker, H., O. Hattenhauer, et al. (1998). "Characterization of a murine type II sodium-phosphate cotransporter expressed in mammalian small intestine." Proc Natl Acad Sci U S A **95**(24): 14564-14569.

Hill, J. W., K. W. Williams, et al. (2008). "Acute effects of leptin require PI3K signaling in hypothalamic proopiomelanocortin neurons in mice." J Clin Invest **118**: 1796-1805.

Hinshelwood, M. M., J. J. Repa, et al. (2003). "Expression of LRH-1 and SF-1 in the mouse ovary: localization in different cell types correlates with differing function." Mol Cell Endocrinol **207**(1-2): 39-45.

Hiza, H. and L. Bente (2011). Nutrient Content of the U.S. Food Supply: Developments Between 2000 and 2006. Center for Nutrition Policy and Promotion. Washington, D.C., U.S. Department of Agriculture.

Hokken-Koelega, A. C., P. Saenger, et al. (2001). "Unresolved problems concerning optimal therapy of puberty in children with chronic renal diseases." J Pediatr Endocrinol Metab **14 Suppl 2**: 945-952.

Holley, J. L. (2004). "The hypothalamic-pituitary axis in men and women with chronic kidney disease." Adv Chronic Kidney Dis **11**(4): 337-341.

Hruska, K. A., S. Mathew, et al. (2008). "Hyperphosphatemia of chronic kidney disease." Kidney Int **74**(2): 148-157.

Hsuchou, H., W. Pan, et al. (2007). "The fasting polypeptide FGF21 can enter brain from blood." Peptides **28**(12): 2382-2386.

Hu, M. C., M. Shi, et al. (2010). "Klotho: a novel phosphaturic substance acting as an autocrine enzyme in the renal proximal tubule." FASEB J **24**(9): 3438-3450.

Ibels, L. S., A. C. Alfrey, et al. (1978). "Preservation of function in experimental renal disease by dietary restriction of phosphate." N Engl J Med **298**(3): 122-126.

Ichikawa, S., E. A. Imel, et al. (2007). "A homozygous missense mutation in human KLOTHO causes severe tumoral calcinosis." J Clin Invest **117**(9): 2684-2691.

Imura, A., A. Iwano, et al. (2004). "Secreted Klotho protein in sera and CSF: implication for post-translational cleavage in release of Klotho protein from cell membrane." FEBS Lett **565**(1-3): 143-147.

Jin, H., S. K. Hwang, et al. (2006). "A high inorganic phosphate diet perturbs brain growth, alters Akt-ERK signaling, and results in changes in cap-dependent translation." Toxicol Sci **90**(1): 221-229.

Jonsson, K. B., R. Zahradnik, et al. (2003). "Fibroblast growth factor 23 in oncogenic osteomalacia and X-linked hypophosphatemia." N Engl J Med **348**(17): 1656-1663.

Kamel, F. and C. L. Kubajak (1987). "Modulation of gonadotropin secretion by corticosterone: interaction with gonadal steroids and mechanism of action." Endocrinology **121**(2): 561-568.

Kastin, A. J., V. Akerstrom, et al. (2001). "Validity of multiple-time regression analysis in measurement of tritiated and iodinated leptin crossing the blood-brain barrier: meaningful controls." Peptides **22**(12): 2127-2136.

Kato, K., C. Jeanneau, et al. (2006). "Polypeptide GalNAc-transferase T3 and familial tumoral calcinosis. Secretion of fibroblast growth factor 23 requires O-glycosylation." J Biol Chem **281**(27): 18370-18377.

Kato, Y., E. Arakawa, et al. (2000). "Establishment of the anti-Klotho monoclonal antibodies and detection of Klotho protein in kidneys." Biochem Biophys Res Commun **267**(2): 597-602.

Kauffman, A. S., M. L. Gottsch, et al. (2007). "Sexual differentiation of Kiss1 gene expression in the brain of the rat." Endocrinology **148**(4): 1774-1783.

Khoshniat, S., A. Bourgine, et al. (2011). "Phosphate-dependent stimulation of MGP and OPN expression in osteoblasts via the ERK1/2 pathway is modulated by calcium." Bone **48**(4): 894-902.

Khoshniat, S., A. Bourgine, et al. (2011). "The emergence of phosphate as a specific signaling molecule in bone and other cell types in mammals." Cell Mol Life Sci **68**(2): 205-218.

Kido, S., K. Miyamoto, et al. (1999). "Identification of regulatory sequences and binding proteins in the type II sodium/phosphate cotransporter NPT2 gene responsive to dietary phosphate." J Biol Chem **274**(40): 28256-28263.

Kinsey-Jones, J. S., X. F. Li, et al. (2009). "Down-regulation of hypothalamic kisspeptin and its receptor, Kiss1r, mRNA expression is associated with stress-induced suppression of luteinising hormone secretion in the female rat." J Neuroendocrinol **21**(1): 20-29.

Kinuta, K., H. Tanaka, et al. (2000). "Vitamin D is an important factor in estrogen biosynthesis of both female and male gonads." Endocrinology **141**(4): 1317-1324.

Knobil, E. (1980). "The neuroendocrine control of the menstrual cycle." Recent Prog Horm Res **36**: 53-88.

Kolek, O. I., E. R. Hines, et al. (2005). "1alpha,25-Dihydroxyvitamin D3 upregulates FGF23 gene expression in bone: the final link in a renal-gastrointestinal-skeletal axis that controls phosphate transport." Am J Physiol Gastrointest Liver Physiol **289**(6): G1036-1042.

Kronenberg, H. M., S. Melmed, et al. (2008). Williams Textbook of Endocrinology. Philadelphia, PA, Saunders Elsevier.

Kuro-o, M., Y. Matsumura, et al. (1997). "Mutation of the mouse klotho gene leads to a syndrome resembling ageing." Nature **390**(6655): 45-51.

Kurosu, H., Y. Ogawa, et al. (2006). "Regulation of fibroblast growth factor-23 signaling by klotho." J Biol Chem **281**(10): 6120-6123.

Kurosu, H., M. Yamamoto, et al. (2005). "Suppression of aging in mice by the hormone Klotho." Science **309**(5742): 1829-1833.

Kurumaji, A., T. Ito, et al. (2008). "Effects of FG7142 and immobilization stress on the gene expression in the neocortex of mice." Neurosci Res **62**(3): 155-159.

Lane, P. H. (2005). "Puberty and chronic kidney disease." Adv Chronic Kidney Dis **12**(4): 372-377.

Li, S. A., M. Watanabe, et al. (2004). "Immunohistochemical localization of Klotho protein in brain, kidney, and reproductive organs of mice." Cell Struct Funct **29**(4): 91-99.

Lim, V. S., C. Henriquez, et al. (1980). "Ovarian function in chronic renal failure: evidence suggesting hypothalamic anovulation." Ann Intern Med **93**(1): 21-27.

Liu, H., M. M. Fergusson, et al. (2007). "Augmented Wnt signaling in a mammalian model of accelerated aging." Science **317**(5839): 803-806.

Liu, S., R. Guo, et al. (2003). "Regulation of fibroblastic growth factor 23 expression but not degradation by PHEX." J Biol Chem **278**(39): 37419-37426.

Liu, S., L. Vierthaler, et al. (2008). "FGFR3 and FGFR4 do not mediate renal effects of FGF23." J Am Soc Nephrol **19**(12): 2342-2350.

Liu, X., D. Qin, et al. (2010). "The effect of calcium phosphate nanoparticles on hormone production and apoptosis in human granulosa cells." Reprod Biol Endocrinol **8**: 32.

Lorenz-Depiereux, B., M. Bastepe, et al. (2006). "DMP1 mutations in autosomal recessive hypophosphatemia implicate a bone matrix protein in the regulation of phosphate homeostasis." Nat Genet **38**(11): 1248-1250.

Lotscher, M., Y. Scarpetta, et al. (1999). "Rapid downregulation of rat renal Na/P(i) cotransporter in response to parathyroid hormone involves microtubule rearrangement." J Clin Invest **104**(4): 483-494.

Mankin, H. J. (1974). "Rickets, osteomalacia, and renal osteodystrophy. Part II." J Bone Joint Surg Am **56**(2): 352-386.

Martin, K. J. and E. A. Gonzalez (2011). "Prevention and control of phosphate retention/hyperphosphatemia in CKD-MBD: what is normal, when to start, and how to treat?" Clin J Am Soc Nephrol **6**(2): 440-446.

Masoro, E. J. (2005). "Overview of caloric restriction and ageing." Mech Ageing Dev **126**(9): 913-922.

Matteri, R. L., G. P. Moberg, et al. (1986). "Adrenocorticotropin-induced changes in ovine pituitary gonadotropin secretion in vitro." Endocrinology **118**(5): 2091-2096.

McSheehy, P. M. and T. J. Chambers (1986). "Osteoblast-like cells in the presence of parathyroid hormone release soluble factor that stimulates osteoclastic bone resorption." Endocrinology **119**(4): 1654-1659.

Milenkovic, L., G. D'Angelo, et al. (1994). "Inhibition of gonadotropin hormone-releasing hormone release by prolactin from GT1 neuronal cell lines through prolactin receptors." Proc Natl Acad Sci U S A **91**(4): 1244-1247.

Miller, W. L. and J. F. Strauss, 3rd (1999). "Molecular pathology and mechanism of action of the steroidogenic acute regulatory protein, StAR." J Steroid Biochem Mol Biol **69**(1-6): 131-141.

Mirams, M., B. G. Robinson, et al. (2004). "Bone as a source of FGF23: regulation by phosphate?" Bone **35**(5): 1192-1199.

Mitamura, R., K. Yano, et al. (1999). "Diurnal rhythms of luteinizing hormone, follicle-stimulating hormone, and testosterone secretion before the onset of male puberty." J Clin Endocrinol Metab **84**(1): 29-37.

Mitamura, R., K. Yano, et al. (2000). "Diurnal rhythms of luteinizing hormone, follicle-stimulating hormone, testosterone, and estradiol secretion before the onset of female puberty in short children." J Clin Endocrinol Metab **85**(3): 1074-1080.

Moallem, E., R. Kilav, et al. (1998). "RNA-Protein binding and post-transcriptional regulation of parathyroid hormone gene expression by calcium and phosphate." J Biol Chem **273**(9): 5253-5259.

Morishita, K., A. Shirai, et al. (2001). "The progression of aging in klotho mutant mice can be modified by dietary phosphorus and zinc." J Nutr **131**(12): 3182-3188.

Nakatani, T., M. Ohnishi, et al. (2009). "Inactivation of klotho function induces hyperphosphatemia even in presence of high serum fibroblast growth factor 23 levels in a genetically engineered hypophosphatemic (Hyp) mouse model." FASEB J **23**(11): 3702-3711.

Navarro, V. M., J. M. Castellano, et al. (2004). "Developmental and hormonally regulated messenger ribonucleic acid expression of KiSS-1 and its putative receptor, GPR54, in rat hypothalamus and potent luteinizing hormone-releasing activity of KiSS-1 peptide." Endocrinology **145**(10): 4565-4574.

Navarro, V. M., J. M. Castellano, et al. (2005). "Effects of KiSS-1 peptide, the natural ligand of GPR54, on follicle-stimulating hormone secretion in the rat." Endocrinology **146**(4): 1689-1697.

Oakley, A. E., D. K. Clifton, et al. (2009). "Kisspeptin signaling in the brain." Endocr Rev **30**(6): 713-743.

Ohnishi, M., T. Nakatani, et al. (2009). "Reversal of mineral ion homeostasis and soft-tissue calcification of klotho knockout mice by deletion of vitamin D 1alpha-hydroxylase." Kidney Int **75**(11): 1166-1172.

Ohnishi, M. and M. S. Razzaque (2010). "Dietary and genetic evidence for phosphate toxicity accelerating mammalian aging." FASEB J **24**(9): 3562-3571.

Ohyama, Y., M. Kurabayashi, et al. (1998). "Molecular cloning of rat klotho cDNA: markedly decreased expression of klotho by acute inflammatory stress." Biochem Biophys Res Commun **251**(3): 920-925.

Oury, F., G. Sumara, et al. (2011). "Endocrine regulation of male fertility by the skeleton." Cell **144**(5): 796-809.

Palmer, S. C., A. Hayen, et al. (2011). "Serum levels of phosphorus, parathyroid hormone, and calcium and risks of death and cardiovascular disease in individuals with chronic kidney disease: a systematic review and meta-analysis." JAMA **305**(11): 1119-1127.

Peng, N., J. W. Kim, et al. (2003). "The role of the orphan nuclear receptor, liver receptor homologue-1, in the regulation of human corpus luteum 3beta-hydroxysteroid dehydrogenase type II." J Clin Endocrinol Metab **88**(12): 6020-6028.

Plant, T. M. (2001). "Neurobiological bases underlying the control of the onset of puberty in the rhesus monkey: a representative higher primate." Front Neuroendocrinol **22**(2): 107-139.

Plotnikov, A. N., S. R. Hubbard, et al. (2000). "Crystal structures of two FGF-FGFR complexes reveal the determinants of ligand-receptor specificity." Cell **101**(4): 413-424.

Quarles, L. D. (2012). "Role of FGF23 in vitamin D and phosphate metabolism: Implications in chronic kidney disease." Exp Cell Res.

Razzaque, M. S. (2009). "The FGF23-Klotho axis: endocrine regulation of phosphate homeostasis." Nat Rev Endocrinol **5**(11): 611-619.

Richards, J. S. and K. Bogovich (1982). "Effects of human chorionic gonadotropin and progesterone on follicular development in the immature rat." Endocrinology **111**(5): 1429-1438.

Richards, J. S., J. A. Jonassen, et al. (1980). "Evidence that changes in tonic luteinizing hormone secretion determine the growth of preovulatory follicles in the rat." Endocrinology **107**(3): 641-648.

Riminucci, M., M. T. Collins, et al. (2003). "FGF-23 in fibrous dysplasia of bone and its relationship to renal phosphate wasting." J Clin Invest **112**(5): 683-692.

Ritthaler, T., M. Traebert, et al. (1999). "Effects of phosphate intake on distribution of type II Na/Pi cotransporter mRNA in rat kidney." Kidney Int **55**(3): 976-983.

Rivier, C. and W. Vale (1984). "Influence of corticotropin-releasing factor on reproductive functions in the rat." Endocrinology **114**(3): 914-921.

Roa, J., J. M. Castellano, et al. (2009). "Kisspeptins and the control of gonadotropin secretion in male and female rodents." Peptides **30**(1): 57-66.

Sage, A. P., J. Lu, et al. (2011). "Hyperphosphatemia-induced nanocrystals upregulate the expression of bone morphogenetic protein-2 and osteopontin genes in mouse smooth muscle cells in vitro." Kidney Int **79**(4): 414-422.

Saito, H., A. Maeda, et al. (2005). "Circulating FGF-23 is regulated by 1alpha,25-dihydroxyvitamin D3 and phosphorus in vivo." J Biol Chem **280**(4): 2543-2549.

Sarnak, M. J., A. S. Levey, et al. (2003). "Kidney disease as a risk factor for development of cardiovascular disease: a statement from the American Heart Association Councils on Kidney in Cardiovascular Disease, High Blood Pressure Research, Clinical Cardiology, and Epidemiology and Prevention." Hypertension **42**(5): 1050-1065.

Sauder, S. E., M. Frager, et al. (1984). "Abnormal patterns of pulsatile luteinizing hormone secretion in women with hyperprolactinemia and amenorrhea: responses to bromocriptine." J Clin Endocrinol Metab **59**(5): 941-948.

Schaefer, F., C. Seidel, et al. (1991). "Pulsatile immunoreactive and bioactive luteinizing hormone secretion in adolescents with chronic renal failure. The Cooperative Study Group on Pubertal Development in Chronic Renal Failure (CSPCRF)." Pediatr Nephrol **5**(4): 566-571.

Schaefer, F., J. D. Veldhuis, et al. (1994). "Immunoreactive and bioactive luteinizing hormone in pubertal patients with chronic renal failure. Cooperative Study Group on Pubertal Development in Chronic Renal Failure." Kidney Int **45**(5): 1465-1476.

Schipper, I., W. C. Hop, et al. (1998). "The follicle-stimulating hormone (FSH) threshold/window concept examined by different interventions with exogenous FSH during the follicular phase of the normal menstrual cycle: duration, rather than magnitude, of FSH increase affects follicle development." J Clin Endocrinol Metab **83**(4): 1292-1298.

Schumacher, B., I. van der Pluijm, et al. (2008). "Delayed and accelerated aging share common longevity assurance mechanisms." PLoS Genet **4**(8): e1000161.

Seeburg, P. H. and J. P. Adelman (1984). "Characterization of cDNA for precursor of human luteinizing hormone releasing hormone." Nature **311**(5987): 666-668.

Segawa, H., I. Kaneko, et al. (2002). "Growth-related renal type II Na/Pi cotransporter." J Biol Chem **277**(22): 19665-19672.

Segawa, H., S. Yamanaka, et al. (2007). "Correlation between hyperphosphatemia and type II Na-Pi cotransporter activity in klotho mice." Am J Physiol Renal Physiol **292**(2): F769-779.

Segawa, H., S. Yamanaka, et al. (2007). "Parathyroid hormone-dependent endocytosis of renal type IIc Na-Pi cotransporter." Am J Physiol Renal Physiol **292**(1): F395-403.

Seminara, S. B., S. Messager, et al. (2003). "The GPR54 gene as a regulator of puberty." N Engl J Med **349**(17): 1614-1627.

Shimada, T., H. Hasegawa, et al. (2004). "FGF-23 is a potent regulator of vitamin D metabolism and phosphate homeostasis." J Bone Miner Res **19**(3): 429-435.

Shimada, T., M. Kakitani, et al. (2004). "Targeted ablation of Fgf23 demonstrates an essential physiological role of FGF23 in phosphate and vitamin D metabolism." J Clin Invest **113**(4): 561-568.

Shimada, T., S. Mizutani, et al. (2001). "Cloning and characterization of FGF23 as a causative factor of tumor-induced osteomalacia." Proc Natl Acad Sci U S A **98**(11): 6500-6505.

Shimada, T., T. Muto, et al. (2002). "Mutant FGF-23 responsible for autosomal dominant hypophosphatemic rickets is resistant to proteolytic cleavage and causes hypophosphatemia in vivo." Endocrinology **143**(8): 3179-3182.

Silver, J., J. Russell, et al. (1985). "Regulation by vitamin D metabolites of messenger ribonucleic acid for preproparathyroid hormone in isolated bovine parathyroid cells." Proc Natl Acad Sci U S A **82**(12): 4270-4273.

Sitara, D., M. S. Razzaque, et al. (2004). "Homozygous ablation of fibroblast growth factor-23 results in hyperphosphatemia and impaired skeletogenesis, and reverses hypophosphatemia in Phex-deficient mice." Matrix Biol **23**(7): 421-432.

Stenvinkel, P., B. Lindholm, et al. (2000). "Increases in serum leptin levels during peritoneal dialysis are associated with inflammation and a decrease in lean body mass." J Am Soc Nephrol **11**(7): 1303-1309.

Stevens, L. A., S. Li, et al. (2010). "Prevalence of CKD and comorbid illness in elderly patients in the United States: results from the Kidney Early Evaluation Program (KEEP)." Am J Kidney Dis **55**(3 Suppl 2): S23-33.

Stubbs, J. R., S. Liu, et al. (2007). "Role of hyperphosphatemia and 1,25-dihydroxyvitamin D in vascular calcification and mortality in fibroblastic growth factor 23 null mice." J Am Soc Nephrol **18**(7): 2116-2124.

Taal, M. W., G. M. Chertow, et al. (2011). Brenner and Rector's The Kidney, Saunders.

Tani, Y., T. Sato, et al. (2007). "Effects of prolonged high phosphorus diet on phosphorus and calcium balance in rats." J Clin Biochem Nutr **40**(3): 221-228.

Ten Hagen, K. G., T. A. Fritz, et al. (2003). "All in the family: the UDP-GalNAc:polypeptide N-acetylgalactosaminyltransferases." Glycobiology **13**(1): 1R-16R.

The HYP Consortium (1995). "A gene (PEX) with homologies to endopeptidases is mutated in patients with X-linked hypophosphatemic rickets. The HYP Consortium." Nat Genet **11**(2): 130-136.

Thompson, E. L., K. G. Murphy, et al. (2006). "Chronic subcutaneous administration of kisspeptin-54 causes testicular degeneration in adult male rats." Am J Physiol Endocrinol Metab **291**(5): E1074-1082.

Tonelli, M., F. Sacks, et al. (2005). "Relation between serum phosphate level and cardiovascular event rate in people with coronary disease." Circulation **112**(17): 2627-2633.

Toyama, R., T. Fujimori, et al. (2006). "Impaired regulation of gonadotropins leads to the atrophy of the female reproductive system in klotho-deficient mice." Endocrinology **147**(1): 120-129.

Trogan, E., R. P. Choudhury, et al. (2002). "Laser capture microdissection analysis of gene expression in macrophages from atherosclerotic lesions of apolipoprotein E-deficient mice." Proc Natl Acad Sci U S A **99**(4): 2234-2239.

United States Institute of Medicine Standing Committee on the Scientific Evaluation of Dietary Reference Intakes (1997). Dietary reference intakes

: for calcium, phosphorus, magnesium, vitamin D, and fluoride. Washington, D.C., National Academy Press.

United States Nutrient Data Laboratory (2005). USDA National Nutrient Database for Standard Reference. United States Nutrient Data Laboratory. Riverdale, Md., Nutrient Data Laboratory, Agricultural Research Service, Beltsville Human Nutrition Research Center.

Urakawa, I., Y. Yamazaki, et al. (2006). "Klotho converts canonical FGF receptor into a specific receptor for FGF23." Nature **444**(7120): 770-774.

Uribarri, J. (2009). "Phosphorus additives in food and their effect in dialysis patients." Clin J Am Soc Nephrol **4**(8): 1290-1292.

van den Broek, F. A. and A. C. Beynen (1998). "The influence of dietary phosphorus and magnesium concentrations on the calcium content of heart and kidneys of DBA/2 and NMRI mice." Lab Anim **32**(4): 483-491.

van der Pluijm, I., G. A. Garinis, et al. (2007). "Impaired genome maintenance suppresses the growth hormone--insulin-like growth factor 1 axis in mice with Cockayne syndrome." PLoS Biol **5**(1): e2.

Vergara, G. J., M. H. Irwin, et al. (1997). "In vitro fertilization in mice: Strain differences in response to superovulation protocols and effect of cumulus cell removal." Theriogenology **47**(6): 1245-1252.

Wahl, P. and M. Wolf (2012). "FGF23 in chronic kidney disease." Adv Exp Med Biol **728**: 107-125.

Weber, T. J., S. Liu, et al. (2003). "Serum FGF23 levels in normal and disordered phosphorus homeostasis." J Bone Miner Res **18**(7): 1227-1234.

Weinman, E. J., R. Biswas, et al. (2011). "Increased renal dopamine and acute renal adaptation to a high-phosphate diet." Am J Physiol Renal Physiol **300**(5): F1123-1129.

White, K. E., G. Carn, et al. (2001). "Autosomal-dominant hypophosphatemic rickets (ADHR) mutations stabilize FGF-23." Kidney Int **60**(6): 2079-2086.

White, K. E., K. B. Jonsson, et al. (2001). "The autosomal dominant hypophosphatemic rickets (ADHR) gene is a secreted polypeptide

overexpressed by tumors that cause phosphate wasting." J Clin Endocrinol Metab **86**(2): 497-500.

Williams, K. W., L. O. Margatho, et al. (2010). "Segregation of acute leptin and insulin effects in distinct populations of arcuate proopiomelanocortin neurons." J Neurosci **30**(7): 2472-2479.

Winters, R. W., J. B. Graham, et al. (1958). "A genetic study of familial hypophosphatemia and vitamin D resistant rickets with a review of the literature." Medicine (Baltimore) **37**(2): 97-142.

Wu, F. C., G. E. Butler, et al. (1996). "Ontogeny of pulsatile gonadotropin releasing hormone secretion from midchildhood, through puberty, to adulthood in the human male: a study using deconvolution analysis and an ultrasensitive immunofluorometric assay." J Clin Endocrinol Metab **81**(5): 1798-1805.

Xiao, E., J. Luckhaus, et al. (1989). "Acute inhibition of gonadotropin secretion by corticotropin-releasing hormone in the primate: are the adrenal glands involved?" Endocrinology **124**(4): 1632-1637.

Yamamoto, T., J. J. Carrero, et al. (2009). "Leptin and uremic protein-energy wasting--the axis of eating." Semin Dial **22**(4): 387-390.

Yamashita, T., M. Yoshioka, et al. (2000). "Identification of a novel fibroblast growth factor, FGF-23, preferentially expressed in the ventrolateral thalamic nucleus of the brain." Biochem Biophys Res Commun **277**(2): 494-498.

Yoshida, T., T. Fujimori, et al. (2002). "Mediation of unusually high concentrations of 1,25-dihydroxyvitamin D in homozygous klotho mutant mice by increased expression of renal 1alpha-hydroxylase gene." Endocrinology **143**(2): 683-689.

Yoshiko, Y., H. Wang, et al. (2007). "Mineralized tissue cells are a principal source of FGF23." Bone **40**(6): 1565-1573.

Yoshizawa, T., Y. Handa, et al. (1997). "Mice lacking the vitamin D receptor exhibit impaired bone formation, uterine hypoplasia and growth retardation after weaning." Nat Genet **16**(4): 391-396.